Nanoscale Advances

REVIEW

View Article Online
View Journal | View Issue

Cite this: *Nanoscale Adv.*, 2019, **1**, 3325

Preparation and applications of electrochemical chemosensors based on carbon-nanomaterial-modified molecularly imprinted polymers

Rijun Gui, †*[a] Huijun Guo†[b] and Hui Jin*[a]

The past few decades have witnessed a rapid development in electrochemical chemosensors (ECCSs). The integration of carbon nanomaterials (CNMs) and molecularly imprinted polymers (MIPs) has endowed ECCSs with high selectivity and sensitivity toward target detection. Due to the integrated merits of MIPs and CNMs, CNM-modified MIPs as ECCSs have been widely reported and have excellent detection applications. This review systematically summarized the general categories, preparation strategies, and applications of ECCSs based on CNM-modified MIPs. The categories include CNM-modified MIPs often hybridized with various materials and CNM-encapsulated or CNM-combined imprinting silica and polymers on working electrodes or other substrates. The preparation strategies include the polymerization of MIPs on CNM-modified substrates, co-polymerization of MIPs and CNMs on substrates, drop-casting of MIPs on CNM-modified substrates, self-assembly of CNMs/MIP complexes on substrates, and so forth. We discussed the *in situ* polymerization, electro-polymerization, and engineering structures of CNM-modified MIPs. With regard to potential applications, we elaborated the detection mechanisms, signal transducer modes, target types, and electrochemical sensing of targets in real samples. In addition, this review discussed the present status, challenges, and prospects of CNM-modified MIP-based ECCSs. This comprehensive review is desirable for scientists from broad research fields and can promote the further development of MIP-based functional materials, CNM-based hybrid materials, advanced composites, and hybrid materials.

Received 23rd July 2019
Accepted 29th July 2019

DOI: 10.1039/c9na00455f

rsc.li/nanoscale-advances

1. Introduction

1.1. Development process and preparation of MIPs

Before discussing molecularly imprinted polymers (MIPs), we review the development process of the molecular imprinting technology (MIT). The history of MIT seems to be somewhat

[a]*College of Chemistry and Chemical Engineering, Intellectual Property Research Institute, Qingdao University, Shandong 266071, PR China. E-mail: guirijun@qdu.edu.cn; jinhui@qdu.edu.cn; Fax: +86 532 85953981; Tel: +86 532 85953981*

[b]*Advanced Fiber and Composites Research Institute, Jilin Institute of Chemical Technology, Jilin 132022, PR China*

† These authors have the equivalent contribution to this work.

Rijun Gui received his BS degree in 2005 and completed his MS in Applied Chemistry from Shanghai Ocean University in 2009. Then, he studied at the East China University of Science and Technology to pursue his PhD (2012) in Physical Chemistry. Thereafter, he worked as a Postdoctoral Fellow at Shanghai Jiao Tong University. In 2014, he joined Qingdao University, where he is currently an Associate Professor. His research interests focus on fluorescent and electroactive nanomaterials.

Huijun Guo was born in 1992. Since 2015, she has been a Master's candidate in the College of Chemistry and Chemical Engineering, Qingdao University, China. After completing her MS in 2018, she joined the Jilin Institute of Chemical Technology, where she is currently a Laboratory Assistant. Her research interests focus on the preparation and applications of electrochemical sensors.

older. The first report on MIT dates back to the 1930s. As early as 1931, Polyakov first interpreted the selective template effects of polymers.[1] Templates and additives were included in template-participated polymerization. In 1940, Pauling postulated molecular recognition and involved antigens as the template in the self-assembly of protein antibodies.[2] During the subsequent few decades, there was no significant progress in MIT. Thereafter, Wulff *et al.* prepared organic polymers *via* reversible chemical bonds.[3] Vlatakis *et al.* prepared MIP based on non-covalent MIT.[4] After the pioneering studies, numerous scientists have paid close attention to MIT. Since then, MIT-related studies have started to grow rapidly.[5]

The general preparation of MIP involves covalence, non-covalence, or semi-covalence binding interactions between the templates and monomers. Wulff *et al.* first proposed a covalent approach to fabricate reversible covalent bonds between the templates and monomers before polymerization.[3] A marked merit of the covalent approach is the high stability of the template–monomer interactions, which yield considerable homogenous binding sites.[6] However, intense actions result in difficulty to thoroughly remove the templates. Arshady *et al.* employed a noncovalent approach to combine templates with monomers through *in situ* noncovalent interactions including van der Waals forces, hydrogen binding, and electrostatic interactions.[7] Under weak interactions, the preparation procedure of MIPs is relatively facile, and most of the monomers can interact with most of the templates. This approach has been widely used for MIP preparation,[8–12] but certain drawbacks inevitably exist because of the low selectivity of the binding sites. A semi-covalent approach has the combined features of both covalent and noncovalent approaches. MIPs prepared from covalent interactions can re-recognize templates *via* the noncovalent molecular imprinting process and reversible bonds.[13,14] Due to the advantages of two binding interactions, a semi-covalent imprinting approach can be used to fabricate stable, stoichiometric complexes in covalent imprinting, realizing fast guest binding in noncovalent imprinting.[15]

Various strategies involve the preparation of MIP. One of the most frequently used strategies is bulk polymerization. MIPs serve as the receptors to recognize the target molecules or templates. A general procedure for MIP preparation includes three steps. Step (I) is the prepolymerization of the functional monomers. Step (II) is the preparation of molecular recognition sites on high cross-linked polymers *via* noncovalent or covalent interactions. Step (III) is the generation of recognition cavities after template removal. These cavities are complementary to the target molecules with specific shapes, sizes, structures, and functional groups.[16–19] Bulk polymerization is simple and universal, but it is time-consuming and labor-intensive. The resulting MIP particles are often accompanied by irregular shapes and have low recovery as useable particles.[20] With regard to suspension polymerization, water as a dispersing agent reduces the number and strength of binding sites between the functional monomers and templates.[21] Precipitation polymerization belongs to a well-suited strategy to synthesize MIP microspheres with desirable features. During the polymerization process, the growing polymer chains are insoluble in porogens and tend to precipitate. The noticeable advantage of this strategy is the convenient achievement of MIP in the micron-size range, without surfactants and the control of polymerization conditions.[22,23] A two-step or multiple swelling polymerization process can be used to fabricate MIP beads *via* laborious steps. The uniformed-sized seed particles remain suspended in water. After the addition of suitable organic solvents, the initial particles swell to their final size with the desired performance.[5,24] In addition, the surface imprinting technique attracts considerable interest and serves as a new alternative for the preparation of MIP with improved performance. The imprinted binding sites are located on or near the surface of polymers. These characteristics conquer some limitations, such as limited mass transfer, small binding capacity, and incomplete removal of templates.[25,26] Two principal strategies are used for the preparation of surface-imprinted polymers. One involves the synthesis of a thin polymer film with the bulk imprinting technique. The other comprises the attachment of templates on the surface of flat or spherical substrates through polymerization.

Hui Jin received her BS degree in 2005 and completed her MS in Applied Chemistry from Shanghai Ocean University in 2008. Then, she studied at Tongji University to purse her PhD in Organic Chemistry. After completing her PhD in 2012, she worked as a Research Assistant at Shanghai Jiao Tong University. In 2015–2016, she joined Qingdao University as a Postdoctoral Fellow. Currently, she is an Associate Professor in Qingdao University. Her research interests focus on the synthesis and applications of nanomaterials with luminescence properties and electronic activities.

1.2. Characteristics of MIP and applications as electrochemical chemosensors (ECCSs)

MIP is similar to an antibody or bioreceptor. With regard to synthetic polymers, MIP has predetermined selectivity toward recognizing particular targets or other species with structural similarities to the targets or templates. Due to the existence of artificially created recognition sites, MIP is complementary to the sizes, shapes, molecular structures, or functional groups of the templates. MIP can specifically bind targets and imitate natural receptor systems, such as enzymes, antibodies, and hormones.[27,28] The significant characteristics of MIPs are facile preparation, specific identification, high stability and selectivity, wide practicability, *etc.* MIPs have attracted considerable attention in current research fields, such as extraction, separation, optical elements, electronic and optoelectronic devices, sensors, catalysis, *etc.* The prepared MIPs often lack electrocatalytic and conductive activities. Other drawbacks are low

sensitivity toward target recognition, large sizes, heterogeneous size distribution, partial embedding of binding sites, poor site accessibility for templates, *etc.* In this context, a proper modification of MIP with active substances is essential and can improve the performance of MIP applications. During the past few decades, numerous studies have reported using MIPs as ECCSs. There are more than 1000 target molecules and imprinting structures using different templates, such as inorganic ions, drugs, nucleic acids, proteins, viruses, and even cells.[11] MIP-based ECCSs integrate the merits of MIP and ECCS, exhibiting high selectivity, sensitivity, stability, facile preparation, low cost, reusability, and miniaturization.[29]

In recent years, MIP-based ECCSs have attracted tremendous interest in promising applications, such as biomedical diagnosis, biochemical analysis, environmental monitoring, and food safety evaluation. In particular, they have been widely used for the accurate analysis of important biomolecules, such as proteins, hormones, drugs, nucleic acids, *etc.* Mechanical and thermal stabilities as well as high specificity and sensitivity of MIP-based ECCSs toward targets endow them with promising potential toward high-performance sensing applications over the traditional instruments, techniques, and sensors. As tailor-made biomimetic materials, MIPs have obvious priority over other recognition elements. MIP-based ECCSs use MIPs as the specific recognition elements of templates (targets) and act as smart devices for signal outputs. High selectivity and sensitivity are two major requirements in the design of efficient sensors. To improve the sensitivity of MIP-based ECCSs, the principal routes involve enlarging the effective sensing surface areas and the modification of sensing surfaces with electroactive substances. To enlarge the sensing surface areas, commercial electrodes and other electrochemical substrates are widely used to fabricate ECCSs, such as nickel foam (NF), conducting glass, Cu wire, Au film, indium tin oxide, *etc.* Sensitive electrochemical sensing devices can be prepared by constructing ECCSs on various substrates with higher surface areas. The modification of MIP with electroactive substances is a superior route to improve the sensitivity of MIP-based ECCSs.

1.3. Carbon nanomaterials (CNMs)-modified MIPs as ECCSs and introduction of this review

In earlier reports, various electroactive substances have been used to construct MIP-based ECCSs, such as CNMs; noble metal nanoparticles (NPs); alloyed, bimetal, and metal oxide NPs; nanospheres and nanosheets; ionic liquids (ILs); polymers; organic–inorganic hybrid materials; and composite materials. Among these electroactive substances, CNMs have attracted considerable attention because of their unique electrical, optical, thermal, mechanical, and chemical properties; low cost; easy availability of raw materials; high biocompatibility; and deformability. Currently, CNMs have been widely used in electronics, optoelectronics, photovoltaics, flexible sensors, advanced devices, and bioassay technology (biosensors). Their excellent properties majorly depend on the functional atomic structures of CNMs and the synergistic interactions of CNMs with other materials. Typical CNMs include graphene (GR), graphene oxide (GO), reduced graphene oxide (rGO), single- and multiwalled carbon nanotubes (SWCNTs and MWCNTs), mesoporous/porous/three-dimensional (3D) carbon structures, GR, and carbon quantum dots (QDs). In this review, we systematically summarize numerous earlier studies regarding ECCSs based on CNM-modified MIPs. Prior to this current review, recent reviews involving MIP or MIP-based sensors have been introduced.[11,29–42] Whitcombe *et al.* reviewed the rational development of MIP-based sensors for protein detection.[38] Huynh *et al.* reviewed MIP as the recognition material for use in electronic tongues.[39] Ashley *et al.* summarized MIPs for sample preparation and biosensing in food analyses.[40] Dabrowski *et al.* reported a nanostructured MIP for protein chemosensing.[41]

During the past decade, numerous studies have investigated ECCSs based on CNM-modified MIPs due to the integrated merits of MIPs, ECCSs, and CNMs. Such a type of ECCS was largely prepared and widely used for the electrochemical sensing of various targets, with obvious superiority over other analytical techniques. Earlier reviews have referred to MIP-based sensors, but a timely and comprehensive review that summarizes the currently significant topic of CNM-modified MIPs as ECCSs is still lacking. In this review (Scheme 1), we systematically summarize the recent advances in CNM-modified-MIP-based ECCSs, focusing on the general categories, preparation strategies, and analytical applications. With regard to categories, we review the CNM-modified MIPs without or with the hybridization of other materials, and ECCSs fabricated on various work electrodes and substrates. With regard to preparation strategies, we firstly introduce CNM-encapsulated or CNM-combined imprinted silica and polymers. Then, we summarize the various preparation strategies, including the polymerization of MIPs on CNM-modified substrates, copolymerization of MIPs and CNMs on substrates, dropcasting of

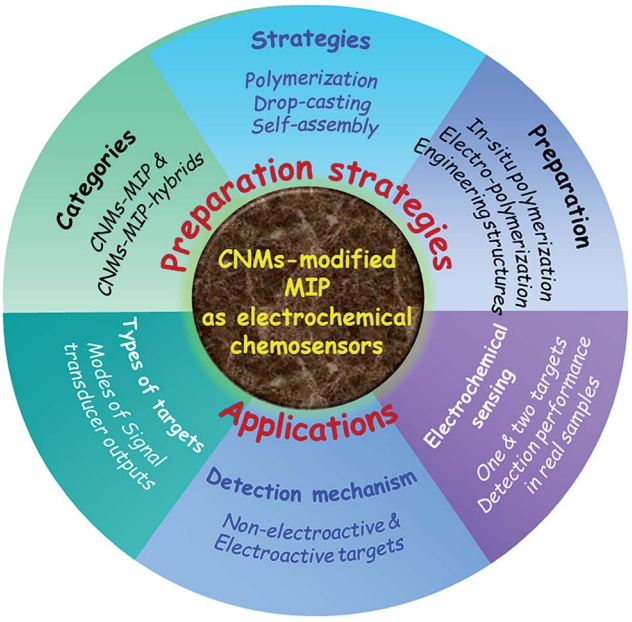

Scheme 1 Total architecture of this review, involving the preparation strategies and applications of CNM-modified MIP-based ECCSs.

MIPs on CNM-modified substrates, dropcasting of MIP/CNMs on substrates, self-assembly of CNMs/MIP/hybrids on substrates, dropcasting of self-assembled MIP/CNMs/hybrids on substrates. Further, we discuss the *in situ* chemical polymerization of monomers, electropolymerization of electroactive monomers, dummy templates, and engineering structures of CNM-modified MIPs. With regard to analytical applications, we elaborate the detection mechanisms of nonelectroactive and electroactive targets, signal transducer modes, target types, electrochemical sensing of one and two types of targets, and real samples for detection. This review discusses the present status, challenges, and perspectives in CNM-modified-MIP-based ECCSs. This review is timely, comprehensive, in-depth, and desirable for scientists in broad fields. It will promote the further development of MIP-based functional materials, CNM-based hybrid materials, and other functionalized composites or hybrid materials.

2. Categories of ECCSs based on CNM-modified MIPs

2.1. MIPs modified with CNMs without hybridization

In this review, we summarize the general categories of ECCSs based on CNM-modified MIPs. On the surfaces of work electrodes and other sensing substrates, CNMs usually are dropcasted or grown *in situ* to form CNM-modified electrodes or substrates, followed by the *in situ* polymerization of MIPs or dropcasting of MIPs to fabricate CNM-modified MIPs. We have regularly summarized studies involving CNM-modified-MIP-based ECCSs,[43–92] often fabricated onto the surface of commercial glassy carbon electrodes (GCE, Table 1), other work electrodes, and electrochemical substrates (Table 2). There are two general categories to prepare such ECCSs. One is to prepare CNM-modified MIPs on the surface of the work electrodes or other substrates without the hybridization of other materials. The other is to prepare CNM-modified MIPs with the hybridization of inorganic, organic, mixed, hybrid, or composite materials,[93–197] as summarized in Tables 3–6.

The fabrication of CNM-modified MIPs widely involves different CNMs, including zero-, one-, two-, and three-dimensional (0D, 1D, 2D, and 3D, respectively), or micro-scale CNMs. 0D CNMs comprise GR quantum dots (GQDs), carbon dots (CDs), and C_{60}, while 1D CNMs majorly contain CNTs, CNT–COOH, SWCNTs, MWCNTs, SWCNT-/MWCNT–COOH, and C_3N_4 nanotubes. Typical 2D CNMs comprise GR, GO, rGO, GR/N-doped GR/GO/rGO nanoribbons, NH_2–GR, N,S-activated GR, rGO–COOH, Ag–N-doped rGO, or GR nanoplatelets. Principally, 3D CNMs include 3D porous GR, porous rGO, and boron-doped/ordered mesoporous carbon (CKM-3). As a type of microscale CNM, graphite powder participates in the modification of MIPs with CNMs and other materials.

With regard to the use of "MIP modified with CNMs without hybridization" to fabricate ECCSs, GCE is widely used as the work electrode (Table 1). One or more types of CNMs are prepared and used for the modification of electrodes or substrates, followed by the preparation of MIPs on CNM-modified electrodes or substrates. Bai *et al.* designed an electrochemical artemisinin (ART) sensor by the *in situ* polymerization of ART-imprinted membrane on GR-modified GCE surfaces.[52] Acrylamide (AM) and ethylene glycol dimethacrylate (EGDMA) acted as the monomer and cross-linking agent, respectively (Fig. 1a). In addition to GCE, other commercial work electrodes often serve as the substrates to fabricate CNM-modified MIPs (Table 2), such as carbon paste electrode, Cu electrode, Pt electrode, Au electrode, magnetic electrode, pencil graphite electrode (PGE), ceramic electrode, acetylene black paste electrode, carbon electrode (CE), screen-printed/ceramic CE, glassy electrode, *etc.* Huang *et al.* synthesized N,S-doped activated GR (N,S-AGR) that was dropcasted on a glassy electrode.[85] The MIP layer was *in situ* electropolymerized on an N,S-AGR-modified electrode to form a platform for cyclophosphamide (CPA) detection (Fig. 1b).

Moreover, different types of CNMs can simultaneously participate in the surface modification of electrodes and substrates. Thereafter, MIP can be prepared on multiple CNM-modified electrodes and substrates,[72–75,90–92] which have improved electron transfer capabilities and enhanced surface areas. Based on a composite of GR and SWCNT–COOH, an imprinted sol–gel electrochemical sensor was developed for the detection of propyl gallate (PG).[72] GR–SWCNTs composite was synthesized by the *in situ* hydrothermal reduction of exfoliated GO in the presence of hydrazine and ammonia solution. The dropping of GR–SWCNTs on GCE aims to prepare a modified electrode. By the *in situ* electropolymerization of phenyltrimethoxysilane (PTMOS as a functional monomer), a sol–gel MIP was grown on GR–SWCNTs-modified GCE to form MIP/GR–SWCNTs/GCE. The modification of MIP with GR–SWCNTs obviously improves the sensitivity of this sensor, which originates from the synergistic interactions between GR and SWCNTs to accelerate the electron transfer during the reaction process.

2.2. MIPs modified with CNMs and hybridized with other materials

In addition to the use of CNMs to prepare CNM-modified MIPs, in earlier studies, researchers have mostly used other materials to hybridize with CNMs in order to fabricate ECCSs based on MIPs modified with CNMs and hybridized with other materials. As summarized in Tables 3–6, various materials have been widely used in the hybridization with CNMs, including noble metal NPs, alloyed/bimetal NPs, metal oxide NPs, nanosheets, small molecules, biomolecules, polymers, organic–inorganic hybrid materials, and composite materials. One or more types of these materials can be prepared and used for hybridization with CNMs, followed by the preparation of MIPs on CNMs and other materials in the form of dual-modified electrodes or substrates. Ji *et al.* constructed an electrochemical sensor for cholesterol (CHO) detection[94] through the MIP membrane on MWCNTs and gold NPs (AuNPs)-modified GCE. CHO and *p*-aminothiophenol (*p*-ATP) were assembled on the modified surface of GCE by Au–S bonds and hydrogen bonds, followed by the generation of an MIP membrane *via* the electropolymerization in a prepolymer solution containing *p*-ATP, $HAuCl_4$, tetrabutyl ammonium perchlorate (TBAP), and CHO

Table 1 CNMs-modified-MIP-based ECCSs that were fabricated on GCE[a]

Sensing materials	Targets	Modes	LOD	Detection ranges	Detected samples	Ref.
Polypyrrole/CNTs/GCE	Dopamine	DPV	1×10^{-11} M	5×10^{-11} to 5×10^{-6} M	Human serum, urine	43
Polydopamine/MWCNTs/GCE	Sunset yellow	DPV	1.4 nM	2.2 nM to 4.64 μM	Jelly, drink, chocolate, juice, ice cream, candy	44
Poly(*o*-aminophenol)/MWCNTs/GCE	Levofloxacin	DPV	1 μM	3–200 μM	Pharmaceuticals	45
Polypyrrole/MWCNTs–COOH/GCE	Dopamine	DPV	6×10^{-8} M	6.25×10^{-7} to 1×10^{-4} M	—	46
Poly(APVIMBF$_4$)/MWCNTs–COOH/GCE	BSA	CV	3.91×10^{-10} M	1.5×10^{-9} to 1.5×10^{-6} M	Liquid milk	47
Chitosan/graphene/GCE	L-Dopa	DPV	0.012 μM	0.4–100 μM	Tablet, blood serum	48
Chitosan/graphene/GCE	Dopamine	DPV	1×10^{-11} M	1×10^{-9} to 8×10^{-8} M, 1×10^{-7} to 1×10^{-4} M	Human blood serum	49
Polyaniline/graphene/GCE	2,4,6-Trinitrotoluene (picric acid)	DPV	—	0.73–31.55 μM	—	50
Polypyrrole/graphene/GCE	Trimethoprim	SWV	1.3×10^{-7} M	1×10^{-6} to 1×10^{-4} M	Human urine	51
Polyacrylamide/graphene/GCE	Artemisinin	DPV	2×10^{-9} M	1×10^{-8} to 4×10^{-5} M	Extract of *Artemisia annua* L.	52
Poly(4-vinylpyridine)/graphene/GCE	MDA, aniline	DPV	—	1–15 μM	White spoon, black spatula, black spoon	53
Poly(methacrylic acid)/graphene/GCE	4-Nitrophenol	DPV	5 nM	0.01–100, 200–1000 μM	Lake, tap water	54
Poly(acrylamide)/graphene/GCE	Phoxim	DPV	2×10^{-8} M	8×10^{-7} to 1.4×10^{-4} M	Cucumber	55
Poly(4-vinylbenzoic acid)/graphene/GCE	Thiamethoxam	LSV	0.04 μM	0.5–20 μM	Brown rice	56
Poly(*p*-vinylbenzoic acid)/graphene/GCE	Imidacloprid	LSV	0.1 μM	0.5–15 μM	Brown rice	57
SiO_2/GO/GCE	Paracetamol	DPV	20 nM	0.1–80 μM	Urine, tablets	58
Polypyrrole/GO/GCE	Quercetin	DPV	4.8×10^{-8} M	6×10^{-7} to 1.5×10^{-5} M	Apple juices	59
Polydopamine/GO/GCE	Bovine hemoglobin	DPV	2×10^{-10} mg mL^{-1}	1×10^{-9} to 1×10^{-1} mg mL^{-1}	Bovine blood plasma	60
Poly(β-cydodextrin)/GO/GCE	Epigallocatechin gallate	DPV	8.78×10^{-9} M	3×10^{-8}∼1×10^{-5} M	Tea samples	61
Poly(methacrylic acid)/GO/GCE	2,4-Dichlorophenol	DPV	0.5 nM	0.004–10 μM	Lake water	62
Imprinted silica sol–gel/GO/GCE	Mesalazine	DPV	0.97 μM	2–20, 20–150 μM	Drug tablet	63
Polypyrrole/rGO/GCE	Melamine	EIS	0.83 nM	4–240 nM	Liquid milk	64
Poly(*o*-phenylenediamine)/rGO/GCE	Imidacloprid	LSV	4×10^{-7} M	7.5×10^{-7} to 7×10^{-5} M	Pears	65
Poly(methacrylic acid)/rGO/GCE	4-Nitrophenol	DPV	0.005 μM	0.01–100 μM	Tap/river water	66
Poly(AMT)/rGO/GCE	Uric acid, tyrosine	DPV	3.2 nM, 0.046 μM	0.01–100, 0.1–400 μM	Human serum, urine	67
Poly(5-amino-8-hydroxyquinoline)/rGO/GCE	Dopamine	DPV	32.7 nM	1×10^{-7} to 14×10^{-7} M	Human blood plasma	68
Poly(*o*-phenylenediamine)/Ag–N-doped rGO/GCE	Salbutamol	DPV	7 nM	0.03–20 μM	Human urine, pork	69
Polypyrrole/GQDs/GCE	Bisphenol A	DPV	0.04 μM	0.1–50 μM	Sea, bottled water	70
Poly(3,4-ethylenedioxythiophene)/graphene nanoribbons/GCE	Octylphenol	LSV	6 nM	0.04–8 μM	River, bottled mineral water, urine	71
Poly(phenyl trimethoxysilane)/SWCNTs/graphene/GCE	Propyl gallate	DPV	5×10^{-8} M	8×10^{-8} to 2.6×10^{-3} M	Edible oil, instant noodles, cookies	72
Polypyrrole/rGO–carbon dots/GCE	Rutoside	DPV	3 nM	0.01–6.5 μM	Human serum	73
Poly(3-aminopropyltriethoxysilane)/GQDs/graphene nanoplatelets/GCE	Metronidazole	DPV	0.52 nM	0.005–0.75, 0.75–10 μM	Human blood plasma	74
Poly(C16VimCl)/MWCNTs/mesoporous carbon/porous rGO/GCE	Chloramphenicol	DPV	1×10^{-10} M	5×10^{-9} to 5×10^{-7} M, 5×10^{-7} to 4×10^{-6} M	Milk, honey	75

[a] Abbreviation carbon nanotubes, CNTs; glassy carbon electrode, GCE; multiwalled carbon nanotubes, MWCNTs; 3-(3-aminopropyl)-1-vinylimidazole tetrafluoroborate, APVIMBF$_4$; graphene oxide, GO; reduced graphene oxide, rGO; 2-amino-5-mercapto-1,3,4-thiadiazole, AMT; graphene quantum dots, GQDs; single-walled carbon nanotubes, SWCNTs; 3-hexadecyl-1-vinylimidazolium chloride, C16VimCl; bovine serum albumin, BSA; 4,4-methylene diphenylamine, MDA; differential pulse voltammetry, DPV; cyclic voltammetry, CV; square wave voltammetry, SWV; linear sweep voltammograms, LSV; electrochemical impedance spectroscopy, EIS.

Table 2 CNMs-modified-MIP-based ECCSs that were fabricated on other work electrodes[a]

Sensing materials	Targets	Modes	LOD	Detection ranges	Detected samples	Ref.
Poly(itaconic acid)/MWCNTs/carbon paste electrode	Bi^{3+}	DPV	8.9 nM	0.2–2 μM	Bi substrate, sea, river water, human plasma	76
Poly(methacrylic acid)/MWCNTs/Cu electrode	γ-HCCH	LSV	1×10^{-10} M	1×10^{-10} to 1×10^{-3} M	Fruits, vegetables, water	77
Polybenzidine/MWCNTs–COOH/pencil graphite electrode	L-Methionine	DPCSV	2.4–3 ng L^{-1}	11.7–206.3 ng L^{-1}	Tablet, human blood serum	78
Poly(TEGMPA)/MWCNTs–COOH/ceramic electrode	BSA	DPV	0.42 ng mL^{-1}	1.99–30.91 ng mL^{-1}	Aqueous, human serum, milk, pharmaceutics	79
Polyacrylamide/MWCNTs–COOH/Pt electrode	Pb(II) ions	DPV	0.02 μM	1–5 ppm	Mining effluent, lake water, food, cosmetics	80
Chitosan/graphene/acetylene black paste electrode	Bisphenol A	LSV	6 nM	8 nM to 1 μM, 1–20 μM	Plastic bottled drinking water, canned beverages	81
Poly(methacrylic acid)/graphene/carbon paste electrode	Chlordiazepoxide	SWV	2.61×10^{-10} M	6×10^{-10} to 7.5×10^{-8} M	Tablets, human serum, urine	82
Polypyrrole/graphene/carbon electrode	4-Nonylphenol	DPV	3.5×10^{-12} g mL^{-1}	1×10^{-11} to 1×10^{-8} g mL^{-1}	Rain water, lake water	83
Polypyrrole/NH_2–graphene/screen-printed electrode	Methcathinone, cathinone	DPV	3.3, 8.9 pg mL^{-1}	4.9×10^{-6} to 9.8×10^{-3}, 1.5×10^{-5} to 1.1×10^{-2} μg mL^{-1},	Practical serum samples	84
Poly(*o*-aminophenol)/N,S-activated graphene/glassy electrode	Cyclophosphamide	CV	3.4×10^{-12} M	8×10^{-12} to 8×10^{-7} M	Male rabbit blood plasma	85
Polyaniline/rGO/carbon paste electrode	Diclofenac	DPV	1.1 mg L^{-1}	5–80 mg L^{-1}	Injection, tablet, urine	86
Poly(pyrrole–COOH)/rGO/screen-printed electrode	Human cardiac troponin T	DPV	0.006 ng mL^{-1}	0.01–0.1 ng mL^{-1}	Blood serum	87
Poly(*N*-ABA)/GQDs/screen-printed carbon electrode	Ifosfamide	DPASV	0.08–0.11 ng mL^{-1}	0.25–121.35 ng mL^{-1}	Aqueous, blood plasma, urine, pharmaceutical	88
Polyaniline/CNTs/graphene/carbon electrode	BSA	DPV	6.2×10^{-11} g mL^{-1}	1×10^{-4} to 1×10^{-10} g mL^{-1}	Human serum	89
Polypyrrole/graphene/CNTs/carbon electrode	Tetrabromo bisphenol A	DPV	3.7×10^{-12} M	1×10^{-11} to 1×10^{-8} M	Catfish, chub, carp	90
Polyacrylamide/rGO–C_{60}/pencil graphite electrode	D-serine, L-serine	DPASV	0.24, 0.25 ng mL^{-1}	0.83–20.63, 0.87–20.45 ng mL^{-1}	Serum, cerebrospinal fluid, pharmaceutics	91
Poly(*o*-phenylenediamine)/CNTs/graphene/nickel foam	Dopamine	CV	6.67×10^{-16} M	2×10^{-15} to 1×10^{-12} M	—	92

[a] Abbreviation: multiwalled carbon nanotubes, MWCNTs; tetraethylene glycol-3-morpholine propionate acrylate, TEGMPA; reduced graphene oxide, rGO; *N*-acryloyl-4-aminobenzamide, *N*-ABA; graphene quantum dots, GQDs; carbon nanotubes, CNTs; lindane (γ-hexachlorocyclohexane), γ-HCCH; bovine serum albumin, BSA; differential pulse voltammetry, DPV; linear sweep voltammograms, LSV; differential pulse cathodic stripping voltammetry, DPCSV; square wave voltammetry, SWV; cyclic voltammetry, CV; differential pulse anodic stripping voltammetry, DPASV.

(Fig. 2a). The copolymerization of poly(*p*-ATP) and AuNPs on MWCNT-modified GCE can maximize the amount of effective imprinted sites and enhance conductivity.

Xia *et al.* fabricated a molecularly imprinted electrochemical sensor for bovine serum albumin (BSA) detection based on chitosan/IL–GR (CS/IL–GR)-modified GCE.[130] IL is suitable for use as a supporting electrolyte due to its high ionic conductivity and chemical stability. As compared to GR, the GR/IL composite has an improved electrocatalytic ability for electrochemical sensing. Chitosan (CS) has –OH and –NH– active groups and can serve as a matrix to immobilize protein molecules containing –COOH groups. To produce MIPs on the surface of CS/IL–GR/GCE, a polypyrrole was electropolymerized by using BSA as the template molecule (Fig. 2b). As typical GR-based CNMs, CS/IL–GR nanocomposites contain the hybridization of GR with CS and IL. Synergistic interactions among CS, IL, and GR in nanocomposites improve the electrochemical responses and detection sensitivity of this sensor. Most of the relevant studies mention two or more types of materials that can hybridize with CNMs during the preparation process of CNM-modified MIPs. The synergistic effects between CNMs and other materials during hybridization further improve the sensitivity and electrochemical responses of ECCSs for efficient target detection. Xu *et al.* prepared MoS_2/GR–CNTs nanocomposites *via* the hydrothermal method.[183] MoS_2/GR–CNTs combined the high catalysis of MoS_2 and superior electronic conductivity of GR–CNTs, yielding high electrochemical

Table 3 ECCSs based on carbon-nanotubes-modified MIPs[a]

Sensing materials	Targets	Modes	LOD	Detection ranges	Detected samples	Ref.
Polyacrylamide/AuNPs/MWCNTs/GCE	Isoniazid	LSSV	0.3×10^{-9} M, 5×10^{-8} M	1×10^{-9} to 1.4×10^{-8} M, 2×10^{-8}~1×10^{-7} M	Body fluid, pharmaceutics	93
Poly(aminothiophenol)/AuNPs/MWCNTs/GCE	Cholesterol	DPV	3.3×10^{-14} M	1×10^{-13}–1×10^{-9} M	—	94
Poly(2,2′-dithiodianiline)/AuNPs/MWCNTs/GCE	Valganciclovir	ASDPV	0.3 nM	1–500, 500–2000 nM	Tablet, human blood serum	95
Poly(*o*-phenylenediamine)/AuNPs/MWCNTs–COOH/GCE	Olaquindox	DPV	2.7 nM	10–200 nM	Pork, fish	96
Poly(methacrylic acid)/MWCNTs–COOH/AuNPs/Pt electrode	Ampicillin	DPV	1×10^{-9} M	1×10^{-8} to 5×10^{-6} M	Milk, animal feed, fresh egg	97
Poly(triaminotriazine)/AuNPs/MWCNTs–COOH/pencil graphite electrode	Norepinephrine, uric acid	DPASV	0.62, 0.43 ng mL^{-1}	2.98–40.69, 1.94–43.59 ng mL^{-1}	Aqueous, serum, urine, pharmaceutics	98
Poly(NAPD)/TiO_2 NPs/MWCNTs/pencil graphite electrode	L-Aspartic acid	DPASV	1.73–179 ng mL^{-1}	9.98–532.72 ng mL^{-1}	Serum, cerebrospinal fluid, pharmaceutics	99
Poly(itaconic acid)/Mn NPs/MWCNTs/pencil graphite electrode	PSA	SWSV, DPSV	0.25 pg L^{-1}, 3.04 pg L^{-1}	0.99–5.99 pg L^{-1}, 9.99 pg L^{-1} to 5.99 ng L^{-1}	Blood serum, urine, forensic samples	100
Poly(4-vinylpyridine)/IL@PtNPs/MWCNTs/GCE	Tartrazine	DPV	8 nM	0.03–5, 5–20 μM	Fanta, mirinda drink, orange powder	101
Polypyrrole/Fe@AuNPs/2AET–MWCNTs/*p*-aminothiophenol/GCE	Cefexime	SWV	2.2×10^{-11} M	1×10^{-10} to 1×10^{-8} M	Human plasma	102
Poly(methacrylic acid)/PMMA/Fe_3O_4/MWCNTs/ceramic electrode	Kanamycin	DPV	2.3×10^{-11} M	1×10^{-10} to 1×10^{-6} M	Chicken, pig liver, milk	103
Poly(*o*-aminophenol)/polypyrrole/MWCNTs–BiCoPc/GCE	Metolcarb	CV	7.88×10^{-9} M	1×10^{-8} to 0.6×10^{-6} M	Cucumber, cabbage	104
Poly(4-vinylpyridine-methacrylic acid)/GPTS-vinyl/MWCNTs/GCE	Bisphenol A	DPV	0.2×10^{-11} M	1×10^{-10} to 4×10^{-4} M	Baby feeding bottle	105
Polyarginine/sodium alginate–MWCNTs/GCE	Theophylline	DPV	3.2 nM	0.01–60 μM	Tablet, oral solution, human blood serum	106
Poly(3-aminophenylboronic acid)/MWCNTs/chitosan/GCE	Epinephrine	DPV	35 nM	0.2–800 μM	Human serum, injection	107
Polydopamine/glutaraldehyde/chitosan/MWCNTs/GCE	Chorionic gonadotropin	DPV	0.035 pg mL^{-1}	0.5 pg mL^{-1} to 250 ng mL^{-1}	Human serum	108
Polyacrylamide/glutaraldehyde/chitosan/MWCNTs/GCE	HIV-p24	DPV	0.083 pg cm^{-3}	1×10^{-4} to 2 ng cm^{-3}	Human serum	109
Poly(VOIm PF_6)/MWCNTs@polydopamine–SWCNTs–COOH/GCE	Vanillin	DPV	0.1 μM	0.2–10 μM	Biscuit, cake, milk tea	110
Imprinted SiO_2/sol–gel/MWCNTs/carbon paste electrode	Bisphenol A	DPV	4.4×10^{-9} M	4×10^{-9} to 1×10^{-7}, 5×10^{-7} to 5×10^{-5} M	Polycarbonate bottled drinking water	111
Imprinted SiO_2/polytyramine/sol–gel/MWCNTs/AuNPs/pencil graphite electrode	Ketamine	SWV	0.7 nM	1–50, 50–1000 nM	Drug-free urine, human plasma	112
Imprinted SiO_2 film/sol–gel/MWCNTs–chitosan/GCE	Quinoxaline-2-carboxylic acid	DPV	4.4×10^{-7} M	2×10^{-6} to 1×10^{-3} M	Pork samples	113

[a] Abbreviation: gold nanoparticles, AuNPs, multiwalled carbon nanotubes, MWCNTs; glassy carbon electrode, GCE; *N*-acryloyl-pyrrolidine-2,5-dione, NAPD; nanoparticles, NPs; 2-aminoethanethiol, 2AET; polymethyl methacrylate, PMMA; binuclear phthalocyanine cobalt(ii) sulfonate, BiCoPc; glycidoxypropyl trimethoxysilane, GPTS; 1-vinyl-3-octylimidazole hexafluoride phosphorus, VOIm PF6; single-walled carbon nanotubes, SWCNTs; human immunodeficiency virus, HIV; linear sweep stripping voltammetry, LSSV; differential pulse voltammetry, DPV; anodic stripping differential pulse voltammograms, ASDPV; differential pulse anodic stripping voltammetry, DPASV; differential pulse and square wave stripping voltammetry, DPSV/SWSV; square wave voltammetry, SWV; cyclic voltammetry, CV.

sensitivity toward luteolin. A MIP film was deposited through electropolymerization using the carbazole (Cz) monomer and luteolin template. The electrochemical sensor of MIP/MoS_2/GR–CNTs/GCE had high performance for luteolin detection.

2.3. ECCSs fabricated on work electrodes or other substrates

In the fabrication of ECCSs based on CNM-modified MIPs, various commercial work electrodes have frequently served as substrates to support CNM-modified MIPs. In addition, certain

Table 4 ECCSs based on graphene-modified MIPs[a]

Sensing materials	Targets	Modes	LOD	Detection ranges	Detected samples	Ref.
Polypyrrole/CdS–graphene/FTO	4-Aminophenol	PEC	2.3×10^{-8} M	5×10^{-8} to 3.5×10^{-6} M	Lake water	114
Polypyrrole/IL/graphene/GCE	Bovine hemoglobin	DPV	3.09×10^{-11} g L^{-1}	1×10^{-1} to 1×10^{-3} g L^{-1}	Bovine blood	115
Poly(methacrylic acid)/PDDA–graphene/GCE	4-Chlorophenol	DPV	0.3 μM	0.8–100 μM	Tap, lake water	116
Poly(methacrylic acid)/hemin–graphene/GCE	*p*-Aminophenol	DPV	0.06 μM	0.3–25 μM	Tap, lake water	117
Polypyrrole/graphene–AuNPs/GCE	Levofloxacin	DPV	0.53 μM	1–100 μM	Capsule samples	118
Poly(methacrylic acid)/graphene–AuNPs/GCE	Colchicine	DPV	4.8×10^{-9} M	1.2×10^{-8} to 1.2×10^{-6}, 1.2×10^{-6} to 1×10^{-4} M	Colchicine tablets, human serum	119
Polypyrrole/graphene–Prussian blue/GCE	Butylated hydroxytoluene	CV	0.02 ppb	0.02–1 ppb	—	120
Polypyrrole/graphene–Prussian blue/GCE	Butylated hydroxyanisole	CA	7.63×10^{-8} M	9×10^{-8} to 7×10^{-5} M	Potato chip	121
Poly(*o*-phenylenediamine)/HSO_3–graphene/Au electrode	Dopamine	CV	0.11 mg L^{-1}	0.5–7 mg L^{-1}	Human serum	122
Polypyrrole/graphene/benzenediazonium/carbon electrode	Tetrabromo bisphenol A	DPV	0.23 nM	0.5–4.5 nM	Rain, lake water	123
Poly(methacrylic acid)/graphene sheets/Congo red/GCE	Dopamine	LSV	20 μM	1×10^{-7} to 8.3×10^{-4} M	—	124
Poly(vinyl ferrocene)/cyclodextrin-graphene nanosheet/GCE	1-Naphthylamine	DPV	0.1 μM	0.3–100 μM	Lake water	125
Polypyrrole/β-cydodextrin/AuNPs/graphene/GCE	Quercetin	DPV	1×10^{-10} M	1×10^{-9} to 1×10^{-6} M	Compound tablets	126
AuNPs/over-oxidized polypyrrole/graphene/GCE	Dopamine	CV	0.1 μM	0.5–8 μM	Rabbit serum, rabbit urine	127
Polypyrrole/Co–Ni NPs/graphene/carbon electrode	Octylphenol	DPV	3.6×10^{-11} M	1×10^{-10} to 1×10^{-7} M	Plastic, metal bottle, food packaging bags	128
Poly(Zn-porphyrin)/chitosan/AuNPs/graphene/GCE	Methyl parathion	DPV	3.16×10^{-10} M	1×10^{-6} to 8×10^{-9} M	Apple samples	129
Polypyrrole/chitosan/IL/graphene/GCE	BSA	DPV	2×10^{-11} g L^{-1}	1×10^{-10} to 1×10^{-4} g L^{-1}	Bovine plasma	130
Poly(methacrylic acid)/IL–graphene/chitosan/GCE	6-Benzylamino purine	DPV	0.2 μM	0.5–50 μM	Bean sprout, potato, tomato, lake water	131
Poly(methacrylic acid)/SiO_2/IL/graphene/GCE	2,6-Diamino pyridine	CV	0.0275 mg kg^{-1}	0.05–35 mg kg^{-1}	Hair dyes, L'Oréal, HUYO, Zhanghua	132
Poly(*o*-phenylenediamine)/AuNPs/IL/graphene/GCE	Ractopamine	DPV	0.46 μg L^{-1}	10–5000 μg L^{-1}	Swine urine	133
Poly(*p*-aminothiophenol)/AuNPs/IL–graphene/GCE	4-Nonylphenol	DPV	0.01 ng mL^{-1}	50–500 ng mL^{-1}	Boxes, plastic bag, milk package bottle	134
Poly(*o*-aminophenol-resorcinol)/Au–Prussian blue/graphene/AuNPs/GCE	Tebuconazole	DPV	1.25×10^{-8} M	5×10^{-8} to 4×10^{-4} M	Cucumber, green vegetable, strawberry	135
Imprinted SiO_2/sol–gel/boronic acid-graphene/GCE	Glycoprotein	DPV	2×10^{-11} mg mL^{-1}	1×10^{-10}–1×10^{-4} mg mL^{-1}	Chicken, quail eggs	136
Poly(L-cysteine)/graphene/Ag@NH_2–MIL–125Ti/GCE	BSA	DPV	4.147×10^{-19} g mL^{-1}	1×10^{-18} to 1×10^{-12} g mL^{-1}	Liquid milk	137

Table 4 (*Contd.*)

Sensing materials	Targets	Modes	LOD	Detection ranges	Detected samples	Ref.
Poly(aminothiophenol)/AuNPs–bionic poly dopamine film/ dopamine@graphene/GCE	Cholesterol	DPV	3.3×10^{-19} M	1×10^{-18} to 1×10^{-13} M	Human serum	138
Poly(*p*-aminothiophenol)/graphene-IL-nano Au/chitosan- AuPt alloy NPs/GCE	Carbaryl	DPV	8 nM	0.03–6 μM	Cabbage, apple peel	139
Poly(6-mercaptonicotinic acid)–AuNPs/ graphene–AuNPs/chitosan–PtNPs/gold electrode	Erythromycin	CV	2.3×10^{-8} M	7×10^{-8} to 9×10^{-5} M	Milk, honey	140
Graphene–Au/BSA/anti-AFP@rApo–Cd, anti-CEA@rApo-Pb/polydopamine/ Fe_3O_4/magnetic electrode	AFP, CEA	SWV	0.3 pg mL^{-1}, 0.35 ng mL^{-1}	0.001–5 ng mL^{-1}	Human serum	141

[a] Abbreviation: F-doped SnO_2 conducting glass, FTO; ionic liquid, IL; glassy carbon electrode, GCE; poly(diallyldimethylammonium chloride), PDDA; gold nanoparticles, AuNPs, nanoparticles NPs; AuNPs-supported amino-functionalized Ti-benzenedicarboxylate porous metal–organic frameworks, Au/NH_2–MIL–125Ti; bovine serum albumin, BSA; alpha-fetoprotein, AFP; carcinoembryonic antigen, CEA; apoferritin-encoded metallic labels, rApo; photoelectrochemical, PEC; differential pulse voltammetry, DPV; cyclic voltammetry, CV; chronoamperometry, CA; linear sweep voltammograms, LSV; square wave voltammetry, SWV.

functionalized materials can serve as electrochemical sensing substrates to construct CNM-modified-MIP-based ECCSs, such as NF,[92,160] F-doped SnO_2 conducting glass (FTO),[114] GO,[142] Au film electrode,[145] Cu wire,[151] laser-induced GR electrode,[171] 3D GR electrode,[172] and indium tin oxide (ITO).[176] Jin *et al.* reported an electrochemical coreduction method to synthesize rGO and silver NPs (AgNPs) on the surface of NF.[160] After the *in situ* electropolymerization of polypyrrole in the presence of the gastrodin (GAS) template, MIP was prepared on rGO–AgNPs-modified NF. After modification with electroactive substances, NF exhibits abundant active sites on its surface and high electronic conductivity because of the presence of desirable porous and 3D nanostructures. The modified NF acts as an excellent electrode material for GAS sensing (Fig. 3a). Feng *et al.* designed a photoelectrochemical (PEC) sensor of triclosan.[176] A MIP layer of poly(*o*-phenylenediamine, *o*-PD) was electropolymerized on GR-like carbon nitride (g-C_3N_4) and AuNPs dual-modified ITO electrode (Fig. 3b). The MIP/g-C_3N_4–AuNPs/ITO sensor had highly sensitive and selective PEC response toward triclosan detection.

3. Preparation strategies of ECCSs based on CNM-modified MIPs

3.1. CNM-encapsulated or CNM-combined imprinting of silica and polymers

There are three major routes to achieve CNM-modified MIPs. Route I is to prepare CNM-encapsulated imprinting of silica (hard inorganic matrix). Route II is to prepare CNM-encapsulated imprinting of polymers (soft organic matrix). Route III is to prepare MIPs combined with CNMs. Silica as a promising inorganic material has high acid, thermostability, excellent permeability to templates, and biocompatibility. The classic Stöber method is often employed to synthesize silica NPs,[58,111] and it involves the hydrolysis of tetraethoxysilane (TEOS) under basic conditions. Luo *et al.* reported the one-pot synthesis of GO that was coated with molecularly imprinted sol–gel SiO_2 for the electrochemical sensing of paracetamol (PR).[58] A GO/MIP complex was synthesized by mixing GO with phenyltriethoxysilane (PTEOS), tetramethoxysilane (TMOS) monomers, and PR template, followed by sol–gel copolymerization and extraction (Fig. 4). By depositing a GO/SiO_2–MIP thin film on GCE, a molecular recognition element was constructed and used as an electrochemical sensor of PR. This work described a facile imprinting complex that combined the merits of surface molecular imprinting, CNMs, SiO_2, and sol–gel technology, which enabled the specific recognition and detection of PR.

Patra *et al.* developed an electrochemical sensor of the prostate-specific antigen (PSA) based on surface imprinting nanotechnology.[100] Through the decoration of MWCNTs with MnNPs and further functionalization with thiol groups, a nanoiniferter was prepared and served as the platform to synthesize 3D MIP matrixes for PSA based on a controlled radical polymerization technique. With regard to polymerization on a PGE surface, a prepolymer solution containing itaconic acid as the monomer, PSA as the template, and EGDMA as the cross-

Table 5 ECCSs based on graphene/carbon-derivatives-modified MIPs[a]

Sensing materials	Targets	Modes	LOD	Detection ranges	Detected samples	Ref.
Poly(methacrylic acid)/SiO_2/GO	Dopamine	DPV	3×10^{-8} M	5×10^{-8} to 1.6×10^{-4} M	HCl injections, urine	142
Poly(methacrylic acid)/IL–GO/GCE	Methyl parathion	DPV	6 nM	0.01–7 μM	Cabbage, apple peel	143
Polypyrrole/NiNPs/GO/carbon electrode	Tetrabromo bisphenol A	DPV	1.3×10^{-10} M	5×10^{-10} to 1×10^{-5} M	Tap, rain, lake water	144
Poly(3-aminophenylboronic acid)/Fe_3O_4@GO/Au film electrode	Interleukin-8	CV	0.04 pM	0.1–10 pM	Human saliva	145
Poly(*o*-phenylenediamine)/SiO_2/GO/GCE	2,4-Dinitrophenol	DPV	0.4 μM	1–150 μM	Tap water, artificial wastewater	146
EGDMA-vinyl/NH_2–SiO_2/GO/GCE	Bisphenol A	DPV	0.003 μM	0.006–0.1/0.2–20 μM	Milk, mineral water	147
Polyphenol/cubic AuNPs/2AET–GO/GCE	Tyrosine	DPV	1.5×10^{-10} M	1×10^{-9} to 2×10^{-8} M	Milk samples	148
Poly(methacrylic acid)/AuNPs/Fe_3O_4/GO/GCE	Dibutyl phthalate	DPV	8×10^{-10} M	2.5×10^{-9} to 5×10^{-6} M	Brand wine drinks	149
Poly(*o*-phenylenediamine)/polypyrrole/BiCoPc/GO/GCE	Quinoxaline-2-carboxylic acid	SWV	2.1 nM	1×10^{-8} to 1×10^{-4}, 1×10^{-4} to 5×10^{-4} M	Pork, chicken muscle	150
Polyvinyl acetate/MnO_2/GO/CuO/Cu wire	Glucose	CV	53 μM	0.5–4.4 mM	—	151
Polypyrrole/AuNPs/β-cydodextrin/Fe_3O_4/GO/GCE	Chrysoidine	DPV	1.7×10^{-8} M	5×10^{-8} to 5×10^{-6} M	Tap water	152
Poly(methacrylic acid)/AuNPs/β-cydodextrin–IL/Fe_3O_4/GO/GCE	Sunset yellow	DPV	2×10^{-9} M	5×10^{-9} to 2×10^{-6} M	Water, mirinda drink, minute maid	153
SiO_2@Ag/rhodamine B-labeled/DNA/poly(methacrylic acid)/AuNPs–GO/chitosan/GCE	BRCA-1	DPV	2.53 fM	10 fM to 100 nM	Clinical human serum	154
Poly(methacrylic acid)/Fe_3O_4@rGO/GCE	17β-Estradiol	DPV	0.819 nM	0.05–10 μM	Water environment	155
Poly(*o*-phenylenediamine)/AuNPs/rGO/GCE	D-Mannitol	DPV	7.7×10^{-13} M	1×10^{-12} to 2×10^{-11}, 2×10^{-11} to 3×10^{-10} M	Sugarcane vinasse samples	156
Poly(methacrylic acid)/rGO@Au/GCE	Carbofuran	DPV	2×10^{-8} M	5×10^{-8} to 2×10^{-5} M	Cabbage, cucumber	157
Poly(*o*-phenylenediamine)/poly(sodium 4-styrenesulfonate)–rGO/GCE	Daidzein	CV	0.5 nM	1–20 nM	Human serum, pueraria extraction	158
Poly(carboxymethyl-β-cydodextrin)/TiO_2/rGO/Pt electrode	Toltrazuril	DPV	0.21 μg L^{-1}	0.43–42.54 μg L^{-1}	Egg, chicken muscle	159
Polypyrrole/rGO–AuNPs/nickel foam	Gastrodin	DPV	1 nM	0.01–1 μM	Human serum	160
Poly(methacrylic acid, 4-vinylpyridine, 1 MA-3AI-Br)/rGO–IL/GCE	Sunset yellow	DPV	4 nM	0.01–1.4, 1.4–16 μM	Fruit juice, mirinda drink, orange juice	161
Polyaniline/Fe_3O_4/rGO/magnetic GCE	Amaranth	DPV	50 nM	0.05–0.5, 0.5–50 μM	Grapes, watermelon, peach flavor	162
Polyaniline@Fe_3O_4/rGO/magnetic GCE	Glutathione	DPV	3 nM	0.05–50 μM	Human whole blood	163
Poly(methacrylic acid)/AuNPs/Fe_3O_4@rGO/GCE	Ractopamine	DPV	0.02 nM	0.002–0.1 μM	—	164
Polyacrylamide/AgNPs–Fe_3O_4–rGO/screen-printed electrode	Quercetin	DPV	13 nM	20 nM to 250 μM	Medicinal tablets	165
Polyphenol/AgNPs/$H_3PW_{12}O_{40}$/rGO/GCE	*Tert*-Butyl hydroquinone	DPV	1.48×10^{-11} M	0.05–1.5 nM	Soybean, blend oil, beef tallow	166
Polypyrrole/PtNPs/polyoxometalate/rGO/GCE	Citrinin	DPV	2×10^{-13} M	1×10^{-12} to 1×10^{-10} M	Rye samples	167
Poly(*p*-aminothiophenol)/AuNPs/polyaniline/rGO/GCE	5-Hydroxy tryptamine	DPV	11.7 nM	0.2–10 μM	Human blood serum	168
Poly(2-mercaptonicotinic acid)/PtNPs/rGO–poly(sodium 4-styrenesulfonate)/PtNPs/GCE	17β-Estradiol	DPV	0.002 μM	0.004–0.06, 0.06–50 μM	Hand cream, facial cleanser	169
Poly(*o*-phenylenediamine)/gold networks@IL/porous PtNPs/COOH-rGO/GCE	Cefotaxime	DPV	1×10^{-10} M	3.9×10^{-9} to 8.9×10^{-6} M	Human serum, urine	170

Table 5 (*Contd.*)

Sensing materials	Targets	Modes	LOD	Detection ranges	Detected samples	Ref.
Poly(eriochrome black T)/PEDOT/laser-induced graphene electrode/polyimide	Chloramphenicol	EIS	0.62 nM	1 nM to 10 mM	—	171
Polypyrrole/$NiCo_2O_4$ nanoneedle arrays/3D graphene electrode	Sulfadimidine	DPV	0.169 ng mL^{-1}	0.2–1000 ng mL^{-1}	Commercial milk	172
Poly(*para*-aminobenzoic acid)/porous PdCu allow NPs/3D porous graphene/GCE	Melamine	DPV	2 nM	0.01–1 μM	Raw milk, milk powder	173
Poly(*o*-phenylenediamine-*co*-*o*-toluidine)/IL–N-doped graphene nanoribbons/GCE	4-Nonyl-phenol	LSV	8 nM	0.04–6 μM	Lake, river, tap water	174
Polyphenol/PtNPs/C_3N_4 nanotubes/GCE	Atrazine	SWV	1.5×10^{-13} M	1×10^{-12} to 1×10^{-10} M	Wastewater	175
Poly(*o*-phenylenediamine)/g–C_3N_4–AuNPs/indium tin oxide	Triclosan	PEC	6.01×10^{-13} M	2×10^{-12} to 8×10^{-10} M	Toothpastes	176
Poly(*p*-aminothiophenol)/AuNs/OMC/screen-printed electrode	Ractopamine	DPV	4.23×10^{-11} M	5×10^{-11} to 1×10^{-9} M	Swine urine	177
Poly(methacrylic acid)/N-carbon nanosheet Fe-frameworks/poly(vinyl pyrrolidone)/GCE	Mebendazole, catechol	DPV	0.004, 0.06 μM	0.01–1.5, 0.5–25 μM	Tap, river water	178
Poly(3,4-ethylenedioxythiophene)/AuNPs/graphene nanoribbons/GCE	Octylphenol	LSV	1 nM	0.02–8 μM	River, bottled mineral water, urine	71
Poly(*para*-aminobenzoic acid)/Prussian blue/CMK-3/GCE	Metolcarb	LSV	9.3×10^{-11} M	5×10^{-10} to 1×10^{-4} M	Cucumber, cabbage, apple juice	179
Poly(*p*-aminothiophenol)/AuNPs/chitosan–carbon dots/GCE	Patulin, 2-oxindole	DPV	7.57×10^{-13} M	1×10^{-12} to 1×10^{-9} M	Fresh apple juice	180
Polypyrrole/GQDs/hollow Ni nanospheres/GCE	Bisphenol S	DPV	0.03 μM	0.1–50 μM	Mineral water, plastic samples	181
Polypyrrole/ZnO@GQDs/pencil graphite electrode	6-Mercaptopurine	DPV	5.72 nM	0.01–50, 50–700 μM	Tablet, serum, urine	182

[a] Abbreviation graphene oxide, GO; ionic liquid, IL; glassy carbon electrode, GCE; nanoparticles, NPs; ethylene glycol dimethacrylate, EGDMA; gold nanoparticles, AuNPs; 2-aminoethanethiol, 2-AET; binuclear phthalocyanine cobalt(II) sulfonate, BiCoPc; reduced graphene oxide, rGO; 1-(α-methyl acrylate)-3-allylimidazolium bromide, 1 MA-3AI-Br; poly(3,4-ethylenedioxythiophene), PEDOT; three-dimensional, 3D; ordered mesoporous carbon material, CMK-3 or OMC; graphene quantum dots, GQDs; breast cancer susceptibility gene, BRCA-1; differential pulse voltammetry, DPV; cyclic voltammetry, CV; square wave voltammetry, SWV; electrochemical impedance spectroscopy, EIS; linear sweep voltammograms, LSV; photoelectrochemical, PEC.

linking agent was dropcasted on the tip of the nano-iniferter-modified PGE and heated at 50 °C for 2 h. The adduct-modified PGE suffered from the template extraction of PSA from the polymer matrix to yield MIP.

The combination of MIP with CNMs is a common route to obtain CNM-modified MIPs. Liang *et al.* designed an electrochemical sensor based on MIP/GO-modified GCE for 2,4-dichlorophenol (2,4-DCP) determination.[62] MIP was synthesized *via* precipitation polymerization using 2,4-DCP as the template, methacrylic acid (MAA) as the functional monomer, and EGDMA as the cross-linking agent in the presence of azodiisobutyronitrile (AIBN) initiator. GO was dropcasted on GCE and MIP was dropped on GO/GCE surface to prepare the MIP/GO/GCE sensing platform (Fig. 5a). Due to the high binding affinity and π–π interactions, MIP/GO/GCE yielded high recognition capability and electrochemical activity toward 2,4-DCP. Liu *et al.* reported a MIP sensor for dopamine (DA) detection based on CS dispersed with GR as the functional matrix and DA as the template molecule.[49] Through the co-electrodeposition of a polymer film on GCE and the potential elution of DA, CS-based MIP–GR/GCE was prepared and had high sensitivity, selectivity, and rapid responses to DA oxidation (Fig. 5b). As natural polymers, CS mixed with GR and DA form a functional matrix. GR–CS–DA composite was co-electrodeposited to generate a MIP film on GCE, aiming to construct a MIP electrochemical sensor for DA sensing.

3.2. Polymerization of MIP on CNM-modified substrates

Different strategies have discussed the preparation of CNM-modified-MIPs as ECCS decorated on various work electrodes or other substrates. Based on earlier studies, we have systematically summarized the major preparation strategies. Strategy I involves the polymerization of MIP on CNM-modified substrates. Strategy II involves the copolymerization of MIP and CNMs on substrates. Strategy III involves the dropcasting of MIPs on CNM-modified substrates. Strategy IV involves the dropcasting of a MIP/CNMs complex on substrates. Strategy V involves the self-assembly of MIP/CNMs/hybrids complex on substrates. Strategy VI involves the dropcasting of the self-

Table 6 ECCSs based on MIPs modified with multiple carbon nanomaterials[a]

Sensing materials	Targets	Modes	LOD	Detection ranges	Detected samples	Ref.
Polycarbazole/MoS_2/graphene–CNTs/GCE	Luteolin	LSV	9 nM	0.04–2 μM	Carrot, chrysanthemum tea	183
WS_2–poly(3,4-ethylenedioxythiophene)/GO–SWCNTs/GCE	Vitamin B_2	LSV	0.7 nM	0.002–0.9 μM	Vitamin B_2 tablets	184
Poly(methacrylic acid)/MWCNTs/graphite/paraffin/carbon paste electrode	Gallic acid	DPV	47 nM	0.12–380 μM	Apple, orange, green tea, pineapple juice	185
Poly(*p*-aminothiophenol-*co*-*p*-aminobenzoic acid)/3D graphene–CNTs–IL/GCE	Eugenol	LSV	1×10^{-7} M	5×10^{-7}~2×10^{-5} M	Curry powder, perfume, capsule	186
Poly(*p*-aminobenzoic acid)/3D PdNPs–porous graphene–CNTs/GCE	Quercetin	DPV	5 nM	0.01–0.5 μM	Pule'an tablet, red wine, honeysuckle juice	187
Silicon alkoxide/graphite powder/cholesteryl chitin carbonate/MWCNTs/ceramic carbon electrode	Cholesterol	LSV	1 nM	10–300 nM	—	188
Poly(*p*-aminothiophenol)/AuNPs/MWCNTs@rGO nanoribbons/GCE	*p*-Nonylphenol	CV, CSDPV	0.73 pM, 4.8 fM	1 pM–1 μM, 10 fM to 1 nM	Tap water, flesh fish, sewage water	189
Poly(C3VimBr)/AuNPs/CMK-3/3D porous graphene/GCE	Dimetridazole	DPV	5×10^{-10} M	2×10^{-9} to 2.5×10^{-7} M, 2.5×10^{-7} to 3×10^{-6} M	Milk, honey, porcine muscle	190
p(GMMA)/poly(4-vinylpyridine)/MWCNTs/graphene–IL/GCE	Brucine	DPV	2 nM	0.006–0.6, 0.6–5 μM	Gujinwan/yaotongning capsule, human serum	191
Poly(*o*-phenylenediamine-*o*-toluidine)/CNTs-AuNPs/boron-doped ordered mesoporous carbon/GCE	Bisphenol A	DPV	5 nM	0.01–10 μM	Milk samples	192
Poly(*o*-phenylenediamine)/PtAu NPs/CNTs–COOH/GO/GCE	Propyl gallate	CV	2.51×10^{-8} M	7×10^{-8} to 1×10^{-5} M	Vegetable oils	193
Polypyrrole/AuNPs/activated MWCNTs@GO nanoribbons/GCE	3-Nitrotyrosine	SWSV	50 nM	0.2–50 μM	Human serum, urine	194
Poly(allylamine-*co*-itaconic acid)/Si-GO-*g*-CMNC-ZnO particles/GCE	Cholesterol	CV, DPV	7.4 μM, 98.6 μM	5.18–25.9 μM, 0.6475–10.36 mM	Blood serum of normal person, a patient	195
Polypyrrole/MWCNTs–COOH/IL/AuNPs/GO/GCE	Vanillin	DPV	6.23×10^{-10} M	1×10^{-8} to 2.5×10^{-6} M	Tap water	196
Poly(*p*-aminobenzoic acid)/hyaluronic acid–MWCNTs/polypyrrole–graphene/GCE	Tryptamine	CV	7.4×10^{-8} M	9×10^{-8} to 7×10^{-5} M	Cheese, lactobacillus beverage	197

[a] Abbreviation: carbon nanotubes, CNTs; glassy carbon electrode, GCE; graphene oxide, GO; single-walled carbon nanotubes, SWCNTs; multiwalled carbon nanotubes, MWCNTs; three-dimensional, 3D; ionic liquid, IL; gold nanoparticles, AuNPs; reduced graphene oxide, rGO; 3-propyl-1-vinylimidazolium bromide, C3VimBr; ordered mesoporous carbon material, CMK-3; poly(glycerol monomethacrylate), p(GMMA); nanoparticles, NPs; silylated graphene oxide-grafted chemically modified nanocellulose, Si-GO-*g*-CMNC; linear sweep voltammograms, LSV; differential pulse voltammetry, DPV; cyclic voltammetry, CV; cathodic stripping different pulse voltammetry, CSDPV; square wave stripping voltammetry, SWSV.

assembled complex of MIP/CNMs/hybrids on substrates. In this section, we introduce some typical studies to summarize MIP polymerization on CNM-modified substrates (Strategy I). This strategy implies MIP preparation on the surface of CNM-modified substrates. The preparation strategies of MIPs focus on electropolymerization and *in situ* chemical polymerization.

Yola *et al.* prepared a platinum NPs/carbon nitride nanotubes (PtNPs/C_3N_4 NTs) complex through a hydrothermal reaction.[175] By a cyclic voltammetry (CV) scan, atrazine-imprinted polyphenol was electropolymerized on the complex-modified GCE to develop a MIP electrochemical sensor of atrazine. Chen *et al.* prepared electro-reduced GR (GP) that covalently modified the surface of the CE.[83] Polypyrrole was electrodeposited on a GP-modified CE to prepare an imprinted sensor of 4-nonylphenol (Fig. 6a). NH_2-terminated GO was covalently modified on a CE surface with diazonium salt reactions to improve the stability and reproducibility of this sensor. GP prepared by the electroreduction of GO enhanced the reactivity of 4-nonylphenol and sensitivity of this sensor. Yola *et al.* prepared 2-aminoethanethiol (2-AET)-functionalized GO (2-AETGO) *via* an amide coupling reaction; 2-AETGO was self-assembled with cubic AuNPs to generate a cAuNPs/2-AETGO mixture.[148] The mixture was dropped on the GCE surface to construct cAuNPs/2-AETGO-modified GCE, followed by the

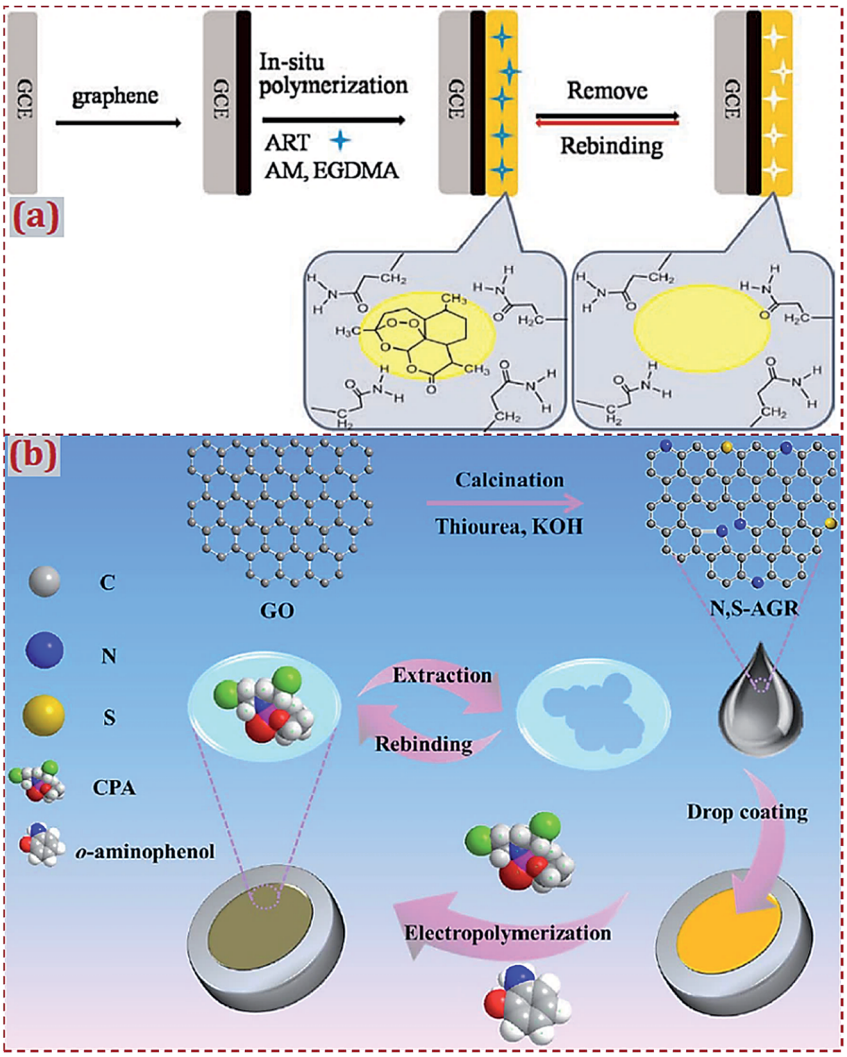

Fig. 1 (a) Detailed procedure diagrams for the fabrication of artemisinin-molecularly imprinted membranes/graphene-modified glassy carbon electrode (ART-MIM/G/GCE) sensor. Reproduced with permission from ref. 52. Copyright 2015, Elsevier. (b) Schematic representation for preparing molecularly imprinted polymer decorated on N,S-co-doped activated graphene on glassy electrode (MIP/N,S-AGR/GE). Reproduced with permission from ref. 85. Copyright 2017, Elsevier.

electropolymerization of polyphenol in the presence of tyrosine as the template (Fig. 6b). A tyrosine-imprinted electrochemical sensor of MIP/cAuNPs/2-AETGO/GCE facilitated the sensitive detection of tyrosine.

In earlier reports, the electropolymerization strategy is widely used to prepare MIPs on substrates that have already been modified with CNMs and CNM-based hybrids. GO was prepared from a graphite powder by the classic Hummers' method. GO often suffers from electroreduction to yield GR. GP has enhanced reactivity and sensitivity during the detection of targets.[54,64,68,83,118,123,128,144] Wang *et al.* synthesized a reduced GR–AuNPs nanocomposite *via* the one-step coreduction reaction of GO and $HAuCl_4$ as the precursors.[118] The GCE surface was drop-casted with GR–AuNPs suspension to generate GR–AuNPs/GCE, followed by the electropolymerization of polypyrrole on modified GCE under a CV scan. Prior to the electropolymerization of MIP-adduct,[61,64,73,87,106,107,113,118,122,137,148,152,167,173,175,178,187,193,196] the direct dropcasting of CNM-complex on the substrates was considered to be a typical strategy to obtain CNM-modified substrates. CNMs or CNM-based hybrids can be electrodeposited on substrates to form CNM-modified substrates.[46,68,156] Kan *et al.* developed an imprinted electrochemical sensor of DA.[46] After the electrodeposition of MWCNT–COOH on GCE, a MIP film was formed by the electropolymerization of polypyrrole in the presence of DA. Beluomini *et al.* designed an electrochemical sensor of D-mannitol based on MIP on GCE modified with AuNP-decorated rGO.[156] rGO was prepared by the electrodeposition of GO on GCE. AuNPs were deposited on the rGO/GCE surface by chronoamperometry. The electropolymerization of MIP was performed on AuNPs/rGO/GCE by a CV scan, using D-mannitol as the template and *o*-PD as the functional monomer.

Except for electropolymerization, MIP is prepared on CNM-modified substrates by *in situ* chemical polymerization.[79,99] Prasad *et al.* fabricated a MWCNT–ceramic electrode (CE)

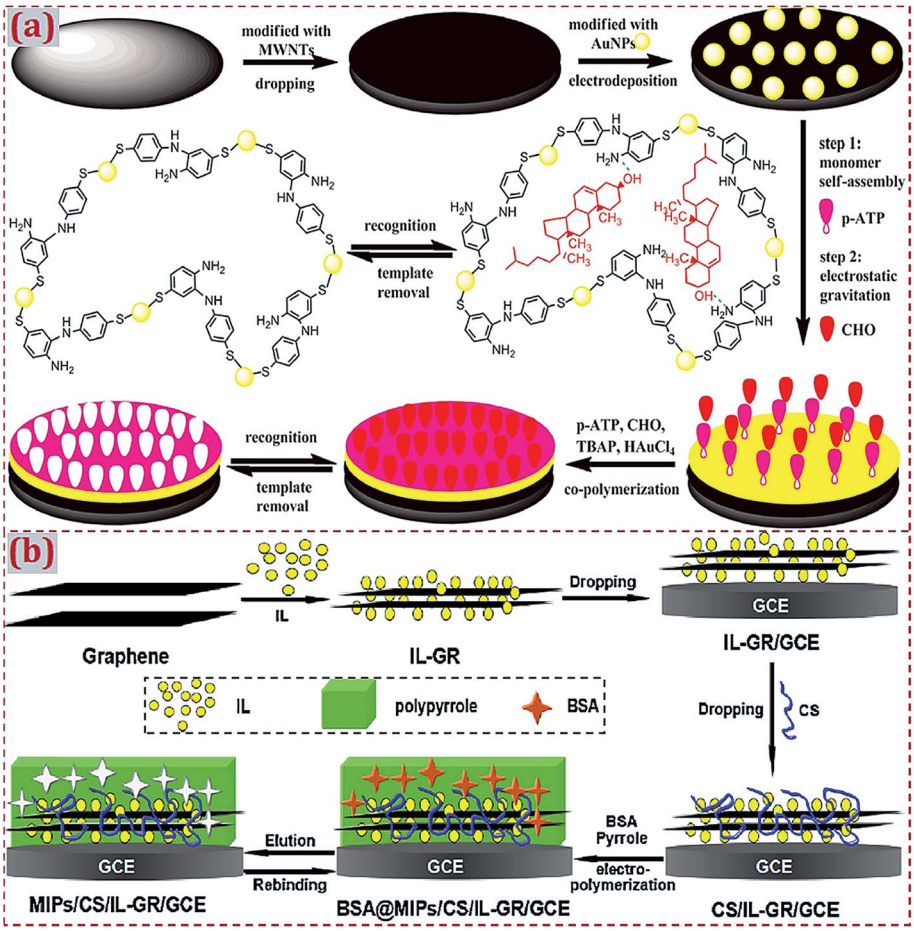

Fig. 2 (a) Preparation of a molecularly imprinted membrane based on a MIP film on AuNP-CNTs-modified GCE. Reproduced with permission from ref. 94. Copyright 2015, Elsevier. (b) Schematic diagram for the preparation procedures of a molecularly imprinted electrochemical sensor of BSA based on chitosan/ionic liquid–graphene (CS/IL–GR)-modified GCE. Reproduced with permission from ref. 130. Copyright 2016, Elsevier.

covered with a substrate-selective imprinted polymer for BSA determination.[79] MWCNTs were dispersed in a ceramic sol–gel matrix to improve the stability of CE. The MWCNT–CE surface is amenable to a "surface grafting" route for growing nanometer-thick MIP thin films. Vinyl-exposed MWCNT–CE was obtained by chemical reactions and physical treatments. This work reported a new way to realize a combination of CNMs with substrates in order to fabricate CNM-modified substrates, which is different from the dropcasting and electrodeposition of CNMs or CNM-based hybrids on substrates. To graft MIPs on vinyl-exposed MWCNT–CE, an *in situ* chemical polymerization reaction was performed in the prepolymer mixture containing BSA as the template, tetraethylene glycol 3-morpholin propionate acrylate (TEGMPA) as the functional monomer, diacryloyl urea (DAU) as the cross-linker, and ammonium persulfate (APS) as the initiator. MIP-modified MWCNT–CE as an electrochemical sensor enabled the ultra-trace detection of BSA.

3.3. Copolymerization of MIP and CNMs on substrates

CNMs or CNM-based hybrids are copolymerized with MIPs to generate a MIP/CNMs complex on substrates. This strategy avoids the modification of substrates with CNMs before the preparation of a MIP on CNM-modified substrates. Prasad *et al.* prepared a nanocomposite of functional GQDs and imprinted a polymer on a screen-printed carbon electrode (SPCE) by using *N*-acryloyl-4-aminobenzamide (*N*-ABA) as the monomer and the anticancer drug ifosfamide (IFO) as the template.[88] GQDs were functionalized to GQD–COCl, followed by covalent bonding with *N*-ABA to form *m*-GQDs. The authors used a surface grafting route for the coating of *m*-GQD–MIP on SPCE. The prepolymer mixture consisted of *m*-GQDs, IFO as the template, AIBN as the initiator, and EGDMA as the cross-linker. The mixture was spin-coated on the SPCE surface and free-radical polymerization on the SPCE surface was initiated to obtain the MIP-adduct@SPCE. The IFO template was retrieved from the MIP-adduct by stirring the modified SPCE in an ammonia solution to obtain *m*-GQD–MIP@SPCE (Fig. 7). The firm coating of *m*-GQDs can be attributed to the interactions of *m*-GQDs with the SPCE surface *via* the cumulative effects of physisorption and π–π interactions. The covalent binding of GQDs with the monomeric units of *N*-ABA helps to obtain an electrochemical sensing platform that has a large surface area for the fast ingress and egress of analytes.

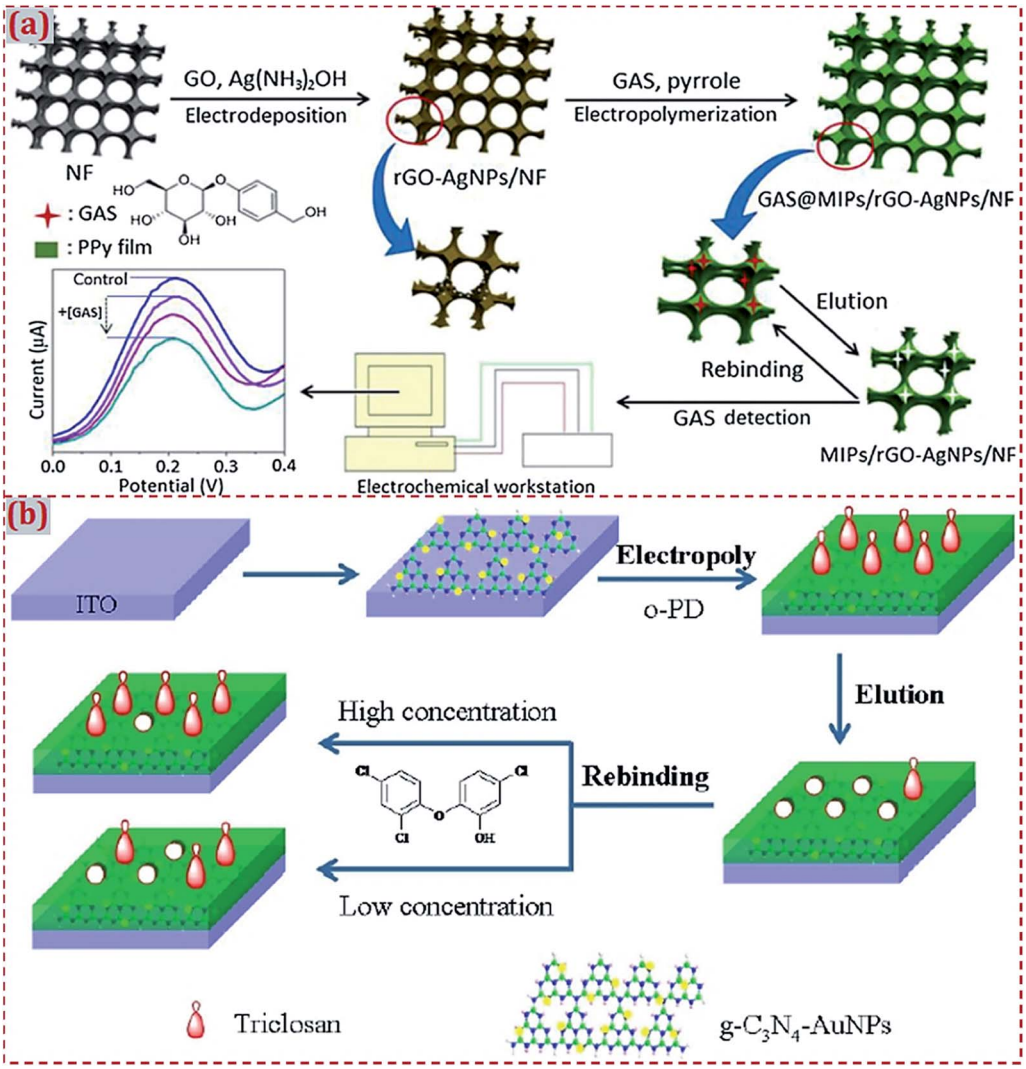

Fig. 3 (a) Schematic illustration of the preparation and application of MIP/rGO–AgNPs/NF sensing system. The control is MIP/rGO–AgNPs/NF without the addition of GAS. Reproduced with permission from ref. 160. Copyright 2018, Elsevier. (b) Schematic of the fabrication of a MIP photoelectrochemical sensor based on g–C_3N_4–AuNP-modified ITO electrode. Reproduced with permission from ref. 176. Copyright 2018, Wiley.

Hatamluyi *et al.* reported an electrochemical biosensor platform using MIP reinforced by ZnO–GR-capped QDs for 6-mercaptopurine (6-MP) detection.[182] ZnO@GQDs core–shell NPs were synthesized by the solvothermal method using GO and $Zn(CH_3COO)_2$ as the precursors. In a prepolymer solution containing ZnO@GQDs, pyrrole monomer, and 6-MP sol, the 6-MP-imprinted sol–gel film was electrodeposited on a PGE surface by performing CV runs. After template elimination by differential pulse voltammetry scanning, a polypyrrole/sol–gel/ZnO@GQDs/MIP/PGE sensor was obtained. The sensor integrated the features of the conducting polymer, sol–gel, and ZnO@GQDs core–shell QDs for the sensitive and selective sensing of 6-MP. As typical 0D CNMs, GQDs or CDs frequently hybridize with other CNMs and electroactive materials to form GQDs and CD-based hybrid materials. The use of hybrid materials to modify the substrates can facilitate the subsequent preparation of MIPs on the modified substrates.[70,73,74,88,180–182] With regard to CNM-modified MIPs as ECCSs involving 0D CNMs, GQDs or CDs with high conductivity improve the electron transfer rate, sensitivity, and electrochemical responses toward analytes. Lin *et al.* fabricated a MIP-based electrochemical sensor of L-3,4-dihydroxy phenylalanine (L-dopa).[48] A mixture was prepared by dispersing GR in a CS solution containing L-dopa. A pretreated GCE was immersed in the mixture solution, followed by electrodeposition under CV scans. This one-step electrodeposition method, namely, the copolymerization of MIP and CNMs on substrates, yielded an L-dopa-imprinted CS/GR/GCE sensing platform.

3.4. Dropcasting of MIPs on CNM-modified substrates

As a facile strategy to form CNM-modified-MIP-based ECCSs, Strategy III involves the dropcasting of already formed MIPs on substrates modified by CNMs or CNM-based complexes.[62,97,116,117,129,132,190,191] Liang *et al.* synthesized MIPs

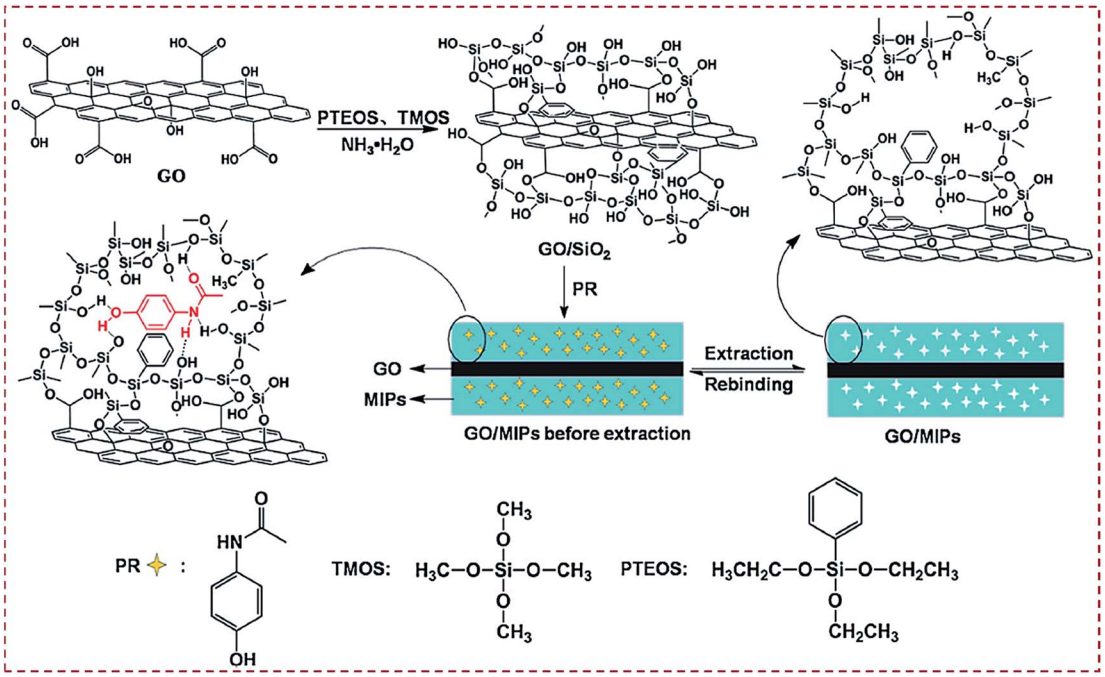

Fig. 4 Preparation routes for molecularly imprinted sol–gel polymer (GO/SiO_2 MIP) *via* a one-pot room-temperature polymerization reaction in an aqueous solution. Reproduced with permission from ref. 58. Copyright 2014, Springer.

via precipitation polymerization using 2,4-DCP as the template, MAA as the functional monomer, EGDMA as the cross-linker, and AIBN as the initiator.[62] GO-based GCE was made by dropping GO dispersion on GCE. MIP suspension was dropped on GO/GCE to formulate MIP/GO/GCE for 2,4-DCP detection (Fig. 5a). Wang *et al.* prepared MIP *via* bulk polymerization using 4-chlorophenol as the template, as well as MAA, EGDMA, and AIBN.[116] Poly(diallyldimethylammonium chloride)-functionalized GR (PDDA-G) was prepared through hydrazine hydride reduction. PDDA-G was used to modify GCE to obtain PDDA-G/GCE. MIP suspension was transferred to PDDA-G/GCE to fabricate MIP/PDDA-G/GCE for the electrochemical detection of 4-chlorophenol. Wei *et al.* prepared MIP, using ampicillin as the template, as well as MAA, EGDMA, and AIBN.[97] AuNPs were dropped on a Pt electrode. MWCNT–COOH was added on AuNP-modified electrodes, followed by the dropcasting of a MIP solution on AuNPs/MWCNTs-modified electrode to develop an ampicillin-imprinted sensor.

He *et al.* reported a biomimetic sensor based on Zn–porphyrin MIP microspheres (MIPM–Zn), AuNPs, and carboxyl-GR (CG).[129] MIPM–Zn was prepared *via* the precipitation polymerization of a prepolymer mixture containing methyl parathion as the template, as well as Zn–porphyrin, EGDMA, and AIBN. AuNPs/CG complex was prepared through the reduction of $HAuCl_4$ with $NaBH_4$. AuNPs/CG suspension was transferred on GCE. MIPM–Zn suspension was dropped on AuNPs/CG/GCE. MIPM–Zn/AuNPs/CG/GCE was constructed and acted as a porphyrin-imprinted electrochemical sensor of methyl parathion. Yang *et al.* reported the preparation of AuNPs@MIP on CKM-3 and 3D porous GR (P-rGO)-modified GCE.[190] IL was added into AuNPs solution to obtain AuNPs@IL *via* self-assembly. AuNPs@MIP was prepared by polymerization using AuNPs@IL as the monomer, dimetridazole as the template, as well as EGDMA and AIBN. P-rGO suspension was dropped on GCE, followed by the coating of CKM-3 suspension on P-rGO-modified GCE. AuNPs@MIP was then dropcasted to obtain AuNPs@MIP/CKM-3/P-rGO/GCE as a sensing platform for the electrochemical detection of dimetridazole. Zhao *et al.* synthesized IL-functionalized GR (GR–IL) dropcasted on GCE.[191] The authors reported the fabrication of surface-imprinted polymer-coated MWCNTs that were grafted with a water-compatible external layer (MWCNTs@GMIP) through reversible addition–fragmentation chain-transfer precipitation polymerization. MWCNTs@GMIP was dropped onto GR–IL/GCE to obtain MWCNTs@GMIP/GR–IL/GCE as an electrochemical sensor for the detection of brucine.

3.5. Dropcasting of MIP/CNMs complex on substrates

Earlier studies have widely involved the strategy of "the dropcasting of MIP/CNMs complex on substrates" to design ECCSs.[44,54,56,57,63,66,103,105,111,124,125,131,142,147,155,164,165,185,188] With regard to this strategy, MIP/CNMs complex, MIP/CNMs complex mixed with other materials, and MIP mixed with CNMs and other materials were dropcasted on the substrates to yield MIP/CNMs-complex-based hybrids-modified substrates. Yin *et al.* synthesized the MWCNTs@MIP–DA complex that was dropped on GCE to design a DA-imprinted film coated on GCE through self-assembly during solvent evaporation in air.[44] Li *et al.* dispersed the Fe_3O_4–MIP@rGO complex in water under sonication.[155] The solution was dropcasted on GCE and dried at room temperature. Kim *et al.* prepared GO/MIP aqueous suspension under ultrasonication.[63] The suspension was

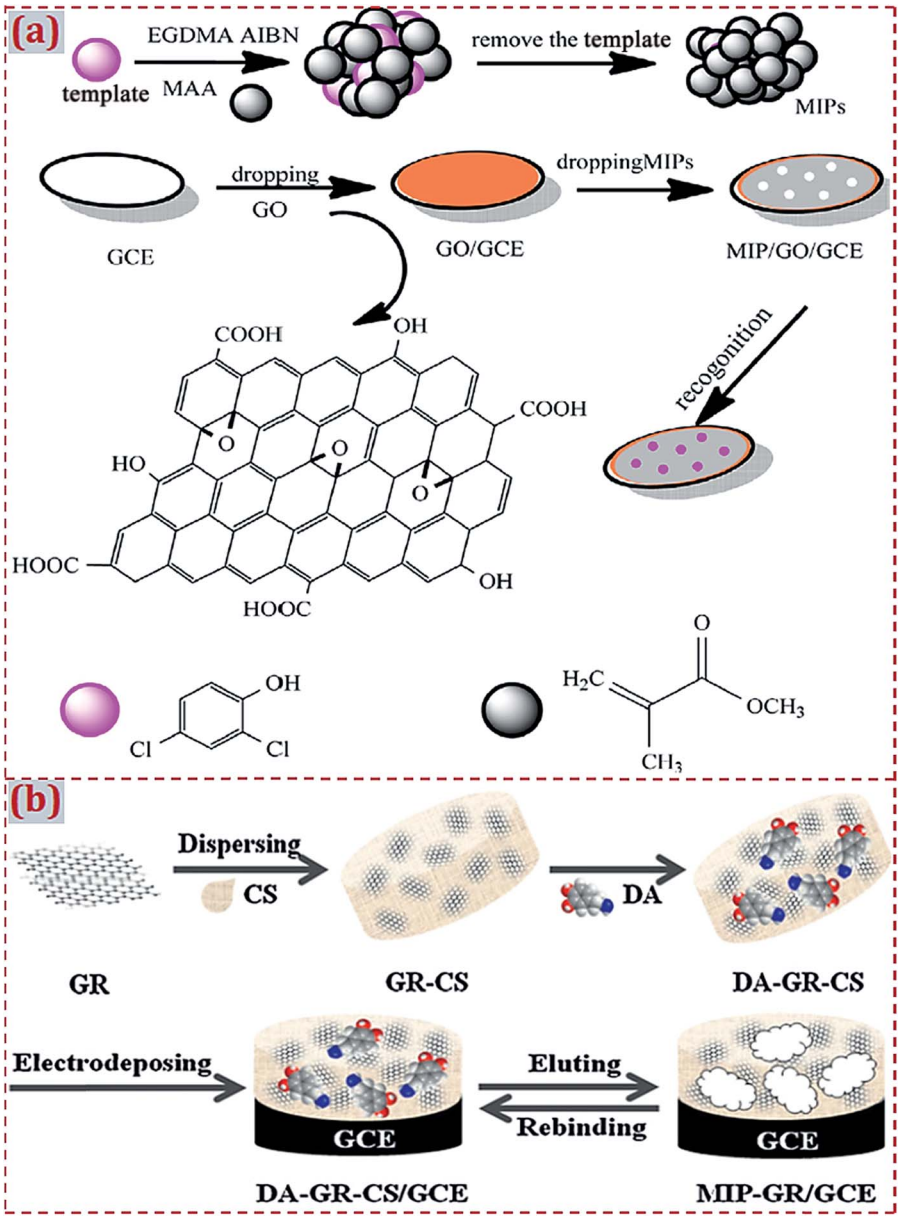

Fig. 5 (a) Schematic illustration for the synthesis procedures of GO/MIP and construction process of a modified electrode. Reproduced with permission from ref. 62. Copyright 2017, Elsevier. (b) Preparation of MIP–GR/GCE and its recognition for DA. Reproduced with permission from ref. 49. Copyright 2012, Elsevier.

transferred on GCE, followed by drying with an infrared lamp. Other studies have reported the dropcasting of MIP/CNMs complexes on substrates to fabricate ECCSs.[54]

Usually, the MIP/CNMs complex is ultrasonically mixed with an acetic acid solution containing CS or Nafion (as a coupling or adhesive agent).[103,105,124,125,131,142,147,165] The suspension is dropped on the surface of the substrates, followed by drying at room temperature in air or irradiation with an infrared lamp. In addition, a CS solution is dropped on MIP/CNMs-modified substrates for immobilization.[56,57] Long *et al.* developed an imprinted electrochemical sensor by using magnetic MIP (MMIP).[103] MMIP was prepared on MWCNT-decorated Fe_3O_4 NPs using kanamycin as the template and MAA as the monomer (Fig. 8a). CS was dissolved into an acetic acid solution under ultrasonication. MMIP was added to form a MMIP/CS mixture and the mixture was coated on a CE surface. A layer of the imprinted film was coated on the electrode to form a MMIP sensor of kanamycin. Zhu *et al.* prepared a composite of GR and MIP using IL as both the monomer and cross-linker for the electrochemical sensing of 6-benzylaminopurine.[131] IL–GR–MIP was dispersed in an acetic acid solution containing CS to form a suspension that was dropped on GCE (Fig. 8b). The solvent was evaporated under an infrared lamp.

Before the dropcasting of the already prepared MIP/CNMs complex on the electrode surface, the electrode is often polished with alumina slurry, followed by rinsing with a water–

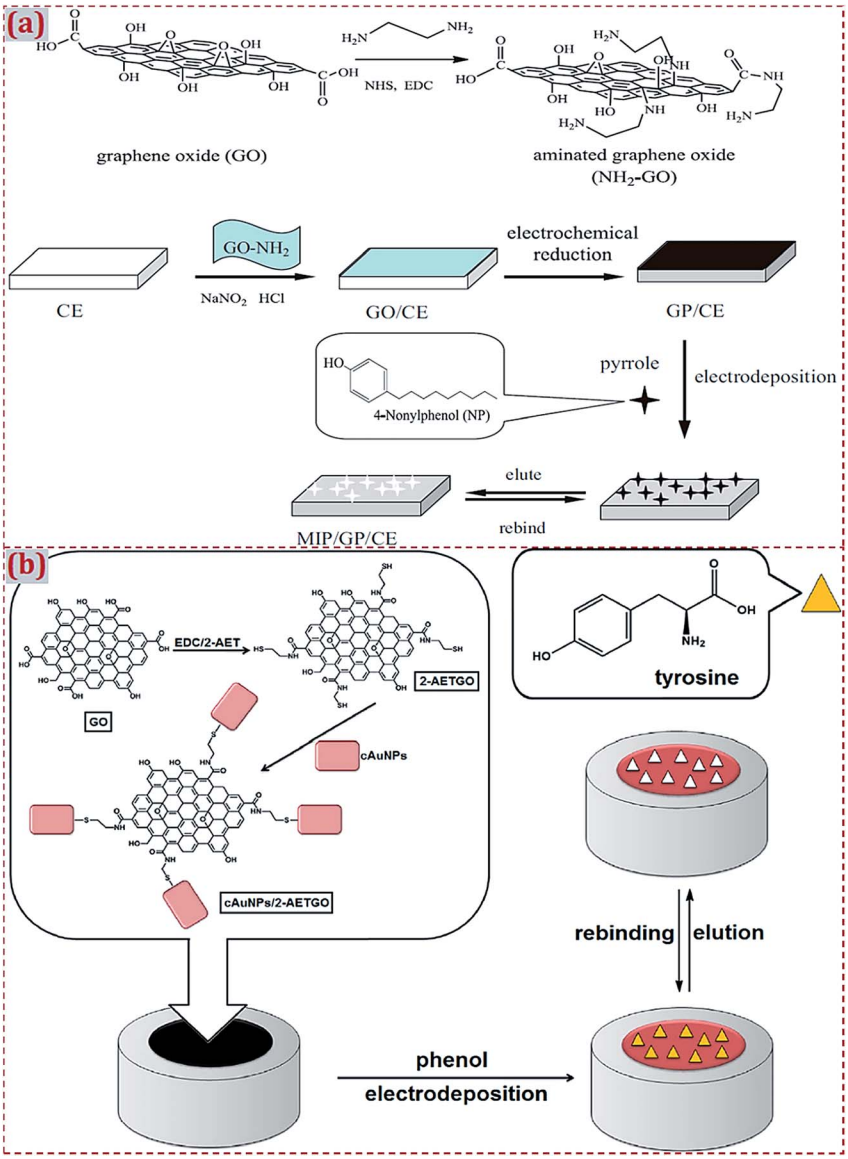

Fig. 6 (a) Detailed procedure diagrams for the fabrication of MIP/GP/CE sensor for 4-nonylphenol. Reproduced with permission from ref. 83. Copyright 2013, Elsevier. (b) Procedures for fabrication of MIP/cAuNPs/2-AETGO/GC sensor for tyrosine detection. Reproduced with permission from ref. 148. Copyright 2015, Elsevier.

ethanol mixture and ultrasonic treatments in nitric acid, NaOH, acetone, and deionized water. The pretreatments aim to achieve a clean and smooth surface on the electrode, which is propitious toward the surface modification of the electrode with other materials in subsequent experiments. Zeng *et al.* prepared a rGO–MIP composite by free-radical polymerization.[66] rGO–MIP was dispersed under ultrasonication in an acetic acid solution containing CS. The suspension was dropped on the pretreated GCE surface together with drying at room temperature (Fig. 9a). Zhang *et al.* employed *p*-vinylbenzoic acid (*p*-VBA) as a monomer to immobilize on GR *via* π–π interactions and the direct polymerization of a uniform MIP layer on the surfaces of GR sheets.[57] The GR/MIP composite was dropped on a well-polished GCE, followed by drying at room temperature. The acetic acid solution containing CS was dropped onto GR/MIP/GCE for the immobilization of GR/MIP on GCE followed by drying in air (Fig. 9b).

Different from dropcasting of the already fabricated MIP/CNMs complex, the mixture of MIP/CNMs and other materials can be poured on substrates to fabricate MIP/CNMs-complex-modified substrates under mechanical pressure. Tong *et al.* investigated an electrochemical cholesterol sensor on ceramic CE modified with the MWCNTs@MIP complex.[188] MWCNTs@MIP, graphite powder, and MIP were added in the solution containing ethyl trimethoxysilane (as a coupling agent), ethanol, and HCl. The mixture was pestled and was firmly packed into the electrode cavity of a Teflon sleeve, followed by drying at room temperature. Güney *et al.* fabricated a carbon paste electrode modified with bisphenol-A-imprinted polymer (BPA-IP), sol–gel, and MWCNTs by mixing BPA-IP,

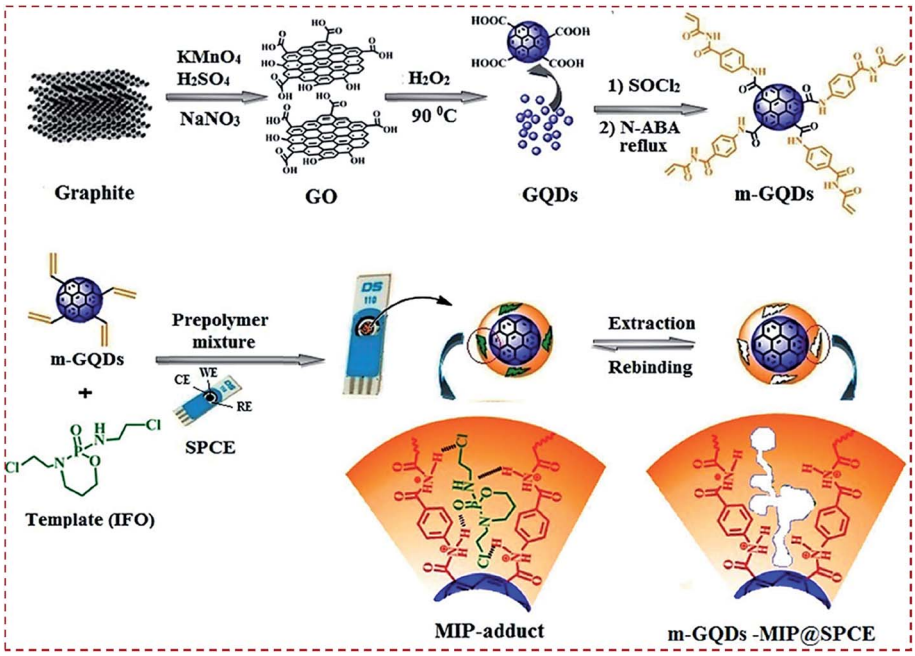

Fig. 7 (a) Schematic illustration for the preparation of monomeric graphene quantum dots (*m*-GQDs) and fabrication of screen-printed carbon electrode (SPCE) modified with *m*-GQD–MIP. Reproduced with permission from ref. 88. Copyright 2017, Elsevier.

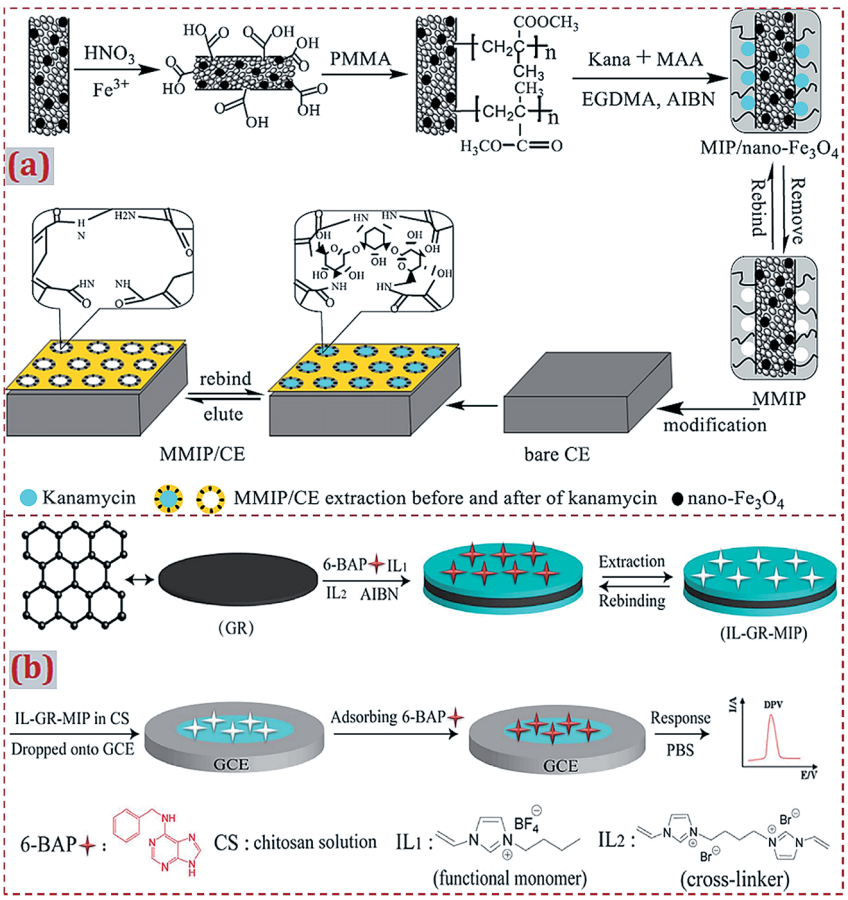

Fig. 8 (a) Schematic of the preparation process of magnetism imprinted electrochemical sensor based on MWCNTs decorated on Fe_3O_4 NPs. Reproduced with permission from ref. 103. Copyright 2015, Elsevier. (b) Schematic illustration for the synthesis of IL–GR–MIP composite dropped on GCE and the detection process for the electrochemical sensor. Reproduced with permission from ref. 131. Copyright 2018, Elsevier.

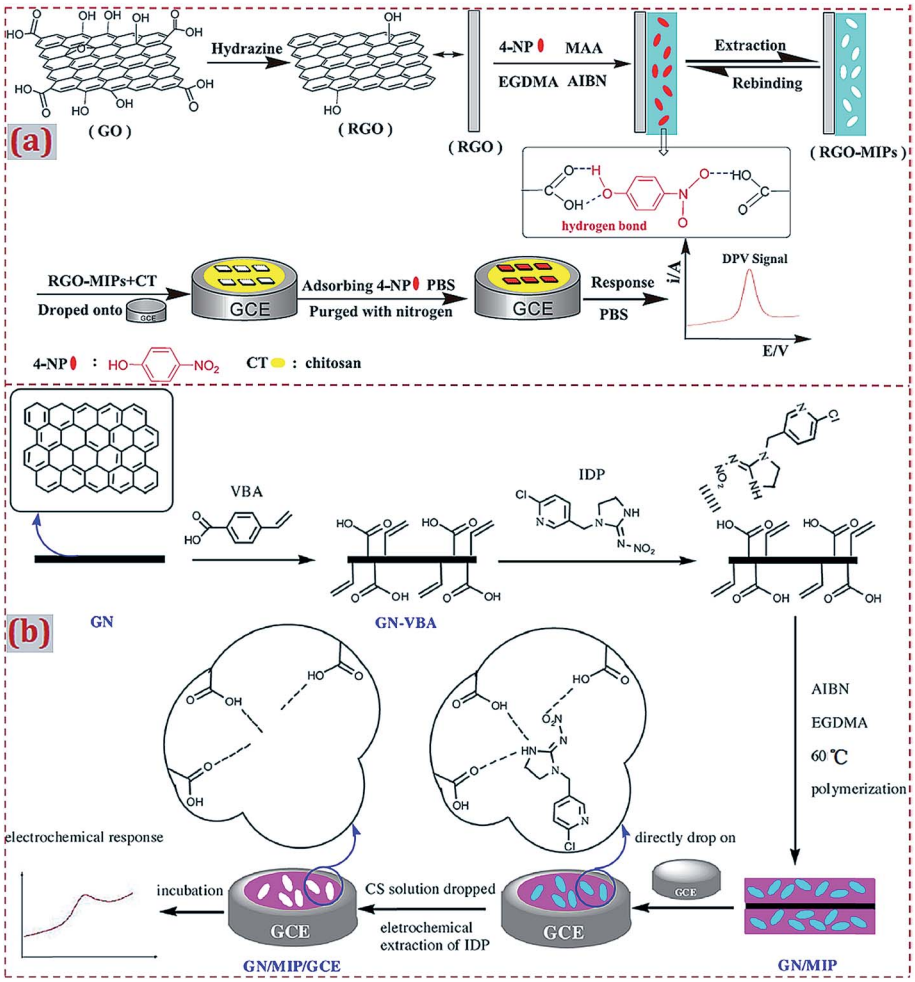

Fig. 9 (a) Illustration of the preparation procedures for rGO-MIPs and the detection process for the electrochemical sensor based on a composite of rGO and MIPs. Reproduced with permission from ref. 66. Copyright 2014, Elsevier. (b) Schematic procedures for the preparation of GN/MIPs/GCE and a concept for the selective electrochemical detection of imidacloprid. Reproduced with permission from ref. 57. Copyright 2017, Elsevier.

carbon-powder–MWCNTs mixture, and paraffin oil in a mortar until a homogeneous paste was formed.[111] The paste was pressed into a glass tube and an electrical contact was achieved by inserting a Cu wire into the glass tube. A new electrode surface was obtained by pushing an excess of the paste out of the glass tube and polishing it on fine smooth paper. Shojaei *et al.* constructed MIP–MWCNTs that were used to modify the carbon paste electrode.[185] Graphite powder was homogenized with MIP and MWCNTs. Paraffin was added to the MIP–MWCNT–graphite blend and mixed with a stainless steel spatula to obtain a homogenous paste. The paste was used to fill a hole at the end of electrode body. MIP–MWCNT–electrode was rinsed with a water–ethanol solution. An excess of the solidified material coming out of the hole was removed with a sheet of paper.

3.6. Self-assembly of MIP/CNMs/hybrids complex on substrates

To prepare CNM-modified-MIP-based ECCSs, earlier studies have reported the preparation of various types of MIPs through *in situ* chemical polymerization and electropolymerization strategies. The resulting MIP is often modified with CNMs, accompanied by hybridization with other materials, to form a MIP/CNMs/hybrids complex. The complex is frequently prepared on work electrodes or other substrates *via* layer-by-layer self-assembly.[75,93,96,108,109,127,128,133–135,138,177,180,181,192] Shen *et al.* reported an imprinted electrochemical sensor of human chorionic gonadotropin (hCG).[108] GCE was modified through a layer-by-layer coating of MWCNTs, CS, and glutaraldehyde. Further, hCG was covalently bonded on the modified GCE followed by the electropolymerization of DA. After template elution, a MIP film was formed on the complex-modified GCE. Guo *et al.* modified the GCE with CDs and CS, followed by the electropolymerization of AuNPs on CS/CDs/GCE, self-assembly of *p*-ATP monomer on AuNPs/CS/CDs/GCE, and H-bonding adsorption of 2-oxindole as a dummy template on *p*-ATP. The authors performed the copolymerization of *p*-ATP and 2-oxindole to generate a polymer film on AuNPs/CS/CDs/GCE and then removed the template to form MIP/AuNPs/CS/CDs/GCE for the electrochemical sensing of patulin.[180]

The layer-by-layer self-assembly for preparing MIP/CNMs/hybrids complex on work electrodes and other substrates was largely reported.[93,96,109,128,133–135,138,177,192] Wen *et al.* reported a sandwich-type MIP electrochemical sensor of 17β-estradiol (E2).[169] By using electrodeposition and cast-coating methods, PtNPs and rGO were fabricated on GCE. 6-Mercaptonicotinic acid (MNA) was self-assembled on the modified GCE with the formation of a Pt–S bond. E2 was assembled by forming a hydrogen bond with MNA. A polymer film was formed by the electropolymerization of MNA. Specific recognition cavities were formed after template removal. Nguyen *et al.* designed a sensitive GCE modified with GR, AuNPs, molecularly imprinted overoxidized polypyrrole for the detection of DA.[127] The authors prepared a GR film by the chemical vapor deposition method. The film was transferred to GCE by chemical etching. An imprinted polypyrrole was electropolymerized on GR/GCE. After template removal, the overoxidization of a MIP film (OPPy) was conducted by CV scans. AuNPs were electrodeposited on the OPPy surface to form AuNPs/OPPy/GR/GCE. The OPPy film exhibited better cation exchange and molecular sieve capability when compared with those of polypyrrole, further enhancing the selectivity and sensitivity for DA detection.

The substrates can be modified with CNMs using Nafion as a coupling or adhesive agent.[93] Moreover, the surface of the substrates can be electroactivated beforehand with functional molecules to facilitate the self-assembly of MIP/CNMs/hybrids complexes on electroactivated substrates. Yola *et al.* reported a MIP sensor of cefixime on GCE.[102] GCE combined with *p*-nitrophenyl *via* a chemical reaction under CV followed by the reduction of a nitro group to amine to prepare *p*-aminophenyl (AP)-modified GCE. COOH-functionalized f-MWCNTs were combined with 2-AET and AP *via* amide coupling. Fe@AuNPs and 2-AET combined with f-MWCNTs were self-assembled on GCE, followed by the electropolymerization of polypyrrole. NH_2-terminated benzene diazonium (NBD) was employed to modify the CE.[123,144] 4-Nitrobenzenediazonium tetrafluoroborate salt was electrodeposited on CE. The nitro group was electroreduced to amine by CV scans. The layer-by-layer self-assembly of CNMs, other materials, and MIP was conducted on NBD-functionalized CE. Chen *et al.* reported a sensor of 3,3′,5,5′-tetrabromo bisphenol A (TBBPA) on CE modified with NiNP–GR complex.[144] GO was covalently combined with NBD-modified CE. GO was electroreduced to GR. NiNPs were electrodeposited on GR/CE, followed by forming a MIP *via* electropolymerization (Fig. 10). Yang *et al.* designed an electrochemical sensor of chloramphenicol through the layer-by-layer self-assembly of MWCNTs@MIP, CKM-3, and P-rGO on GCE.[75] P-rGO was coated on GCE. CKM-3 was coated on P-rGO/GCE followed by the dropcasting of MWCNTs@MIP to fabricate MWCNTs@MIP/CKM-3/P-rGO/GCE.

The fabrication of the MIP/CNMs/hybrids self-assembled complex on substrates is often accompanied by functional and multiple polymerization steps. Xue *et al.* developed a double-layer membrane interface for 5-hydroxytryptamine (5-HT) detection.[168] A polyaniline-coated rGO composite was prepared by a one-step electrodeposition process on GCE. AuNPs@MIP was formed on the modified GCE *via* electropolymerization using 5-HT as the template, functionalized AuNPs as the functional monomer, and *p*-ATP as the cross-linker (Fig. 11a). Kong *et al.* designed a bilayer membrane that consisted of polypyrrole, functionalized MWCNTs, and

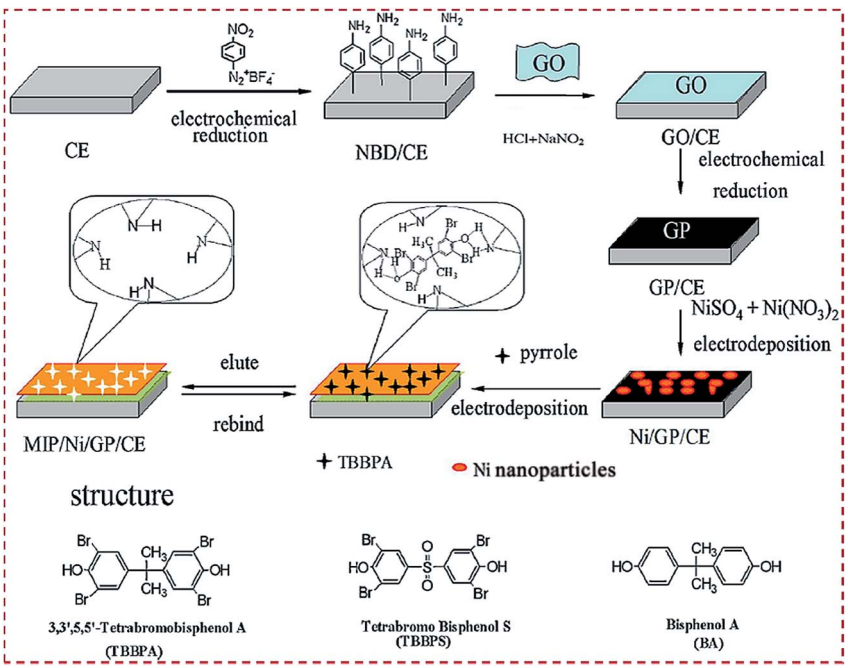

Fig. 10 Detailed procedure diagrams for fabricating a MIP/Ni/GP/CE sensor. The chemical structures of TBBPA, TBBPS, and BPA. Reproduced with permission from ref. 144. Copyright 2014, Elsevier.

binuclear phthalocyanine cobalt(II) sulfonate (BiCoPc) on GCE.[104] The polypyrrole–MWCNT–BiCoPc complex was one-step electrodeposited on GCE *via* chronoamperometry. A MIP membrane was produced on the complex-modified GCE *via* electropolymerization using *o*-aminophenol (*o*-AP) as the monomer and metolcarb (MTMC) as the template (Fig. 11b). Yang *et al.* prepared a bilayer of polypyrrole composite and MIP.[150] A polypyrrole–GO–BiCoPc composite was formed on GCE by CV scans, followed by the electropolymerization of MIP on the composite-modified GCE using *o*-PD as the functional monomer and quinoxaline-2-carboxylic acid as the template. Jaiswal *et al.* fabricated a layer-by-layer imprinted sensor.[91] A PGE was spin-coated with rGO-functionalized D-serine-imprinted polyacrylamide (PAA). The electrode was further modified with fullerene (0D C_{60})-functionalized L-serine-imprinted PAA. This bilayer assembly enabled the enantioselective analyses of D- and L-serine.

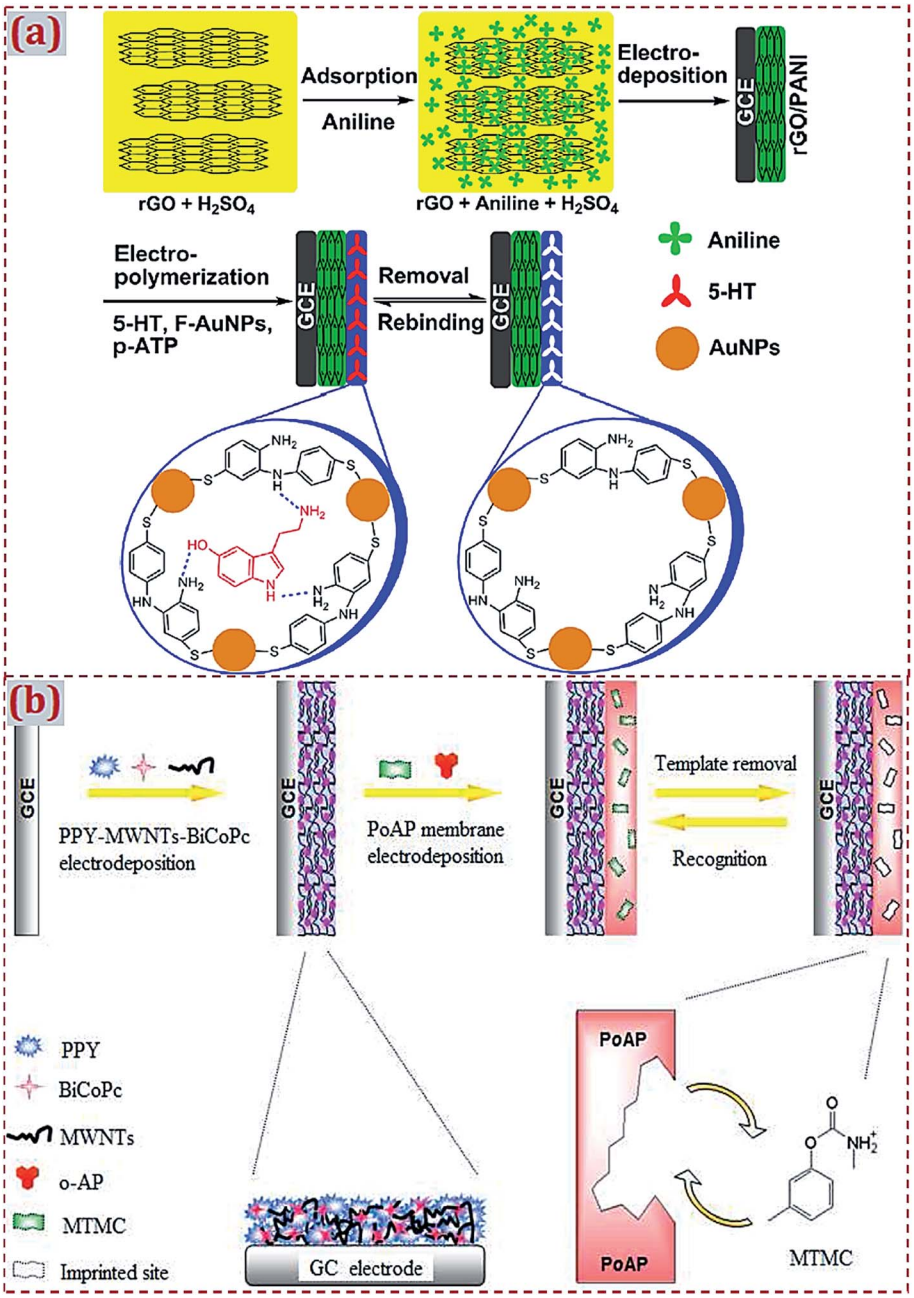

Fig. 11 (a) Schematic representation for the preparation of AuNPs@molecularly imprinted electrochemical sensor (MIES) based on a double-layered membrane of rGO/polyaniline nanocomposites and MIPs embedded with AuNPs. Reproduced with permission from ref. 168. Copyright 2014, Elsevier. (b) Preparation procedures for imprinted PPY–MWCNT–BiCoPc–GCE based on composites consisting of polypyrrole (PPY), functionalized MWCNTs, and binuclear phthalocyanine cobalt(II) sulfonate (BiCoPc) on a GCE surface. Reproduced with permission from ref. 104. Copyright 2015, the Royal Society of Chemistry.

3.7. Dropcasting of self-assembled complex of MIP/CNMs/hybrids on substrates

As an alternative strategy to fabricate CNM-modified-MIP-based ECCSs, a facile and effective strategy is the dropcasting of already prepared self-assembled MIP/CNMs/hybrids complexes on substrates. Li *et al.* developed an electrochemical sensor of dibutyl phthalate (DBP).[149] A complex of AuNPs and GO decorated with Fe_3O_4 NPs (MGO) was synthesized by coprecipitation and self-assembly. DBP, as the template, was absorbed on the complex and then the copolymerization of MAA and EGDMA was conducted. After template extraction *via* potential scans, MIP/MGO@AuNPs complex was prepared and dispersed under ultrasonication in an acetic acid solution containing CS. The suspension was dropped on Au electrodes to generate MIP/MGO@AuNPs/Au-sensing platform. Li *et al.* reported an imprinted sensor of Sunset Yellow (SY).[153] MGO was prepared by the coprecipitation of iron ions with an ammonia solution. Fe_3O_4 NPs were decorated on GO. MGO and β-cyclodextrin (β-CD) were self-assembled in an ammonia and hydrazine solution. With the addition of ILs, the MGO/β-CD/IL complex was formed under sonication. AuNPs were mixed with MGO/β-CD/IL followed by the *in situ* precipitation polymerization using MAA as the monomer, SY as the template, EGDMA as the cross-linker, and AIBN as the initiator. The products were washed with methanol–acetic acid solution to yield the MIP/AuNPs/MGO/β-CD/IL complex. The complex was dispersed under sonication in an acetic acid solution containing CS and was dropped on GCE. After solvent evaporation under an infrared lamp, the self-assembled complex-modified GCE was obtained.

Magnetic-field-directed self-assembly is an effective strategy to implement the dropcasting of MIP/CNMs/hybrids complex on substrates. Han *et al.* prepared the Fe_3O_4@rGO-complex-doped MIP membrane for amaranth detection.[162] The Fe_3O_4@rGO composite was obtained by the initial intercalating of iron ions between the GO layers *via* electrostatic interactions followed by reduction with hydrazine hydrate to deposit Fe_3O_4 NPs on rGO nanosheets. The mixture, containing aniline as the monomer, amaranth as the template, and Fe_3O_4@rGO, was preassembled through π–π stacking and hydrogen bonding interactions and was then self-assembled on magnetic GCE with magnetic field induction before electropolymerization (Fig. 12a). Tang *et al.* fabricated a sensor for interleukin-8 (IL-8) detection.[145] IL-8 surface MIP NPs were synthesized by using GO-modified Fe_3O_4 NPs as the core and IL-8-imprinted polymer as the shell. Fe_3O_4@GO@MIP NPs were self-assembled on Au film electrodes under a magnetic field, which realized the direct dropcasting of self-assembled MIP/CNMs-complex-based materials on the Au film electrode to form ECCSs (Fig. 12b). Zhu *et al.* reported the one-step fabrication of MIP membranes by magnetic-field-directed self-assembly for glutathione sensing.[163] Ternary Fe_3O_4@polyaniline/rGO was prepared by the chemical oxidative polymerization and intercalation of Fe_3O_4@polyaniline into GO layers *via* π–π stacking interactions, followed by the reduction of GO with hydrazine hydrate. The prepolymer mixture, containing glutathione as the template, ternary composite as the monomer, and pyrrole as the cross-linker and comonomer, was assembled *via* N–H hydrogen bonds and electrostatic interactions and was rapidly oriented on magnetic GCE under magnetic field induction. By electropolymerization and template reveal, the self-assembled MIP/Fe_3O_4@polyaniline/rGO–complex-modified magnetic GCE was achieved.

3.8. *In situ* chemical polymerization of functional monomers

The *in situ* chemical polymerization of functional monomers is a classic strategy for the synthesis of MIPs, which is often used to synthesize MIPs used in CNM-modified-MIP-based ECCSs. The prepolymer mixture principally contains monomers, templates, cross-linkers, initiators, catalysts, solvents, and other auxiliary substances. There are noncovalent and covalent interactions among the monomers, templates, and cross-linkers. Driven by initiators, catalysts, and auxiliary substances, the highly cross-linked polymers are prepared and formed as MIP-adduct. The polymerization process is usually undertaken as hydrothermal, solvothermal, or room-temperature reactions. To generate molecular recognition cavities in the MIP-adduct, template molecules need to be removed by rinsing with water or other solvents. MIPs with molecular cavities are obtained by template removal. The cavities are complementary to analytes and have specific shapes, sizes, structures, and functional groups, which are similar to those for template molecules.

With regard to CNM-modified-MIP-based ECCSs (Tables 1–6), the *in situ* chemical polymerization of functional monomers has been popular to prepare MIPs in earlier studies.[52,57,62,66,79,100,103,161] The frequently used functional monomers include AM and MAA. The cross-linkers majorly involve EGDMA and *N*,*N*-methylene-bisacrylamide (MBA). AIBN and APS are popular initiators. Zhao *et al.* reported SY-imprinted IL polymers and IL-functionalized rGO complex films coated on GCE.[161] Water-compatible MIPs were prepared by free-radical polymerization in a water–methanol system using SY as the template and 1-(α-methylacrylate)-3-allylimidazolium bromide (1-MA-3AI-Br) IL as the monomer. The IL interacted with SY through π–π stacking, hydrogen bonding, and electrostatic interactions. MIPs were prepared by a noncovalent method. In the mixture containing SY, IL, AIBN, EGDMA, and methanol–water as the solvents, prepolymerization was performed at room temperature followed by the hydrothermal treatment of the mixture to trigger polymerization. The product was washed with methanol–ammonia, followed by centrifugation collection. IL–rGO suspension was dropcasted on GCE. Solvents were evaporated under an infrared lamp. MIP suspension was dropped on IL–rGO/GCE and was evaporated in air. MIP–IL–rGO/GCE was used as a sensor for the detection of SY.

Anirudhan *et al.* reported the *in situ* chemical copolymerization of dual-functional monomers to prepare MIPs.[105] In the prepolymerization mixture comprising bisphenol A (BPA) as the template, MAA and vinylpyridine as the co-functional monomers, EGDMA as the cross-linker, and AIBN as the initiator, the polymerization reaction was performed at 70 °C for 16 h. The product was centrifuged and then washed with ethanol to remove the unreacted reagents. The BPA templates were

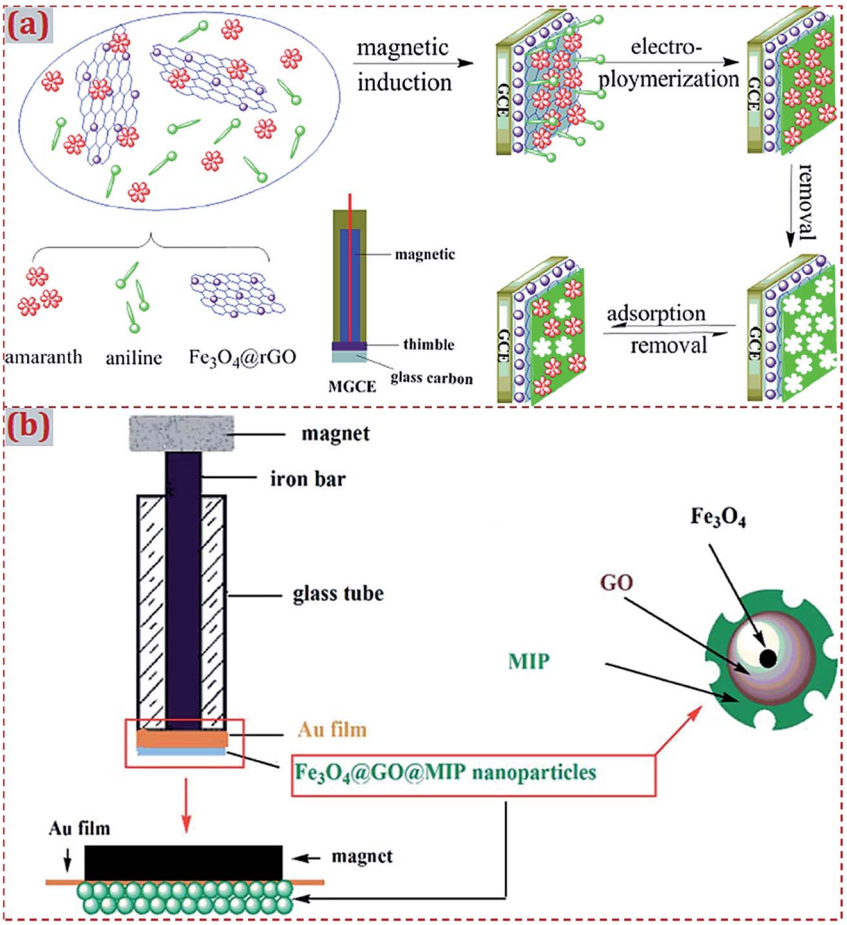

Fig. 12 (a) Schematic representation for the preparation of magnetic molecularly imprinted electrochemical sensor (MIES) based on magnetic GCE modified with MIPs@Fe_3O_4@rGO. Reproduced with permission from ref. 162. Copyright 2014, Elsevier. (b) Schematic representation for preparing a work electrode: full view of Fe_3O_4@GO@MIP-nanoparticle-modified electrode; partially enlarged drawing of the electrode surface; schematic presentation of the nanoparticles. Reproduced with permission from ref. 145. Copyright 2015, the Royal Society of Chemistry.

removed by Soxhlet extraction with methanol and acetic acid. BPA-imprinted MIPs were obtained on the surface of glycidoxypropyl-trimethoxysilane-functionalized MWCNT–CH=CH_2. MIP/MWCNTs composite was mixed with acetic acid and CS solution. The mixture was dropped on bare GCE to form MIP/MWCNTs/GCE for the electrochemical sensing of BPA (Fig. 13). Anirudhan *et al.* prepared silylated GO-grafted chemically modified nanocellulose (Si-GO-*g*-CMNC) for the electrochemical sensing of cholesterol.[195] CMNC was modified by grafting allyl amine on ZnO NCs, followed by the polymerization of itaconic acid to generate –COOH. Si–GO was polymerized with the prepolymerization mixture using MBA as the cross-linker and AIBN as the free-radical initiator in a polymeric chain reaction. Si-GO-*g*-CMNC was dispersed under ultrasonication in acetic acid–CS solution, followed by dropping on GCE and solvent evaporation at 50 °C.

3.9. Electrochemical polymerization of electroactive functional monomers

As a facile strategy to prepare MIPs, electropolymerization is popularly applied in the preparation of MIPs to fabricate CNM-modified-MIP-based ECCSs.[44,45,67,72,78,85,88,93,94,102,104,114,130,138,144,152,160,168,169,172–174,176,179,181,183,186] The electropolymerization of MIP requires the presynthesis of a polymer solution containing template molecules, functional monomers, solvents, electrolyte solution, *etc.* In contrast to *in situ* chemical polymerization, electropolymerization can avoid the use of cross-linkers, initiators, or catalysts during the preparation of MIPs, thereby simplifying the experimental procedures. The electropolymerization of MIPs involves CV scan cycles in a polymer solution together with the potential sweeping within proper scan ranges and rates.

Wen *et al.* developed the one-step fabrication of poly(*o*-AP)/MWCNTs-film-modified electrode for the detection of levofloxacin.[45] Under sonication, a mixture containing *o*-AP, MWCNTs, sodium dodecyl sulfate (SDS), and H_2SO_4 was prepared. GCE was dipped in this mixture solution. By potential scanning in the range of −0.20 to 0.84 V at 0.1 V s^{-1} for 10 cycles, poly(*o*-AP)/MWCNTs/GCE was constructed. SDS increases the conductivity of poly(*o*-AP) and *o*-AP can be easily oxidized to form more monocation radicals on GCE. At the first cycle, a distinct irreversible anodic peak was found at

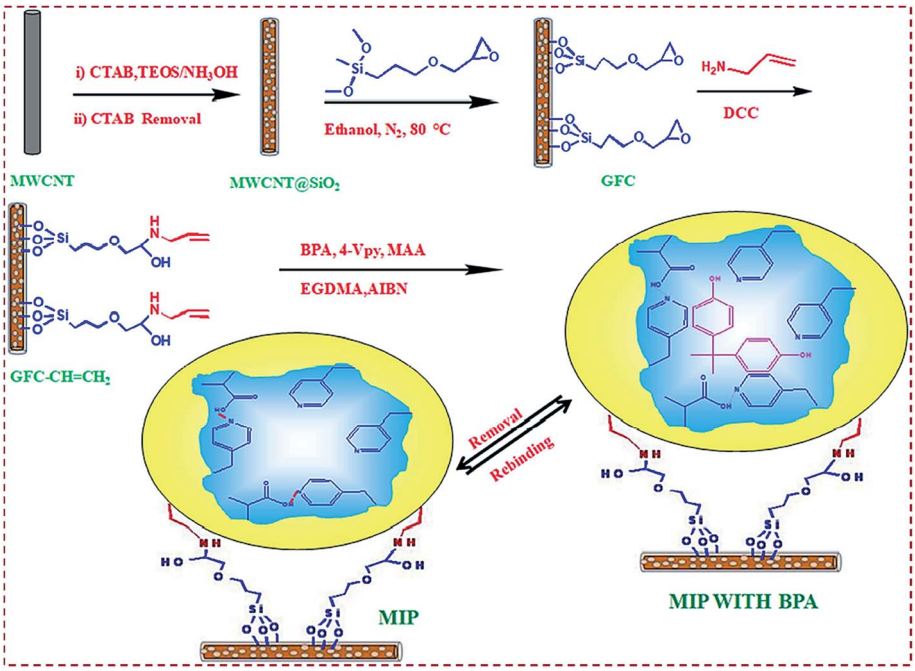

Fig. 13 Schematic illustration of MIP/MWCNTs/GCE for the electrochemical sensing of BPA. Reproduced with permission from ref. 105. Copyright 2018, Elsevier.

0.71 V. Therefore, *o*-AP was irreversibly oxidized at the electrode surface. Two pairs of redox peaks appeared. Redox and redox pairs were respectively ascribed to the redox process of phenoxazine units and intermediate generation in the oxidation process of *o*-AP. Yin *et al.* reported MIP–polydopamine (PDA)-coated MWCNTs for the detection of SY.[44] SY was mixed with DA to induce molecular self-assembly through intermolecular forces, such as hydrogen bonding, π–π, and electrostatic interactions. DPA was formed by the *in situ* spontaneous oxidative polymerization of DA in an alkaline solution and at room temperature. DA adhered on MWCNTs to produce a DPA film. The SY template was embedded in a DPA film through intermolecular forces. After template removal, SY-imprinted MWCNTs@MIP–DPA was obtained and dropped on GCE to fabricate an electrochemical sensor of SY.

In particular, different functional monomers with electroactivity can simultaneously participate in the preparation process of MIPs[174,186,192] with the features of highly cross-linking copolymers. Hu *et al.* explored a BPA sensor based on MIP/CNT–AuNPs/boron-doped ordered CKM-3-composite-modified GCE.[192] MIP was prepared by cycling the potential of 0–0.65 V at 50 mV s^{-1} in an acetate buffer solution using *o*-phenylenediamine (*o*-PD) and *o*-toluidine (*o*-TD) as the co-functional monomers and BPA as the template. Yang *et al.* reported a sensor of eugenol using 3D molecularly imprinted poly(*p*-aminothiophenol-*co*-*p*-aminobenzoic acid), namely, poly(*p*-ATP-*co*-*p*-ABA)-film-modified GCE.[186] The sensor was composed of MIP and IL-functionalized GR–CNTs composite prepared by a one-step hydrothermal method. Porous molecularly imprinted copolymers were prepared on GR–CNT–IL/GCE by CV scans (Fig. 14a). Pan *et al.* presented a sensor of 4-nonyl-phenol (NP) based on molecularly imprinted poly(*o*-phenylenediamine-*co*-*o*-toluidine), *i.e.*, poly(*o*-PD-*co*-*o*-TD)-N-doped GR nanoribbons (NGRRs)–IL film.[174] NGRRs were prepared by unzipping MWCNTs, followed by hydrothermal treatment with ammonium–NaOH solution. MIP was prepared by electropolymerization on NGRR–IL-modified GCE using NP as the template and *o*-PD and *o*-TD as comonomers (Fig. 14b).

3.10. Dummy templates and engineering structures of CNM-modified MIPs

With regard to the preparation of MIPs, certain target molecules are difficult to obtain or harmful. Dummy molecules with similar molecular structures as those of the targets often serve as alternative templates. Patulin (4-hydroxy-4*H*-furo[3,2-*c*]pyran-2(6*H*)-one) as a type of polyketide lactone is a toxic secondary metabolite produced by numerous species of filamentous fungi belonging to the genera. Patulin is toxic to animals. Guo *et al.* adopted 2-oxindole as a dummy template to replace patulin with the purpose of forming a MIP cavity at a lower cost.[180] The authors fabricated a MIP sensor for patulin detection based on GCE modified with CDs, AuNPs, CS, and electropolymerized MIP. Shi *et al.* reported a sensor using MIPs for the recognition of 2,4,6-trinitrotoluene (TNT).[50] The safe detection of TNT cannot be easily achieved. Picric acid has a molecular structure similar to that of TNT and acts as a dummy template of TNT. GR–polyaniline (GR–PANI) composite was prepared by the electropolymerization of aniline on GR. GR–PANI–MIP was formed by *in situ* polymerization using picric acid as the template, AM as the monomer, EGDMA as the cross-linker, and AIBN as the initiator (Fig. 15). After the reaction of the mixture

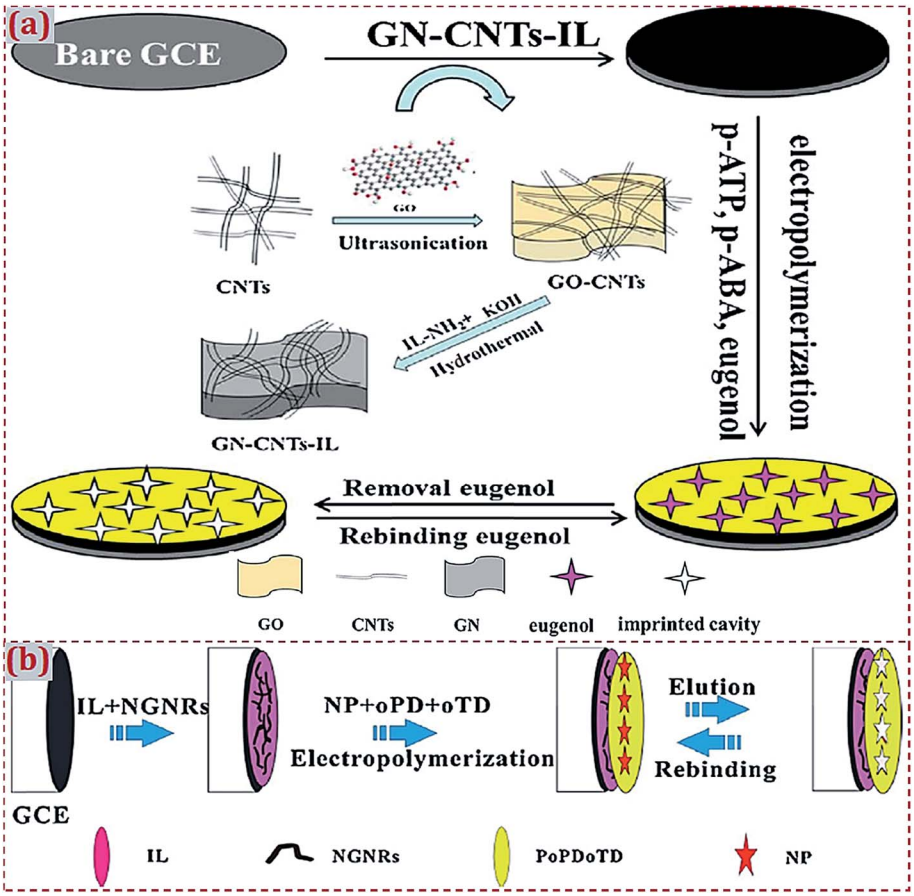

Fig. 14 (a) Preparation routes of MIP/GN–CNT–IL/GCE for the electrochemical determination of eugenol using a 3D molecularly imprinted poly(*p*-ATP-*co*-*p*-ABA)-film-modified electrode. Reproduced with permission from ref. 186. Copyright 2016, Elsevier. (b) Preparation routes for MIP/NGNR–IL/GCE as an electrochemical sensor of 4-nonyl-phenol (NP) based on molecularly imprinted poly(*o*-PD-*co*-*o*-TD)-nitrogen-doped graphene nanoribbons (NGNRs)–ionic liquid (IL) composite film. Reproduced with permission from ref. 174. Copyright 2015, Elsevier.

at 70 °C for 12 h, the product was collected by centrifugation, followed by washing with ethanol and water, and eluting with ethanol and acetic acid. GR–PANI–MIP was dropped on GCE. The modified electrode was used for TNT detection.

There are various engineering structures of CNM-modified MIPs to fabricate ECCSs. Category I involves a core–shell-structured composite that uses CNMs or CNM-based hybrids as the core and MIP as the shell. Category II comprises composite NPs or particles containing CNMs, MIPs and hybrids. Category III involves a layer-by-layer self-assembled complex of CNMs/MIP/hybrids on electrodes. Category IV comprises bulk material containing CNMs, MIP, and hybrids on bulk substrates. Category V includes the surface-imprinted material of CNM-modified MIPs on bulk substrates. Category VI comprises a 3D structural complex of CNMs/MIP/hybrids on electrodes. Wang *et al.* reported a sensor of 4-aminophenol using CdS QD–GR composite and MIP.[114] FTO was treated with poly(diallyldimethyl ammonium chloride) to improve the immobilization of CdS and GO on FTO through electrostatic attraction. CdS–GO-modified FTO was thermally heated for the reduction of GO to GR. A polypyrrole layer with surface imprinting of 4-aminophenol was electropolymerized on CdS–GO-modified FTO (Fig. 16). The template was removed by electrochemical treatments in Na_2HP_4 solution. MIP with surface imprinting was electrodeposited on this modified FTO to fabricate MIP/CdS–GO/FTO sensing platform.

With regard to CNM-modified-MIP-based ECCSs, electrodes or substrates are frequently modified with CNMs/MIP/hybrids complexes with 3D structures.[172,173,186,187,190] 3D-Structured CNMs/MIP/hybrids complexes are synthesized and dropped on substrates or they are directly fabricated on substrates *via* self-assembly. Shang *et al.* fabricated a 3D hybrid film with in- and out-of-plane pores by using porous GR as the framework structure and porous Pd–Cu alloy NPs as the building blocks.[173] A 3D porous hybrid was dropped on GCE, followed by the electropolymerization of *p*-ABA to prepare MIPs. A 3D porous MIP hybrid film was formed on GCE and enabled the electrochemical sensing of melamine. 3D porous GR–CNT–IL composite was prepared by the one-step hydrothermal method and was used to modify the GCE.[186] Eugenol-imprinted poly(*p*-ATP-*co*-*p*-ABA) was electrodeposited on the modified GCE *via* copolymerization to form a MIP electrochemical sensor. 3D PdNP–porous GR–CNTs composite was prepared *via* a one-step hydrothermal method. Quercetin-imprinted poly(*p*-ABA) was deposited on this modified

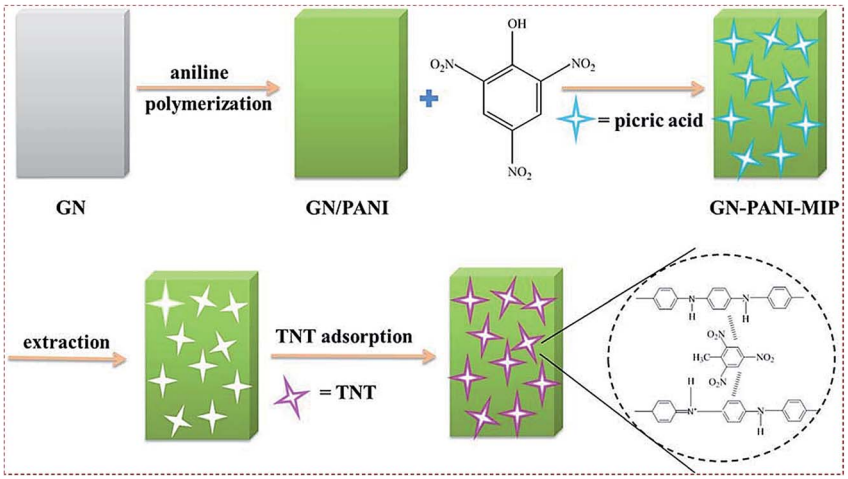

Fig. 15 Schematic of fabricating molecularly imprinted sites for TNT recognition based on GN–PANI–MIP/GCE. Reproduced with permission from ref. 50. Copyright 2015, Wiley.

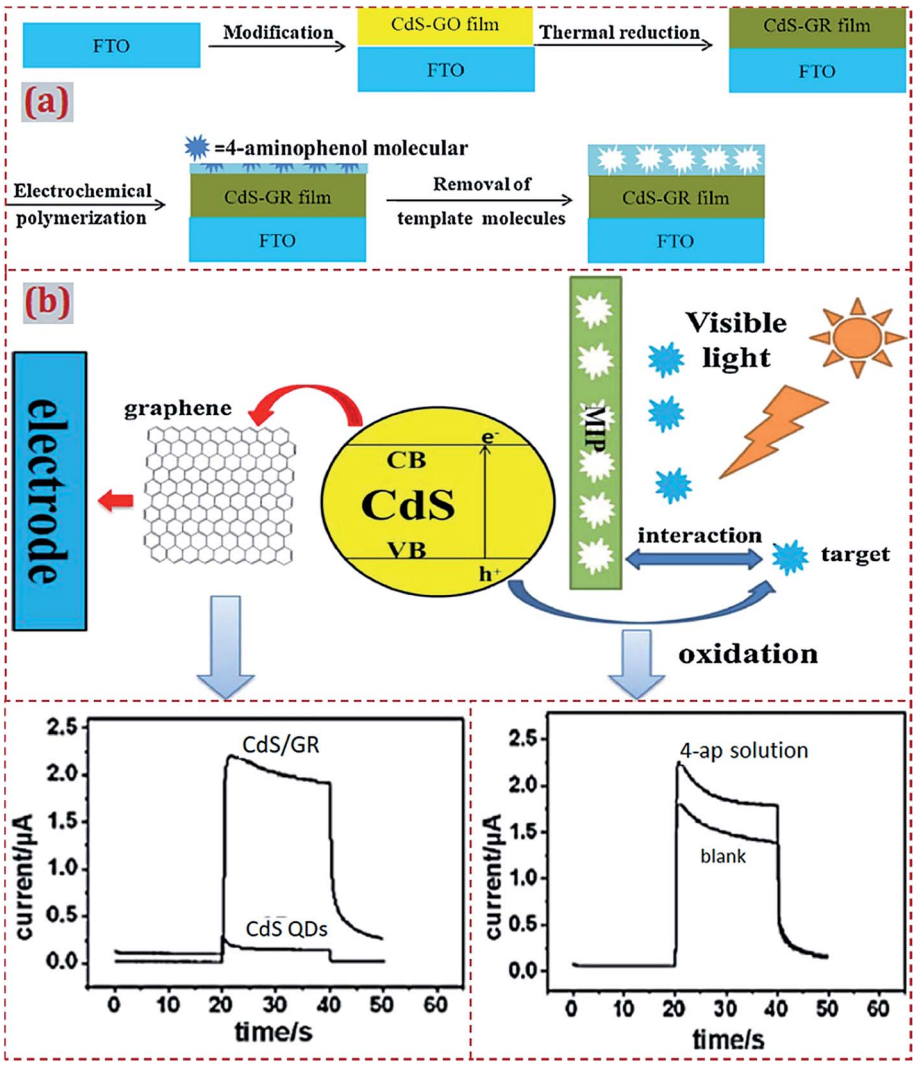

Fig. 16 (a) Schematic illustration for the fabrication of MIP/CdS–GR/FTO-based photoelectrochemical sensor. (b) A proposed mechanism for the photoelectrochemical sensing of 4-aminophenol based on MIP/CdS–GR-modified electrode. Reproduced with permission from ref. 114. Copyright 2014, Elsevier.

GCE *via* the electropolymerization of *p*-ABA.[187] Yang *et al.* reported a sensor of dimetridazole by using AuNPs@MIP, CKM-3, and P-rGO.[190] AuNPs@MIP was coated on CKM-3- and P-rGO-modified GCE to fabricate a 3D porous MIP hybrid film.

Other engineering structures of CNM-modified MIP have been reported. Wei *et al.* prepared MIP/$NiCo_2O_4$ nanoneedle arrays on 3D GR electrodes to detect sulfadimidine (SM2).[172] $NiCo_2O_4$ nanoneedle arrays were decorated on free-standing and conductive 3D GR *via* a hydrothermal process. Polypyrrole was coated on these nanoneedle arrays *via* electropolymerization by using SM2 as the template. SM2-imprinted MIP/nanoneedle arrays/3D GR complex electrodes were thus formed. Cardoso *et al.* reported a sensor of chloramphenicol (CAP) based on CO_2 laser-induced GR technique for electrode patterning.[171] GR produced on a polyimide substrate showed a porous multilayer structure. The sensor was designed as a three-electrode system. Auxiliary and working electrodes were made of GR by laser patterning. The reference electrode was handmade by casting silver ink. MIP was produced at the working electrode through the direct electropolymerization of Eriochrome Black T (EBT) using CAP as the template. GR-based electrodes obtained from the laser-induced GR technique are simple and quick for onsite sensing.

4. Applications of ECCSs based on CNM-modified MIPs

4.1. Targets, signal transducer modes, and real samples for detection

In earlier studies, various template molecules and targets (analytes) have been used to prepare MIPs in CNM-modified-MIP-based ECCSs (Tables 1–6). The targets majorly involve metal ions (Bi^{3+}), small molecules, and biomacromolecules. Small target molecules include various drug molecules used for treating human diseases, biological small molecules from human bodies, molecules that are toxic and harmful toward human health, pesticides for agricultural products, *etc.* The examples of biomacromolecules are proteins, nucleic acids, enzymes, disease biomarkers, *etc.* Other targets focus on industrial raw materials, environmental pollutants, food additives, explosives, *etc.* With regard to CNM-modified-MIP-based ECCSs, different modes of signal transducer outputs are used for the electrochemical sensing of various targets. Different signal transducer modes are used, such as differential pulse voltammetry (DPV), CV, square wave voltammetry (SWV), linear sweep voltammograms (LSV), electrochemical impedance spectroscopy (EIS), differential pulse cathodic stripping voltammetry (DPCSV), differential pulse anodic stripping voltammetry (DPASV), linear sweep stripping voltammetry (LSSV), anodic stripping differential pulse voltammograms (ASDPV), differential pulse stripping voltammetry (DPSV), square wave stripping voltammetry (SWSV), PEC and chronoamperometry (CA), cathodic stripping different pulse voltammetry (CSDPV), *etc.*

CNM-modified-MIP-based ECCSs are widely applied in the electrochemical detection of various targets in real samples. Various samples are involved, including questionable samples containing targets as well as healthy and safe samples without targets. The contents of the targets in questionable samples are determined directly using ECCSs. In addition, the targets are externally introduced into healthy and safe samples and are determined based on a standard addition method. The types of real samples for determination are several and varied (Tables 1–6), including biological and biomedical samples of human bodies or small animals, pharmaceuticals, food samples, agricultural products, industrial and environmental samples, *etc.* In different real samples, various targets were effectively detected by using CNM-modified-MIP-based ECCSs. As confirmed in earlier studies, this type of ECCS exhibited high detection sensitivity and selectivity, stability, and repeatability, as well as high detection recoveries.

4.2. Detection mechanisms of nonelectroactive and electroactive targets

With regard to the electrochemical sensing applications of CNM-modified-MIP-based ECCSs, there are two principal detection mechanisms for nonelectroactive and electroactive targets (Scheme 2). When the targets are nonelectroactive, the redox electrochemical probes from CNM-modified MIPs or MIP/CNMs/hybrids complexes on the substrates or those already added into electrolyte solutions can act as the signal outputs for the sensing of nonelectroactive targets. When the targets are electroactive, redox of the targets acts as the signal outputs. In this case, the targets frequently combine with other electrochemical probes from the ECCS sensing platform or electrolyte solutions to yield dual, triple, and multiple signal outputs, which facilitate the development of dual-signal ratiometric and simultaneous sensing of dual, triple, or multiple targets.

Qian *et al.* proposed a MIP sensor of DA based on molecularly imprinted oxygen-containing polypyrrole coated on CNTs.[43] Polypyrrole/CNT–MIP complex was dropped on GCE to fabricate a sensing platform. DA served as the target and its redox characteristics were used as the signal outputs for DA sensing without the introduction of other electrochemical probes from the sensing platform and electrolyte solutions (Fig. 17). In this case, the sensing platform can produce enhanced electrochemical signal responses to electroactive targets. The targets enter into the MIP cavities, pass through the cavities, and reach the electrode (substrate) surface to undergo redox reactions, which finally yield redox electrochemical signal outputs. This detection mechanism is widely used for the electrochemical sensing of nonelectroactive targets in ECCSs based on CNM-modified MIPs and MIP/CNMs/hybrids complexes.

With regard to the electrochemical sensing of nonelectroactive targets, redox probes are often used for signal outputs. Redox probes include the frequently used $[Fe(CN)_6]^{3-/2-}$,[136,138,158,159] Prussian blue (PB),[120,121,135,179] $N_2H_4 \cdot H_2O$,[173] *etc.* Wang *et al.* reported a 3D MIP electrochemical sensor based on PB-mediated amplification together with signal enhancement of ordered CKM-3 for the quantification of MTMC.[179] PB has high stability and excellent electrocatalytic activity. A PB film is often prepared by electrochemical methods and is widely used as an electronic mediator in ECCSs. Upon modification with

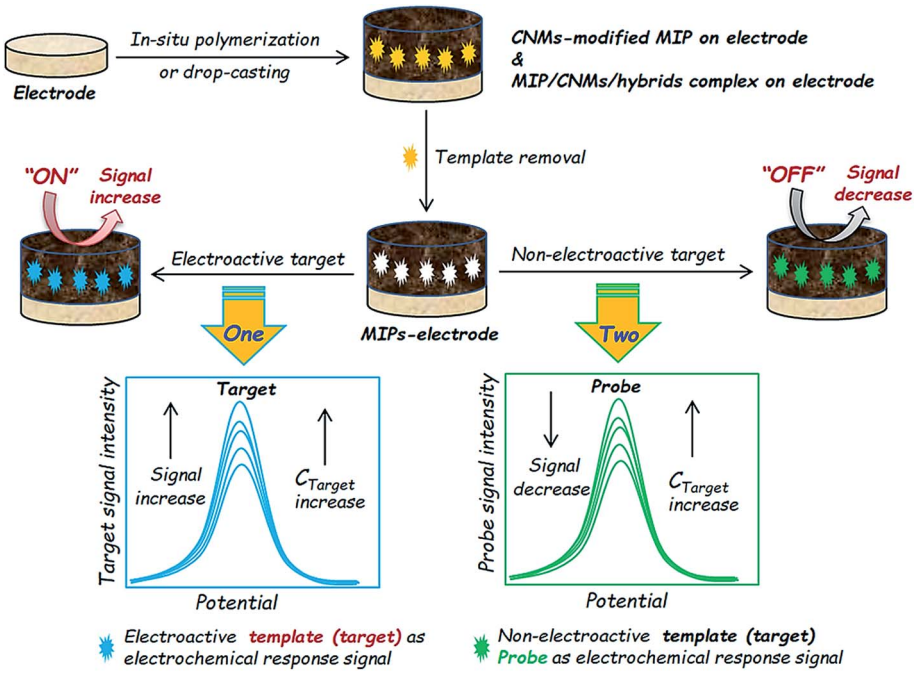

Scheme 2 Scheme illustration of the electrochemical sensing applications of CNM-modified MIP-based ECCSs using two principal detection mechanisms for nonelectroactive and electroactive targets.

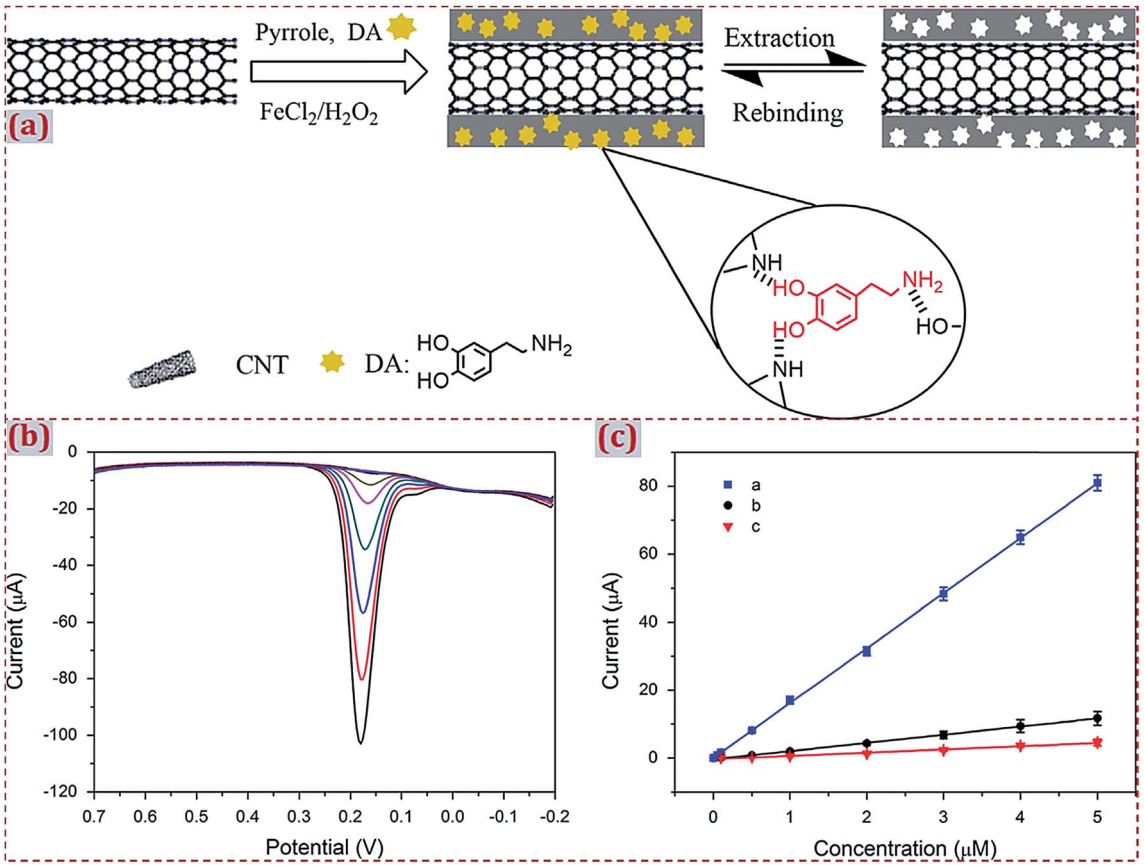

Fig. 17 (a) Chemical routes for the preparation of polypyrrole/CNT–MIP. (b) DPV curves with an increase in DA concentrations in 0.1 M PBS (pH 6.5). DA concentration was 0.05–50 nM and 0.1–5 μM (from top to bottom), respectively. (c) Calibration curves of DA obtained with (blue) polypyrrole/CNT–MIP, (black) polypyrrole/CNT–NIP and (red) CNT-modified GCE. Reproduced with permission from ref. 43. Copyright 2014, Elsevier.

a PB film, the performance of CNMs as transducers gets enhanced. As an inorganic conductive film, a PB film directly produces an electrochemical signal that improves sensitivity. In Fig. 18a, PB–CMK-3 hybrid with a 3D structure is shown, which acts as a low-potential redox mediator and electron transfer carrier. The hybrid has a desirable hosting structure, efficient facilitation effect on electron transfer of CMK-3, and effective low-potential electron transfer mediation of PB. With regard to MIP/PB–CMK-3/GCE, the current reduction of the PB signal indicates the MTMC content.

Huang *et al.* developed a sensor of toltrazuril (TZR) using MIP/TiO_2/rGO-complex-modified Pt electrode.[159] The modified electrode was incubated in a TZR solution and measured in a $K_3[Fe(CN)_6]$ solution containing KCl by DPV (Fig. 18b). The MIP-adduct film was insulating and it hindered the movement of $[Fe(CN)_6]^{3-/4-}$ probe ions through the polymer network for redox reactions. After template removal, a TZR-imprinted polymer had an increased peak current. Upon the incubation of the modified electrode in a TZR solution, the peak current significantly reduced because the partially imprinted sites were occupied by TZR, leading to fewer channels for the diffusion of $[Fe(CN)_6]^{3-/4-}$ on the electrode surface. The current response of $[Fe(CN)_6]^{3-/4-}$ was proportional to the amount of unoccupied imprinted sites and was indirectly correlated to the TZR concentration. Shang *et al.* fabricated 3D porous GR/PdCu alloy NPs complex decorated on MIP for the electrocatalytic assay of melamine.[173] Melamine was detected by DPV using hydrazine as the electrochemical probe. Hydrazine had an oxidation peak at the modified electrode. The detection signal was amplified due to the catalytic oxidation of hydrazine. After the rebinding of melamine, the peak current decreased because electroinactive melamine deterred the access of hydrazine on the surface of the modified electrode. The detection signal was generated from the peak current deduction of hydrazine.

4.3. Electrochemical sensing of different types of targets

CNM-modified-MIP-based ECCSs are popularly used for the electrochemical sensing of various targets (analytes) in the

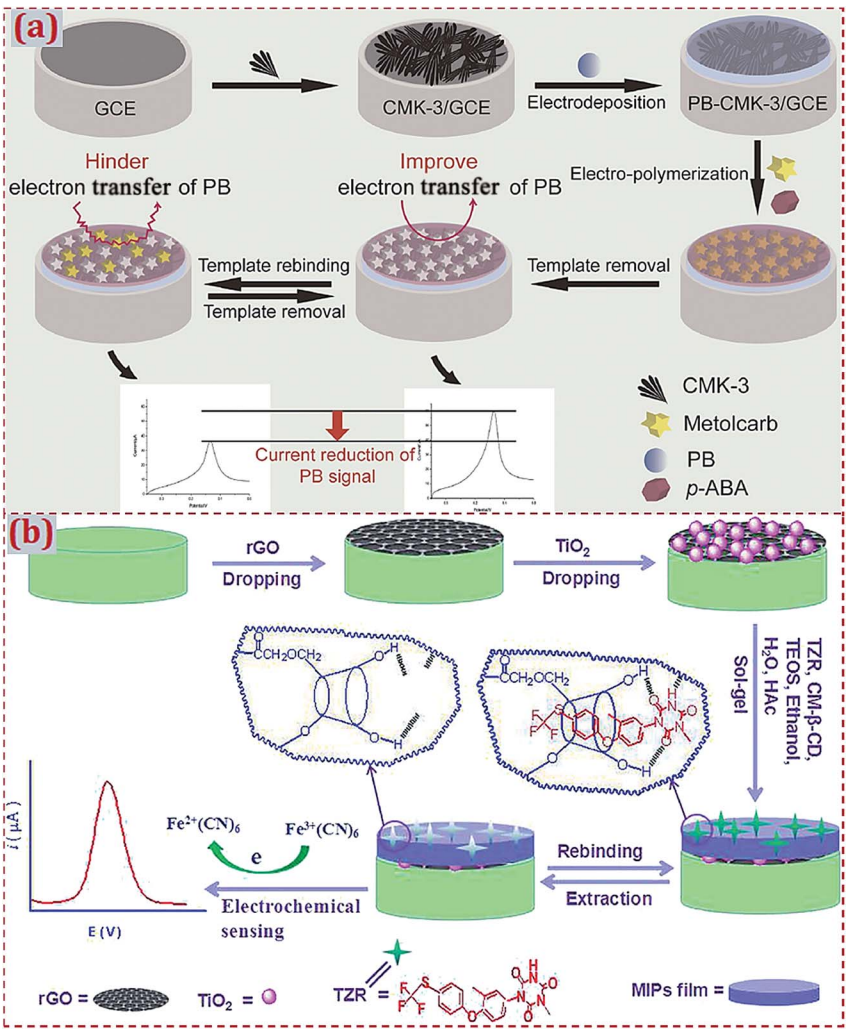

Fig. 18 (a) Schematic representation of the fabrication process of MIP/PB–CMK-3/GCE. Reproduced with permission from ref. 179. Copyright 2015, Elsevier. (b) Schematic illustration for the fabrication of an electrochemical sensor based on MIPs/TiO_2/rGO/Pt electrode. Reproduced with permission from ref. 159. Copyright 2019, Elsevier.

liquid (solution) phase, such as pharmaceuticals, drugs, biomarkers, proteins, nucleic acids, enzymes, food additives, industrial raw materials, environment pollutants, pesticides, explosives, *etc.* The electrochemical sensing applications of ions in solution and gas molecules have been undertaken. By introducing one typical work, we elaborated the applications of CNM-modified-MIP-based ECCSs for the electrochemical sensing of molecules and ions in a solution, as well as the electrochemical sensing of gases. You *et al.* designed an electrochemical sensor to determine the breast cancer susceptibility gene BRCA-1 amplified by SiO_2@AgNPs.[154] AuNPs/GO-composite-modified GCE was covered with a prepared MIP layer using rhodamine B (RhB) as the template, MAA as the monomer, and Nafion as the additive. The signal amplification trace tag SiO_2@AgNPs was prepared by covering AgNPs on SiO_2 NP surface *in situ*. DNA probes were modified on AgNPs by the Ag–S bond to form the SiO_2@Ag/DNA complex. In the presence of the target DNA, homogeneous hybridization was performed with SiO_2@Ag/DNA and RhB-labeled DNA (Fig. 19). SiO_2@Ag/dsDNA/RhB was specifically recognized with MIP *via* interactions between imprinting cavities and RhB. This biosensor had a wide linear range from 10 fM to 100 nM, low detection limit of 2.53 fM, excellent selectivity, reproducibility, stability, and feasibility in serum analyses.

Emam *et al.* reported a MIP electrochemical sensor of gases to detect butylated hydroxytoluene (BHT) in air.[120] A three-layer sensor was formed by depositing a thin layer of GR on a GCE substrate. In the prepolymer solution containing BHT as the template (target) and pyrrole as the monomer, electropolymerization was initiated to form polypyrrole on GR/GCE. After template removal, a MIP layer as the conductive polymer film was generated. The sensor contained molecularly imprinted cavities for the selective recognition of target molecules (Fig. 20). Two sets of sensors were designed. First, a GR sensor was fabricated with a layer of rGO and tested over 5–100 parts per million (ppm). In the second batch, PB was added to GR before polymerization, which enhanced the electrochemical properties. The sensor was tested over 0.02–1 parts per billion (ppb) level of the target. The sensor resistance was monitored. Alizadeh *et al.* designed a sensor for Bi^{3+} detection using nanostructured Bi^{3+}-imprinted polymer-modified carbon/CNTs paste electrode.[76] Bi^{3+}–MIP was prepared by the copolymerization of Bi^{3+}–methylene succinate complex and EGDMA in acetonitrile through precipitation polymerization (Fig. 21). Polymeric NPs were used as Bi^{3+}-selective modifier of carbon/CNTs paste electrode. Bi^{3+} ions were accumulated on the electrode surface in a Bi^{3+} solution. ASDPV signals of the modified electrode were recorded as the analytical signal, which were significantly higher than those of nonimprinted polymer-based electrodes. The electrode had a dynamic linear response range of 0.2–2 μM and detection limit of 8.9 μM for Bi^{3+}. The sensitivity was high and reached 112.25 μA μM^{-1}. This sensor was

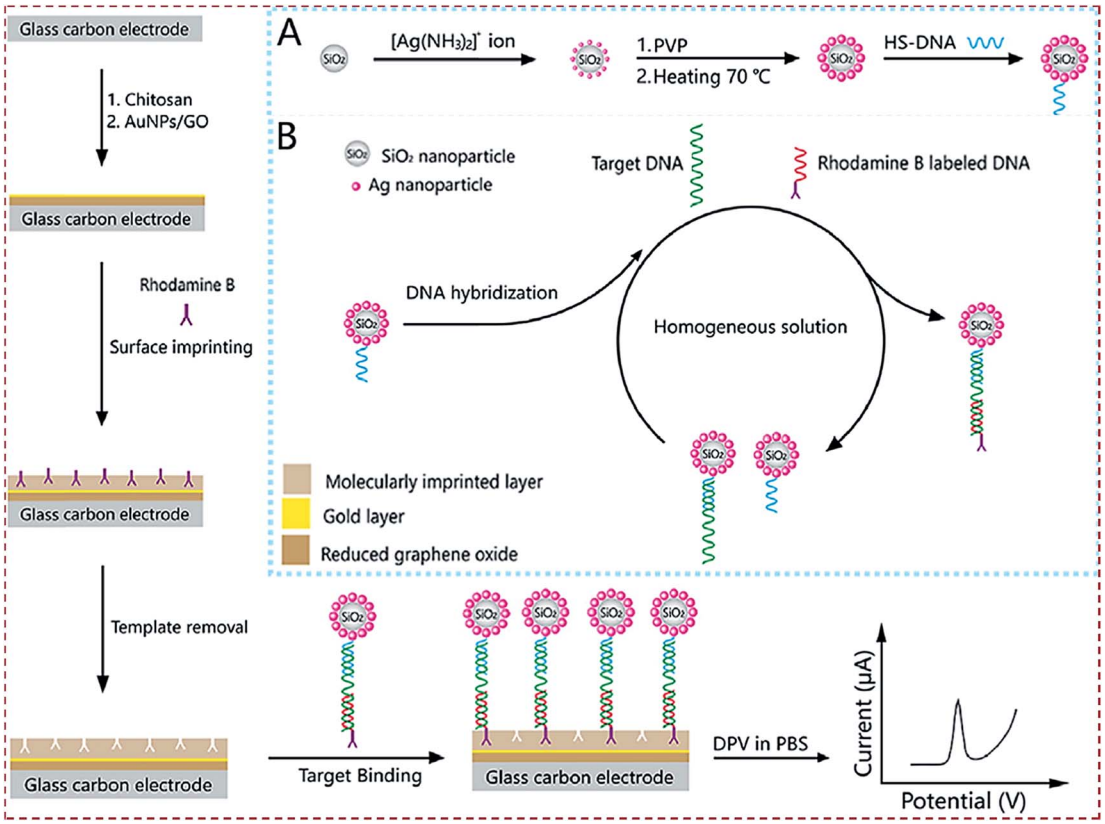

Fig. 19 Schematic illustration of a MIP-based electrochemical DNA biosensor for the determination of breast cancer susceptibility gene (BRCA-1) amplified by SiO_2@Ag. Insets of (A) and (B) show the preparation process of SiO_2@Ag/DNA and homogeneous DNA hybridization. Reproduced with permission from ref. 154. Copyright 2018, Elsevier.

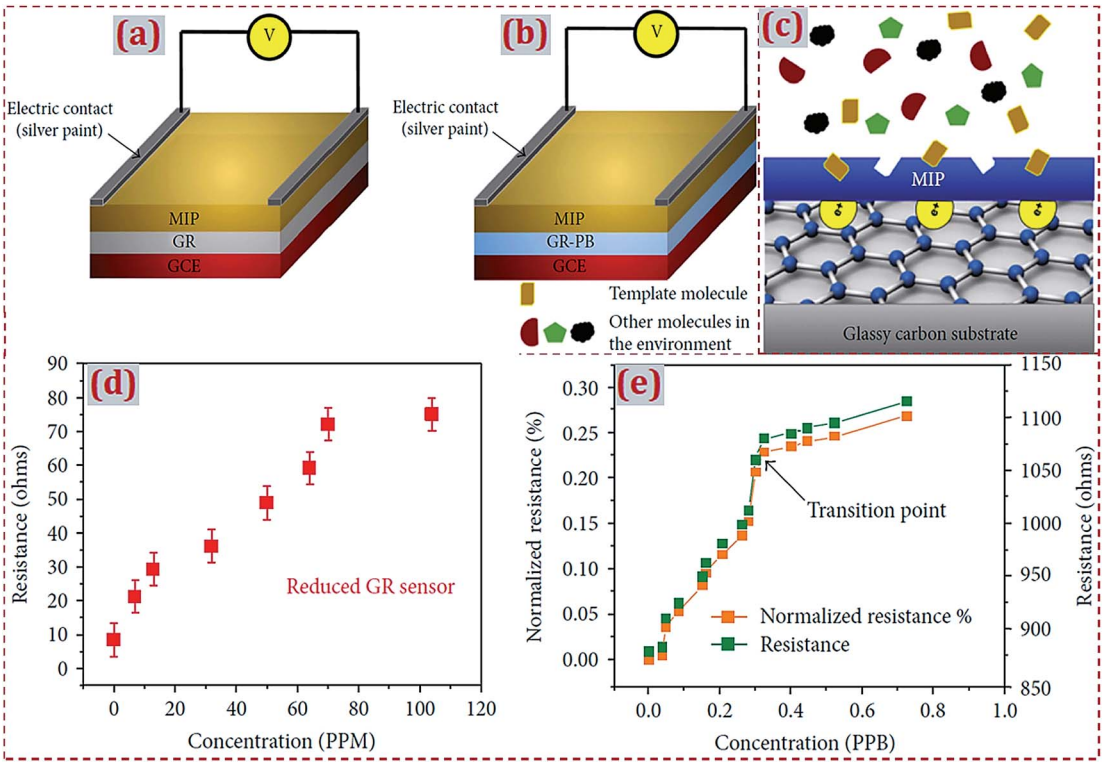

Fig. 20 (a, b) Schematic diagrams of both sensors: a layer of MIP is deposited on graphene (GR) or a GR–Prussian blue (PB)-modified surface of GCE. (c) Mechanism of the sensor among different molecules in environment; only the template can be absorbed on the MIP layer. When the template molecule is trapped on the MIP layer, an extra electron is transferred to the GR layer, which induces a resistance change. Test results of GR sensors in the range of 5–100 ppm in red (d) and GR–PB sensor in the range of 0.02–1 ppb in green (e) along with the normalized resistance change. At a concentration of 0.3 ppb, the vacuum was purged to the sealed chamber; therefore, the resistance increase occurs with a lower slope. Reproduced with permission from ref. 120. Copyright 2018, Hindawi.

used for the electrochemical detection of Bi^{3+} in environmental, pharmaceutical, and biological samples.

4.4. Respective and simultaneous electrochemical sensing of two targets

Most of the earlier reported ECCSs based on CNM-modified MIPs can be used to determine only a single type of targets, with high detection sensitivity and selectivity. Moreover, scientists have investigated different CNM-modified-MIP-based ECCSs for the respective and simultaneous electrochemical determination of two types of targets.[53,67,84,91,98,141] Jaiswal *et al.* presented the enantioselective analysis of D- and L-serine on a layer-by-layer imprinted electrochemical sensor.[91] The authors employed AM-functionalized rGO–fullerene layer-by-layer assembled dual-imprinted polymers to quantify D- and L-serine at the ultra-trace level in real aqueous samples. The sensor exhibited better electronic properties with improved synergism and had a lower detection limit (0.24 ng mL^{-1}) for both the isomers. Zang *et al.* formulated a disposable simultaneous electrochemical sensor array using a MIP film on NH_2–GR-modified screen-printed electrode for the detection of psychotropic drugs.[84] The MIP film was prepared by electropolymerization using methcathinone and cathinone as dual templates and pyrrole as the monomer. This multiplexed immunoassay method had wide linear ranges over 3 orders of magnitude together with detection limits down to 3.3 and 8.9 pg mL^{-1} for methcathinone and cathinone, respectively. This sensor array was applied to detect methcathinone and cathinone in practical serum samples.

Chen *et al.* prepared MIP-grafted GR (MIP-G) for the simultaneous sensing of 4,4-methylene diphenyl amine (MDA) and aniline.[53] MIP-G was prepared through a free-radical polymerization reaction using MDA as the template and 4-vinylpyridine as the monomer. MIP-G had high binding affinity toward MDA and underwent π–π interactions with aniline. The oxidation potentials for MDA at 0.62 V and aniline at 0.72 V were distinguishable. MIP-G-modified GCE had a linear response to MDA and aniline over the range of 1.0–15 μM. MIP-G-based sensors were applied in plastic tableware. Prasad *et al.* adopted Monomer dual-imprinted dendrimer nanofilm-modified electrode for the simultaneous detection of uric acid and norepinephrine.[98] AuNP-functionalized MWCNTs composite was used for growing a thin nanofilm based on the surface grafting route on PGE. This sensor enabled the simultaneous analysis of one target in the presence of the other, without any cross-reactivity involving interferences and false positives. The detection limits were calculated to be 0.62 ng mL^{-1} for norepinephrine and 0.43 ng mL^{-1} for uric acid in aqueous, biological, and pharmaceutical samples.

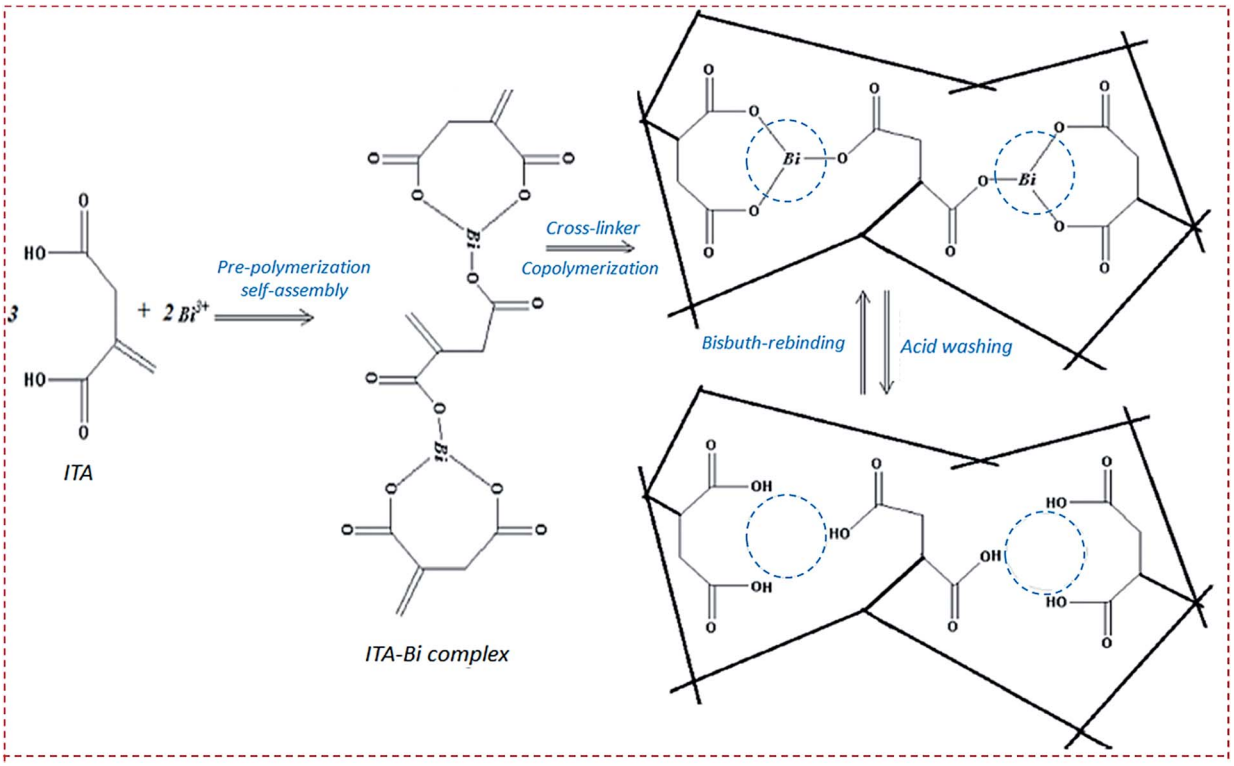

Fig. 21 Schematic representation of Bi^{3+}-imprinted polymer synthesis including Bi^{3+} interaction with itaconic acid (ITA) molecules (pre-polymerization reaction) and copolymerization reaction. Reproduced with permission from ref. 76. Copyright 2017, Elsevier.

Wang *et al.* reported simultaneous immunoassay using GR–AuNPs-grafted recombinant apoferritin-encoded metallic NP labels as the signal tags and dual-template magnetic MIP as the capture probes.[141] This multiplexed immunoassay enabled the simultaneous detection of alpha-fetoprotein (AFP) and carcinoembryonic antigen (CEA). The labels were prepared by loading recombinant apoferritin and separately immobilized primary antibodies *via* AuNP growth on GR. The capture probes

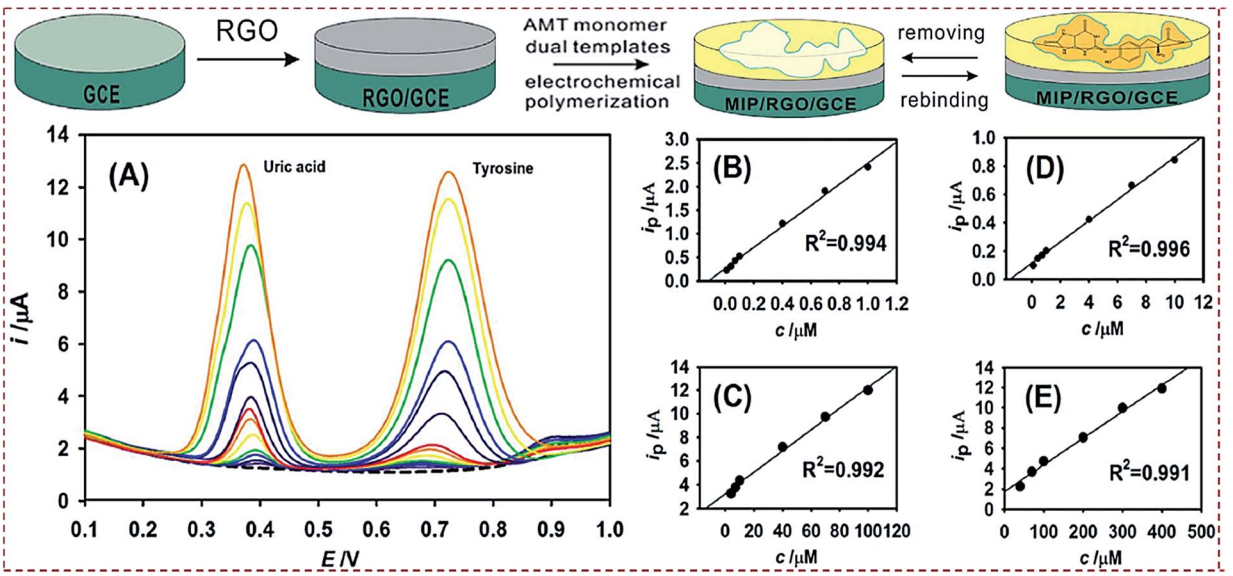

Fig. 22 Preparation process of MIP–rGO composites. (A) DPV responses of a MIP/rGO sensor for different concentrations of uric acid and tyrosine. From bottom to top, the concentrations of uric acid and tyrosine are 0.01 to 100 μM and 0.1 to 400 μM, respectively. The dashed line at the bottom denotes the data obtained from blank PBS. Calibration curves corresponding to uric acid in the concentration ranges of 0.01–1.0 μM (B) and 4–100 μM (C). Calibration curves corresponding to tyrosine in the concentration ranges of 0.1–10 μM (D) and 40–400 μM (E). Reproduced with permission from ref. 67. Copyright 2018, Elsevier.

were prepared by the self-polymerization of DA on Fe_3O_4 NPs using AFP and CEA as the template proteins. The analysis of metal components in an immune complex provided a route to quantify the targets based on the peak currents of Cd and Pb. The immunoassay enabled the simultaneous detection of AFP and CEA, showing broad dynamic ranges of 0.001–5 ng mL^{-1} and low detection limits of 0.3 for AFP and 0.35 pg mL^{-1} for CEA. Zheng *et al.* designed a sensor based on the MIP/rGO composite for the simultaneous determination of uric acid and tyrosine.[67] A MIP layer was electropolymerized on a rGO-modified electrode using dual templates of uric acid and tyrosine (Fig. 22). The sensor had broad linear ranges for uric acid (0.01–100 μM) and tyrosine (0.1–400 μM) with low detection limits of 32 and 46 nM, respectively. The sensor was used to detect uric acid and tyrosine in serum and urine samples.

5. Conclusions and perspectives

5.1. Summary of general categories and preparation strategies

This review systematically summarizes the recent advances in ECCSs based on CNM-modified MIPs, categorized into general categories, preparation strategies, and analytical applications. We introduce the development process and preparation principles of MIPs. Based on the structural characteristics of MIPs, we describe the potential applications of ECCSs. Owing to the integrated merits of MIPs, ECCSs, CNMs, or CNM-based hybrids, numerous studies have been devoted toward CNM-modified-MIP-based ECCSs. During the past decade, ECCSs have been widely investigated toward the electrochemical detection of various targets in real samples, exhibiting high sensitivity and selectivity toward target detection. ECCSs are classified into two general categories: (I) MIP modified with CNMs without hybridization and (II) MIP modified with CNMs and hybridized with other materials. ECCSs can be constructed on commercial work electrodes or other sensing substrates. There are three major routes to achieve CNM-modified MIPs. Route I is to prepare CNM-encapsulated imprinting of silica. Route II is to prepare CNM-encapsulated imprinting of polymers. Route III is to prepare MIP combined with CNMs.

To obtain CNM-modified-MIP-based ECCSs, various preparation strategies have been widely reported. They include the (a) polymerization of MIP on CNM-modified substrates, (b) copolymerization of MIP and CNMs on substrates, (c) dropcasting of already fabricated MIPs on CNM-modified substrates, (d) dropcasting of already made MIP/CNMs complexes on substrates, (e) dropcasting of already made self-assembled complexes of MIP/CNMs/hybrids on substrates, and (f) self-assembly of MIP/CNMs/hybrids complexes on substrates. With regard to the polymerization process of MIPs, the frequently used strategies are the *in situ* chemical polymerization of functional monomers and electrochemical polymerization of electroactive functional monomers. Because some templates are expensive, toxic, and harmful to organisms and the environment, dummy molecules often act as alternative templates to prepare MIPs. There are various engineering structures of CNM-modified MIPs to fabricate ECCSs, majorly involving (i) core–shell-structured composites, (ii) composite NPs or particles, (iii) layer-by-layer self-assembled complexes, (iv) bulk macromaterials, (v) surface-imprinted materials, and (vi) 3D structural complexes.

5.2. Summary of potential applications

With regard to CNM-modified-MIP-based ECCSs, different modes of electrochemical signal from transducer outputs can be employed for the sensing of various targets, focusing on metal ions, small molecules, and macromolecules. Small target molecules include drug molecules used for treating human diseases, biological small molecules from human bodies, molecules that are toxic and harmful toward human health, pesticides for agricultural products, *etc.* Different macromolecules are proteins, nucleic acids, enzymes, disease biomarkers, *etc.* Other targets focus on industrial raw materials, environmental pollutants, food additives, explosives, *etc.* Various practical samples are involved and include questionable samples containing targets and healthy and safe samples without targets. There are two major detection mechanisms for nonelectroactive and electroactive targets. For nonelectroactive targets, redox probes serve as the signal outputs for electrochemical sensing. When the targets are electroactive, redox of the targets can act as signal outputs. Most of the CNM-modified-MIP-based ECCSs enable the determination of only a single type of target. Scientists have explored this type of ECCS for respective and simultaneous electrochemical determination of two types of targets.

5.3. Improvements in preparation strategies

Numerous studies have referred to CNM-modified-MIP-based ECCSs during the past decade, but certain potential challenges inevitably remain. In subsequent studies, scientists should pay close attention to the rational design and optimal preparation of CNM-modified MIPs with functional structures, simplified preparation steps, and high electrical activity, aiming to develop excellent ECCSs for the highly sensitive and selective sensing of various targets. Novel engineering structures of CNM-modified MIPs will be further explored toward multiple functions and applications of ECCSs. Versatile core–shell-engineered MIP_1/MIP_2 hybrids with multi-imprinting cavities from different templates can yield versatile detection applications, such as high-performance detection of dual, triple, or multiple targets. This is imperative for the accurate diagnosis of complex diseases and even cancers. Electropolymerization is considerably suitable for the controllable preparation of MIPs on substrates modified with CNMs or CNM-based hybrids, facilitating the fabrication of various engineering structures of CNM-modified MIPs. The integration of different preparation strategies can be used to design new and multifunctional structures of ECCSs. Different from the *in situ* copolymerization of MIP and CNMs on substrates, magnetic MIP (CNM-modified MIP) already prepared in the solution phase can be absorbed on the magnetic electrode surface. The use of a magnetic electrode avoids the requirements of complicated modification procedures and time-consuming and tedious polymerization operations necessitated in order to prepare MIPs on electrode surfaces. The combination of magnetic MIP complexes with

a magnetic electrode is efficient and ensures high stability of MIP-complex-based ECCSs. Most of the CNM-modified-MIP-based ECCSs involve hybridization with other electroactive materials, which synergistically improves the sensitivity of the responses of the electrochemical signal toward the targets. Several types of materials have been prepared and used for hybridization with CNMs, followed by preparing MIPs on CNMs/other materials dual-modified electrodes or substrates. In the subsequent studies, certain aspects of electroactive materials should be addressed, particularly with respect to low toxicity, cost-effectiveness, facile preparation, colloidal stability, and electrical activity.[198]

5.4. Further exploration of potential applications

With regard to the detection applications of CNM-modified-MIP-based ECCSs, targets frequently combine with other electrochemical probes from the ECCS platforms or electrolyte solutions to yield dual, triple, or multiple signal outputs, which can facilitate the development of dual-signal ratiometric and simultaneous sensing of dual, triple, or multiple targets. Earlier reports have prominently referred to single-signal outputs for the electrochemical sensing of a single target. A single-signal output corresponds to only one type of target. With regard to the detection applications of ECCSs, the dual-signal-ratiometric output is superior to a single-signal output.[199–202] The ratiometry of dual signals is independent of the contents of the sensors and reagents, providing an intrinsic built-in correction to conquer the potentially adverse effects of the sensing systems and background signals.[203–206] Generally, to acquire the accurate intensity of a single signal is difficult in the sensing process of targets. The ratiometry of dual signals can efficiently improve the accuracy and sensitivity of ECCSs for target detection in real samples. Scientists need to rationally design new CNM-modified MIPs and develop versatile ECCSs that have layer-by-layer assembled or core–shell-engineered structures. Different types of electroactive probe molecules can be loaded into different layers and core–shell structures to yield ratiometric ECCSs. Except for commercial work electrodes, other solid sensing substrates have been widely used to develop CNM-modified MIPs. ECCSs constructed on solid substrates show promising potential for various applications, particularly electrochemical sensing elements, as well as flexible and wearable intelligent devices.[207] Except for electrochemical signal from transducer outputs reported in earlier studies, other advanced electrochemical signals from other transducer output modes, such as electrochemiluminescence and photoelectrochemical signals,[208–212] can be introduced in CNM-modified-MIP-based ECCSs. The introduction of advanced electrochemical signal transducer outputs can endow ECCSs with newer opportunities for applications in the visual detection of targets in real samples and electrochemical imaging detection *in vivo*/*in vivo*. These studies demonstrate the promising prospects of CNM-modified-MIP-based ECCSs in current research fields, such as targeting chemo/bioanalysis as well as the accurate diagnosis and therapy of serious diseases and cancers in clinics.

Conflicts of interest

There are no conflicts to declare.

Acknowledgements

This work was financially supported by the Natural Science Foundation of Shandong Province (ZR2019MB026), and the Source Innovation Plan Application Basic Research Project of Qingdao (18-2-2-26 jch, 17-1-1-72-jch).

Notes and references

1 M. V. Polyakov, *Zh. Fiz. Khim.*, 1931, **2**, 799–805.
2 L. Pauling, *J. Am. Chem. Soc.*, 1940, **62**, 2643–2657.
3 G. Wulff and A. Sarhan, *Angew. Chem., Int. Ed.*, 1972, **11**, 341–344.
4 G. Vlatakis, L. I. Andersson, R. Müller and K. Mosbach, *Nature*, 1993, **361**, 645–647.
5 X. Hu, Y. Hu and G. Li, *J. Chromatogr. A*, 2007, **1147**, 1–9.
6 A. Martín-Esteban, *TrAC, Trends Anal. Chem.*, 2013, **45**, 169–181.
7 R. Arshady and K. Mosbach, *Makromol. Chem.*, 1981, **182**, 687–692.
8 F. G. Tamayo, E. Turiel and A. Martín-Esteban, *J. Chromatogr. A*, 2007, **1152**, 32–40.
9 N. M. Bergmann and N. A. Peppas, *Prog. Polym. Sci.*, 2008, **33**, 271–288.
10 C. Malitesta, E. Mazzotta and R. A. Picca, *Anal. Bioanal. Chem.*, 2012, **402**, 1827–1846.
11 O. S. Ahmad, T. S. Bedwell, C. Esen, A. Garcia-Cruz and S. A. Piletsky, *Trends Biotechnol.*, 2019, **37**, 294–309.
12 J. J. BelBruno, *Chem. Rev.*, 2019, **119**, 94–119.
13 Y. Fuchs, O. Soppera and K. Haupt, *Anal. Chim. Acta*, 2012, **717**, 7–20.
14 J. Zhan, G. Z. Fang, Z. Yan, M. F. Pan, C. C. Liu and S. Wang, *Anal. Bioanal. Chem.*, 2013, **405**, 6353–6363.
15 D. L. Huang, R. Z. Wang, Y. G. Liu, G. M. Zeng, C. Lai, P. Xu, B. A. Lu, J. J. Xu, C. Wang and C. Huang, *Environ. Sci. Pollut. Res.*, 2015, **22**, 963–977.
16 S. Wu, L. Tan, G. Wang, G. Peng, C. Kang and Y. Tang, *J. Chromatogr. A*, 2013, **1285**, 124–131.
17 A. A. Volkert and A. J. Haes, *Analyst*, 2014, **139**, 21–31.
18 Y. Ma, S. Xu, S. Wang and L. Wang, *TrAC, Trends Anal. Chem.*, 2015, **67**, 209–216.
19 N. Pérez-Moral and A. G. Mayes, *Anal. Chim. Acta*, 2004, **504**, 15–21.
20 C. Zheng, Y. P. Huang and Z. S. Liu, *Anal. Bioanal. Chem.*, 2013, **405**, 2147–2161.
21 A. G. Mayes and K. Mosbach, *Anal. Chem.*, 1996, **68**, 3769–3774.
22 C. He, Y. Long, J. K. Pan and F. Liu, *J. Biochem. Biophys. Methods*, 2007, **70**, 133–150.
23 S. Yan, Z. Gao, Y. Fang, Y. Cheng, H. Zhou and H. Wang, *Dyes Pigm.*, 2007, **74**, 572–577.
24 E. Turiel and A. Martin-Esteban, *Anal. Bioanal. Chem.*, 2004, **378**, 1876–1886.

25 D. Gao, Z. Zhang, M. Wu, C. Xie, G. Guan and D. Wang, *J. Am. Chem. Soc.*, 2007, **129**, 7859–7866.
26 B. Gao, J. Wang, F. An and Q. Liu, *Polymer*, 2008, **49**, 1230–1238.
27 Z. X. Xu, G. Z. Fang and S. Wang, *Food Chem.*, 2010, **119**, 845–850.
28 S. Ansari, *TrAC, Trends Anal. Chem.*, 2017, **93**, 134–151.
29 R. Gui, H. Jin, H. Guo and Z. Wang, *Biosens. Bioelectron.*, 2018, **100**, 56–70.
30 B. Yang, C. Fu, J. Li and G. Xu, *TrAC, Trends Anal. Chem.*, 2018, **105**, 52–67.
31 L. Uzun and A. P. F. Turner, *Biosens. Bioelectron.*, 2016, **76**, 131–144.
32 J. Wackerlig and P. A. Lieberzeit, *Sens. Actuators, B*, 2015, **207**, 144–157.
33 P. S. Sharma, M. Dabrowski, F. D'Souza and W. Kutner, *TrAC, Trends Anal. Chem.*, 2013, **51**, 146–157.
34 S. Ansari, *TrAC, Trends Anal. Chem.*, 2017, **93**, 134–151.
35 L. Chen, S. Xu and J. Li, *Chem. Soc. Rev.*, 2011, **40**, 2922–2942.
36 L. Chen, X. Wang, W. Lu, X. Wu and J. Li, *Chem. Soc. Rev.*, 2016, **45**, 2137–2211.
37 S. Beyazit, B. T. S. Bui, K. Haupt and C. Gonzato, *Prog. Polym. Sci.*, 2016, **62**, 1–21.
38 M. J. Whitcombe, I. Chianella, L. Larcombe, S. A. Piletsky, J. Noble, R. Porter and A. Horgan, *Chem. Soc. Rev.*, 2011, **40**, 1547–1571.
39 T. P. Huynh and W. Kutner, *Biosens. Bioelectron.*, 2015, **74**, 856–864.
40 J. Ashley, M. A. Shahbazi, K. Kant, V. A. Chidambara, A. Wolff, D. D. Bang and Y. Sun, *Biosens. Bioelectron.*, 2017, **91**, 606–615.
41 M. Dabrowski, P. Lach, M. Cieplak and W. Kutner, *Biosens. Bioelectron.*, 2018, **102**, 17–26.
42 J. Pan, W. Chen, Y. Ma and G. Pan, *Chem. Soc. Rev.*, 2018, **47**, 5574–5587.
43 T. Qian, C. Yu, X. Zhou, P. Ma, S. Wu, L. Xu and J. Shen, *Biosens. Bioelectron.*, 2014, **58**, 237–241.
44 Z. Z. Yin, S. W. Cheng, L. B. Xu, H. Y. Liu, K. Huang, L. Li, Y. Y. Zhai, Y. B. Zeng, H. Q. Liu, Y. Shao, Z. L. Zhang and Y. X. Lu, *Biosens. Bioelectron.*, 2018, **100**, 565–570.
45 W. Wen, D. M. Zhao, X. H. Zhang, H. Y. Xiong, S. F. Wang, W. Chen and Y. D. Zhao, *Sens. Actuators, B*, 2012, **174**, 202–209.
46 X. Kan, H. Zhou, C. Li, A. Zhu, Z. Xing and Z. Zhao, *Electrochim. Acta*, 2012, **63**, 69–75.
47 Y. Wang, M. Han, G. Liu, X. Hou, Y. Huang, K. Wu and C. Li, *Biosens. Bioelectron.*, 2015, **74**, 792–798.
48 L. Lin, H. T. Lian, X. Y. Sun, Y. M. Yu and B. Liu, *Anal. Methods*, 2015, **7**, 1387–1394.
49 B. Liu, H. T. Lian, J. F. Yin and X. Y. Sun, *Electrochim. Acta*, 2012, **75**, 108–114.
50 L. Shi, A. G. Hou, L. Y. Chen and Z. F. Wang, *Polym. Compos.*, 2015, **36**, 1280–1285.
51 H. da Silva, J. G. Pacheco, J. M. Magalhães, S. Viswanathan and C. Delerue-Matos, *Biosens. Bioelectron.*, 2014, **52**, 56–61.
52 H. Bai, C. Wang, J. Chen, J. Peng and Q. Cao, *Biosens. Bioelectron.*, 2015, **64**, 352–358.
53 N. Chen, L. Chen, Y. Cheng, K. Zhao, X. Wu and Y. Xian, *Talanta*, 2015, **132**, 155–161.
54 J. Luo, J. Cong, J. Liu, Y. Gao and X. Liu, *Anal. Chim. Acta*, 2015, **864**, 74–84.
55 X. Tan, J. Wu, Q. Hu, X. Li, P. Li, H. Yu, X. Li and F. Lei, *Anal. Methods*, 2015, **7**, 4786–4792.
56 T. Xie, M. Zhang, P. Chen, H. Zhao, X. Yang, L. Yao, H. Zhang, A. Dong, J. Wang and Z. Wang, *RSC Adv.*, 2017, **7**, 38884–38894.
57 M. Zhang, H. T. Zhao, T. J. Xie, X. Yang, A. J. Dong, H. Zhang, J. Wang and Z. Y. Wang, *Sens. Actuators, B*, 2017, **252**, 991–1002.
58 J. Luo, J. Cong, R. Fang, X. Fei and X. Liu, *Microchim. Acta*, 2014, **181**, 1257–1266.
59 S. Sun, M. Zhang, Y. Li and X. He, *Sensors*, 2013, **13**, 5493–5506.
60 J. Luo, S. Jiang and X. Liu, *Sens. Actuators, B*, 2014, **203**, 782–789.
61 Y. Liu, L. Zhu, Y. Hu, X. Peng and J. Du, *Food Chem.*, 2017, **221**, 1128–1134.
62 Y. Liang, L. Yu, R. Yang, X. Li, L. Qu and J. Li, *Sens. Actuators, B*, 2017, **240**, 1330–1335.
63 S. Kim, N. Wang, Y. Li and X. He, *Anal. Methods*, 2016, **8**, 7780–7788.
64 M. Shamsipur, N. Moradi and A. Pashabadi, *J. Solid State Electrochem.*, 2018, **22**, 169–180.
65 L. Kong, X. Jiang, Y. Zeng, T. Zhou and G. Shi, *Sens. Actuators, B*, 2013, **185**, 424–431.
66 Y. Zeng, Y. Zhou, T. Zhou and G. Shi, *Electrochim. Acta*, 2014, **130**, 504–511.
67 W. Zheng, M. Zhao, W. Liu, S. Yu, L. Niu, G. Li, H. Li and W. Liu, *J. Electroanal. Chem.*, 2018, **813**, 75–82.
68 V. M. A. Mohanan, A. K. Kunnummal and V. M. N. Biju, *J. Mater. Sci.*, 2018, **53**, 10627–10639.
69 J. Li, Z. Xu, M. Liu, P. Deng, S. Tang, J. Jiang, H. Feng, D. Qian and L. He, *Biosens. Bioelectron.*, 2017, **90**, 210–216.
70 F. Tan, L. Cong, X. Li, Q. Zhao, H. Zhao, X. Quan and J. Chen, *Sens. Actuators, B*, 2016, **233**, 599–606.
71 Y. Pan, F. Zhao and B. Zeng, *RSC Adv.*, 2015, **5**, 57671–57677.
72 G. Xu, Y. Chi, L. Li, S. Liu and X. Kan, *Food Chem.*, 2015, **177**, 37–42.
73 H. Guo, R. Gui, H. Jin and Z. Wang, *New J. Chem.*, 2017, **41**, 9977–9983.
74 A. A. Ensafi, P. Nasr-Esfahani and B. Rezaei, *Sens. Actuators, B*, 2018, **270**, 192–199.
75 G. Yang and F. Zhao, *Biosens. Bioelectron.*, 2015, **64**, 416–422.
76 T. Alizadeh, N. Hamidi, M. R. Ganjali and P. Nourozi, *Sens. Actuators, B*, 2017, **245**, 605–614.
77 T. S. Anirudhan and S. Alexander, *Biosens. Bioelectron.*, 2015, **64**, 586–593.
78 B. B. Prasad, I. Pandey, A. Srivastava, D. Kumar and M. P. Tiwari, *Sens. Actuators, B*, 2013, **176**, 863–874.

79 B. B. Prasad, A. Prasad and M. P. Tiwari, *Biosens. Bioelectron.*, 2013, **39**, 236–243.
80 M. Sebastian and B. Mathew, *J. Mater. Sci.*, 2018, **53**, 3557–3572.
81 P. Deng, Z. Xu and Y. Kuang, *Food Chem.*, 2014, **157**, 490–497.
82 A. Motaharian and M. R. M. Hosseini, *Anal. Methods*, 2016, **8**, 6305–6312.
83 H. J. Chen, Z. H. Zhang, R. Cai, X. Chen, Y. N. Liu, W. Rao and S. Z. Yao, *Talanta*, 2013, **115**, 222–227.
84 D. Zang, M. Yan, S. Ge, L. Ge and J. Yu, *Analyst*, 2013, **138**, 2704–2711.
85 B. Huang, L. Xiao, H. Dong, X. Zhang, W. Gan, S. Mahboob, K. A. Al-Ghanim, Q. Yuan and Y. Li, *Talanta*, 2017, **164**, 601–607.
86 M. Mostafavi, M. R. Yaftian, F. Piri and H. Shayani-Jam, *Biosens. Bioelectron.*, 2018, **122**, 160–167.
87 B. V. M. Silva, B. A. G. Rodríguez, G. F. Sales, M. D. P. T. Sotomayor and R. F. Dutra, *Biosens. Bioelectron.*, 2016, **77**, 978–985.
88 B. B. Prasad, A. Kumar and R. Singh, *Biosens. Bioelectron.*, 2017, **94**, 1–9.
89 H. J. Chen, Z. H. Zhang, D. Xie, R. Cai, X. Chen, Y. N. Liu and S. Z. Yao, *Electroanalysis*, 2012, **24**, 2109–2116.
90 Z. Zhang, R. Cai, F. Long and J. Wang, *Talanta*, 2015, **124**, 435–442.
91 S. Jaiswal, R. Singh, K. Singh, S. Fatma and B. B. Prasad, *Biosens. Bioelectron.*, 2019, **124–125**, 176–183.
92 Y. Li, J. Liu, M. Liu, F. Yu, L. Zhang, H. Tang, B. C. Ye and L. Lai, *Electrochem. Commun.*, 2016, **64**, 42–45.
93 B. Wu, L. Hou, T. Zhang, Y. Han and C. Kong, *Anal. Methods*, 2015, **7**, 9121–9129.
94 J. Ji, Z. Zhou, X. Zhao, J. Sun and X. Sun, *Biosens. Bioelectron.*, 2015, **66**, 590–595.
95 M. B. Gholivand and M. Torkashvand, *Mater. Sci. Eng., C*, 2016, **59**, 594–603.
96 H. Wang, S. Yao, Y. Liu, S. Wei, J. Su and G. Hu, *Biosens. Bioelectron.*, 2017, **87**, 417–421.
97 S. Wei, Y. Liu, T. Hua, L. Liu and H. Wang, *J. Appl. Polym. Sci.*, 2014, **131**, 40613.
98 B. B. Prasad and S. Fatma, *Electrochim. Acta*, 2017, **232**, 474–483.
99 B. B. Prasad, A. Srivastava and M. P. Tiwari, *Mater. Sci. Eng., C*, 2013, **33**, 4071–4080.
100 S. Patra, E. Roy, R. Madhuri and P. K. Sharma, *Biosens. Bioelectron.*, 2015, **66**, 1–10.
101 L. Zhao, B. Zeng and F. Zhao, *Electrochim. Acta*, 2014, **146**, 611–617.
102 M. L. Yola, T. Eren and N. Atar, *Biosens. Bioelectron.*, 2014, **60**, 277–285.
103 F. Long, Z. Zhang, Z. Yang, J. Zeng and Y. Jiang, *J. Electroanal. Chem.*, 2015, **755**, 7–14.
104 L. J. Kong, M. F. Pan, G. Z. Fang, X. L. He, Y. Q. Xia and S. Wang, *RSC Adv.*, 2015, **5**, 11498–11505.
105 T. S. Anirudhan, V. S. Athira and V. Chithra Skhar, *Polymer*, 2018, **146**, 312–320.
106 M. Salajegheh, M. Ansari, M. M. Foroghi and M. Kazemipour, *J. Pharm. Biomed. Anal.*, 2019, **162**, 215–224.
107 J. Zhang, X. T. Guo, J. P. Zhou, G. Z. Liu and S. Y. Zhang, *Mater. Sci. Eng., C*, 2018, **91**, 696–704.
108 X. Shen, Y. Ma, Q. Zeng, J. Huang, J. Tao and L. Wang, *ChemistrySelect*, 2017, **2**, 6549–6555.
109 Y. Ma, X. L. Shen, Q. Zeng, H. S. Wang and L. S. Wang, *Talanta*, 2017, **164**, 121–127.
110 W. Wu, L. Yang, F. Zhao and B. Zeng, *Sens. Actuators, B*, 2017, **239**, 481–487.
111 S. Güney and O. Güney, *Electroanalysis*, 2017, **29**, 2579–2590.
112 B. Deiminiat and G. H. Rounaghi, *Sens. Actuators, B*, 2018, **259**, 133–141.
113 Y. Yang, G. Fang, G. Liu, M. Pan, X. Wang, L. Kong, X. He and S. Wang, *Biosens. Bioelectron.*, 2013, **47**, 475–481.
114 R. Wang, K. Yan, F. Wang and J. Zhang, *Electrochim. Acta*, 2014, **121**, 102–108.
115 Z. Wang, F. Li, J. Xia, L. Xia, F. Zhang, S. Bi, G. Shi, Y. Xia, J. Liu, Y. Li and L. Xia, *Biosens. Bioelectron.*, 2014, **61**, 391–396.
116 B. Wang, O. K. Okoth, K. Yan and J. Zhang, *Sens. Actuators, B*, 2016, **236**, 294–303.
117 Y. Liu, K. Yan, B. Wang, C. Yang and J. Zhang, *J. Electrochem. Soc.*, 2017, **164**, B776–B780.
118 F. Wang, L. Zhu and J. Zhang, *Sens. Actuators, B*, 2014, **192**, 642–647.
119 H. Bai, C. Wang, J. Chen, Z. Li, K. Fu and Q. Cao, *J. Electroanal. Chem.*, 2018, **816**, 7–13.
120 S. Emam, A. Adedoyin, X. Geng, M. Zaeimbashi, J. Adams, A. Ekenseair, E. Podlaha-Murphy and N. X. Sun, *J. Sensors*, 2018, **2018**, 1–9.
121 M. Cui, S. Liu, W. Lian, J. Li, W. Xu and J. Huang, *Analyst*, 2013, **138**, 5949–5955.
122 D. Wu, H. Li, X. Xue, H. Fan, Q. Xin and Q. Wei, *Anal. Methods*, 2013, **5**, 1469–1473.
123 H. J. Chen, Z. H. Zhang, R. Cai, X. Q. Kong, X. Chen, Y. N. Liu and S. Z. Yao, *Analyst*, 2013, **138**, 2769–2776.
124 Y. Mao, Y. Bao, S. Gan, F. Li and L. Niu, *Biosens. Bioelectron.*, 2011, **28**, 291–297.
125 H. Tang, J. Chen, Y. Zeng, Z. Li, H. Huang and L. Li, *Anal. Methods*, 2016, **8**, 1681–1689.
126 B. Lu, J. Xia, Z. Wang, F. Zhang, M. Yang, Y. Li and Y. Xia, *RSC Adv.*, 2015, **5**, 82930–82935.
127 P. T. Do, P. Q. Do, H. B. Nguyen, C. N. Van, D. L. Tran, T. H. Le, H. N. Le, H. V. Pham, T. L. Nguyen and Q. H. Tran, *J. Mol. Liq.*, 2014, **198**, 307–312.
128 F. Long, Z. Zhang, J. Wang, L. Yan and B. Zhou, *Electrochim. Acta*, 2015, **168**, 337–345.
129 B. He, Y. L. Mao, Y. Zhang, W. Yin, C. J. Hou, D. Q. Huo and H. B. Fa, *NANO*, 2017, **12**, 1750046.
130 J. Xia, X. Cao, Z. Wang, M. Yang, F. Zhang, B. Lu, F. Li, L. Xia, Y. Li and Y. Xia, *Sens. Actuators, B*, 2016, **225**, 305–311.
131 X. Zhu, Y. Zeng, Z. Zhang, Y. Yang, Y. Zhai, H. Wang, L. Liu, J. Hu and L. Li, *Biosens. Bioelectron.*, 2018, **108**, 38–45.

132 P. Zhao and J. Hao, *Biosens. Bioelectron.*, 2015, **64**, 277–284.
133 T. Li, T. Yao, C. Zhang, G. Liu, Y. She, M. Jin, F. Jin, S. Wang, H. Shao and J. Wang, *RSC Adv.*, 2016, **6**, 66949–66956.
134 L. Zheng, C. Zhang, J. Ma, S. Hong, Y. She, A. M. Abd El-Aty, Y. He, H. Yu, H. Liu and J. Wang, *Anal. Biochem.*, 2018, **559**, 44–50.
135 P. Qi, J. Wang, Z. Wang, X. Wang, X. Wang, X. Xu, H. Xu, S. Di, H. Zhang, Q. Wang and X. Wang, *Electrochim. Acta*, 2018, **274**, 406–414.
136 J. Huang, Y. Wu, J. Cong, J. Luo and X. Liu, *Sens. Actuators, B*, 2018, **259**, 1–9.
137 D. Duan, H. Yang, Y. Ding, D. Ye, L. Li and G. Ma, *Electrochim. Acta*, 2018, **261**, 160–166.
138 H. Yang, L. Li, Y. Ding, D. Ye, Y. Wang, S. Cui and L. Liao, *Biosens. Bioelectron.*, 2017, **92**, 748–754.
139 L. Zhao, F. Zhao and B. Zeng, *Int. J. Electrochem. Sci.*, 2014, **9**, 1366–1377.
140 W. Lian, S. Liu, J. Yu, X. Xing, J. Li, M. Cui and J. Huang, *Biosens. Bioelectron.*, 2012, **38**, 163–169.
141 D. Wang, N. Gan, H. Zhang, T. Li, L. Qiao, Y. Cao, X. Su and S. Jiang, *Biosens. Bioelectron.*, 2015, **65**, 78–82.
142 Y. Zeng, Y. Zhou, L. Kong, T. Zhou and G. Shi, *Biosens. Bioelectron.*, 2013, **45**, 25–33.
143 L. Zhao, F. Zhao and B. Zeng, *Sens. Actuators, B*, 2013, **176**, 818–824.
144 H. Chen, Z. Zhang, R. Cai, W. Rao and F. Long, *Electrochim. Acta*, 2014, **117**, 385–392.
145 P. Tang, H. Zhang, J. Huo and X. Lin, *Anal. Methods*, 2015, **7**, 7784–7791.
146 Y. Liu, L. Zhu, Y. Zhang and H. Tang, *Sens. Actuators, B*, 2012, **171–172**, 1151–1158.
147 S. Dadkhah, E. Ziaei, A. Mehdinia, T. B. Kayyal and A. Jabbari, *Microchim. Acta*, 2016, **183**, 1933–1941.
148 M. L. Yola, T. Eren and N. Atar, *Sens. Actuators, B*, 2015, **210**, 149–157.
149 X. Li, X. Wang, L. Li, H. Duan and C. Luo, *Talanta*, 2015, **131**, 354–360.
150 Y. Yang, G. Fang, X. Wang, M. Pan, H. Qian, H. Liu and S. Wang, *Anal. Chim. Acta*, 2014, **806**, 136–143.
151 M. M. Farid, L. Goudini, F. Piri, A. Zamani and F. Saadati, *Food Chem.*, 2016, **194**, 61–67.
152 X. Wang, X. Li, C. Luo, M. Sun, L. Li and H. Duan, *Electrochim. Acta*, 2014, **130**, 519–525.
153 J. Li, X. Wang, H. Duan, Y. Wang, Y. Bu and C. Luo, *Talanta*, 2016, **147**, 169–176.
154 M. You, S. Yang, W. Tang, F. Zhang and P. He, *Biosens. Bioelectron.*, 2018, **112**, 72–78.
155 Y. Li, X. Zhao, P. Li, Y. Huang, J. Wang and J. Zhang, *Anal. Chim. Acta*, 2015, **884**, 106–113.
156 M. A. Beluomini, J. L. da Silva, G. C. Sedenho and N. R. Stradiotto, *Talanta*, 2017, **165**, 231–239.
157 X. Tan, Q. Hu, J. Wu, X. Li, P. Li, H. Yu, X. Li and F. Lei, *Sens. Actuators, B*, 2015, **220**, 216–221.
158 Y. Liang, C. Qu, R. Yang, L. Qu and J. Li, *Sens. Actuators, B*, 2017, **251**, 542–550.
159 X. Huang, S. Wei, S. Yao, H. Zhang, C. He and J. Cao, *J. Pharm. Biomed. Anal.*, 2019, **164**, 607–614.
160 H. Jin, H. Guo, X. Gao and R. Gui, *Sens. Actuators, B*, 2018, **277**, 14–21.
161 L. Zhao, F. Zhao and B. Zeng, *Electrochim. Acta*, 2014, **115**, 247–254.
162 Q. Han, X. Wang, Z. Yang, W. Zhu, X. Zhou and H. Jiang, *Talanta*, 2014, **123**, 101–108.
163 W. Zhu, G. Jiang, L. Xu, B. Li, Q. Cai, H. Jiang and X. Zhou, *Anal. Chim. Acta*, 2015, **886**, 37–47.
164 Y. Li, W. Xu, X. Zhao, Y. Huang, J. Kang, Q. Qi and C. Zhong, *Analyst*, 2018, **143**, 5094–5102.
165 Z. Yao, X. Yang, X. Liu, Y. Yang, Y. Hu and Z. Zhao, *Microchim. Acta*, 2018, **185**, 70.
166 R. Qin, Q. Wang, C. Ren, X. Dai and H. Han, *Int. J. Electrochem. Sci.*, 2017, **12**, 8953–8962.
167 N. Atar, M. L. Yola and T. Eren, *Appl. Surf. Sci.*, 2016, **362**, 315–322.
168 C. Xue, X. Wang, W. Zhu, Q. Han, C. Zhu, J. Hong, X. Zhou and H. Jiang, *Sens. Actuators, B*, 2014, **196**, 57–63.
169 T. Wen, C. Xue, Y. Li, Y. Wang, R. Wang, J. Hong, X. Zhou and H. Jiang, *J. Electronanal. Chem.*, 2012, **682**, 121–127.
170 G. Yang, F. Zhao and B. Zeng, *Biosens. Bioelectron.*, 2014, **53**, 447–452.
171 A. R. Cardoso, A. C. Marques, L. Santos, A. F. Carvalho, F. M. Costa, R. Martins, M. G. F. Sales and E. Fortunato, *Biosens. Bioelectron.*, 2019, **124–125**, 167–175.
172 X. Wei, Z. Zhang, L. Zhang and X. Xu, *J. Mater. Sci.*, 2019, **54**, 2066–2078.
173 L. Shang, F. Zhao and B. Zeng, *ACS Appl. Mater. Interfaces*, 2014, **6**, 18721–18727.
174 Y. Pan, L. Shang, F. Zhao and B. Zeng, *Electrochim. Acta*, 2015, **151**, 423–428.
175 M. L. Yola and N. Atar, *Ind. Eng. Chem. Res.*, 2017, **56**, 7631–7639.
176 S. Feng, X. Wei, L. Zhong and J. Li, *Electroanalysis*, 2018, **30**, 320–327.
177 M. Ma, P. Zhu, F. Pi, J. Ji and X. Sun, *J. Electroanal. Chem.*, 2016, **775**, 171–178.
178 H. Rao, X. Liu, F. Ding, Y. Wan, X. Zhao, R. Liang, P. Zou, Y. Wang, X. Wang and Q. Zhao, *Chem. Eng. J.*, 2018, **338**, 478–487.
179 Y. Yang, Y. Cao, X. Wang, G. Z. Fang and S. Wang, *Biosens. Bioelectron.*, 2015, **64**, 247–254.
180 W. Guo, F. Pi, H. Zhang, J. Sun, Y. Zhang and X. Sun, *Biosens. Bioelectron.*, 2017, **98**, 299–304.
181 H. Rao, X. Zhao, X. Liu, J. Zhong, Z. Zhang, P. Zou, Y. Jiang, X. Wang and Y. Wang, *Biosens. Bioelectron.*, 2018, **100**, 341–347.
182 B. Hatamluyi and Z. Es'haghi, *Electrochim. Acta*, 2018, **283**, 1170–1177.
183 B. Xu, B. Zhang, L. Yang, F. Zhao and B. Zeng, *Electrochim. Acta*, 2017, **258**, 1413–1420.
184 Z. Zhang, J. Xu, Y. Wen and T. Wang, *Mater. Sci. Eng., C*, 2018, **92**, 77–87.
185 S. Shojaei, N. Nasirizadeh, M. Entezam, M. Koosha and M. Azimzadeh, *Food Anal. Methods*, 2016, **9**, 2721–2731.
186 L. Yang, F. Zhao and B. Zeng, *Electrochim. Acta*, 2016, **210**, 293–300.

187 L. Yang, B. Xu, H. Ye, F. Zhao and B. Zeng, *Sens. Actuators, B*, 2017, **251**, 601–608.
188 Y. Tong, H. Li, H. Guan, J. Zhao, S. Majeed, S. Anjum, F. Liang and G. Xu, *Biosens. Bioelectron.*, 2013, **47**, 553–558.
189 J. Ai, H. Guo, R. Xue, X. Wang, X. Lei and W. Yang, *Electrochem. Commun.*, 2018, **89**, 1–5.
190 G. Yang and F. Zhao, *Sens. Actuators, B*, 2015, **220**, 1017–1022.
191 L. Zhao, F. Zhao and B. Zeng, *Biosens. Bioelectron.*, 2014, **60**, 71–76.
192 X. Hu, Y. Feng, H. Wang, F. Zhao and B. Zeng, *Anal. Methods*, 2018, **10**, 4543–4548.
193 M. Cui, J. Huang, Y. Wang, Y. Wu and X. Luo, *Biosens. Bioelectron.*, 2015, **68**, 563–569.
194 S. Wang, G. Sun, Z. Chen, Y. Liang, Q. Zhou, Y. Pan and H. Zhai, *Electrochim. Acta*, 2018, **259**, 893–902.
195 T. S. Anirudhan, J. R. Deepa and Binussreejayan, *Mater. Sci. Eng., C*, 2018, **92**, 942–956.
196 X. Wang, C. Luo, L. Li and H. Duan, *RSC Adv.*, 2015, **5**, 92932–92939.
197 X. Xing, S. Liu, J. Yu, W. Lian and J. Huang, *Biosens. Bioelectron.*, 2012, **31**, 277–283.
198 Z. Wang, J. Yu, R. Gui, H. Jin and Y. Xia, *Biosens. Bioelectron.*, 2016, **79**, 136–149.
199 H. Jin, R. Gui, J. Yu, W. Lv and Z. Wang, *Biosens. Bioelectron.*, 2017, **91**, 523–537.
200 X. Gao, R. Gui, H. Guo, Z. Wang and Q. Liu, *Sens. Actuators, B*, 2019, **285**, 201–208.
201 H. Jin, C. Zhao, R. Gui, X. Gao and Z. Wang, *Anal. Chim. Acta*, 2018, **1025**, 154–162.
202 C. Zhao, H. Jin, R. Gui and Z. Wang, *Sens. Actuators, B*, 2017, **242**, 71–78.
203 R. Gui, H. Jin, X. Bu, Y. Fu, Z. Wang and Q. Liu, *Coord. Chem. Rev.*, 2019, **383**, 82–103.
204 Y. Fu, H. Jin, X. Bu and R. Gui, *J. Agric. Food Chem.*, 2018, **66**, 9819–9827.
205 R. Gui, X. Bu, W. He and H. Jin, *New J. Chem.*, 2018, **42**, 16217–16225.
206 X. Bu, Y. Fu, H. Jin and R. Gui, *New J. Chem.*, 2018, **42**, 17323–17330.
207 R. Gui, H. Jin, Z. Wang and J. Li, *Chem. Soc. Rev.*, 2018, **47**, 6795–6823.
208 Y. Wang, D. Zang, S. Ge, L. Ge, J. Yu and M. Yan, *Electrochim. Acta*, 2013, **107**, 147–154.
209 B. Babamiri, A. Salimi and R. Hallaj, *Biosens. Bioelectron.*, 2018, **117**, 332–339.
210 B. Babamiri, A. Salimi, R. Hallaj and M. Hasanzadeh, *Biosens. Bioelectron.*, 2018, **107**, 272–279.
211 X. Jin, G. Fang, M. Pan, Y. Yang, X. Bai and S. Wang, *Biosens. Bioelectron.*, 2018, **102**, 357–364.
212 W. Zhang, H. Xiong, M. Chen, X. Zhang and S. Wang, *Biosens. Bioelectron.*, 2017, **96**, 55–61.